AD-A078 477 SYRACUSE UNIV NY DEPT OF ELECTRICAL AND COMPUTER EN--ETC F/G 20/3
ELECTROMAGNETIC TRANSMISSION THROUGH A FILLED SLIT OF ARBITRARY--ETC(U)
OCT 79 D T AUCKLAND , R F HARRINGTON F30602-79-C-0011

UNCLASSIFIED RADC-TR-79-257 NL

1 OF 2
ADA
078477

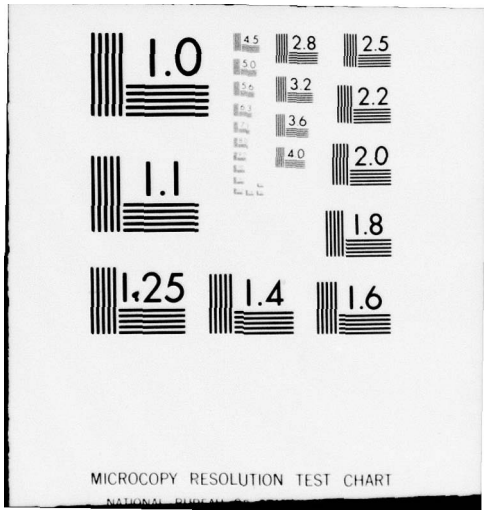
1.0
1.1
1.25
1.4
1.6
1.8
2.0
2.2
2.5
2.8
3.2
3.6
4.0
4.5
5.0
5.6
MICROCOPY RESOLUTION TEST CHART

LEVEL II

RADC-TR-79-257
Phase Report
October 1979

ELECTROMAGNETIC TRANSMISSION THROUGH A FILLED SLIT OF ARBITRARY CROSS SECTION IN A CONDUCTING PLANE OF FINITE THICKNESS

Syracuse University

David T. Auckland
Roger F. Harrington

ROME AIR DEVELOPMENT CENTER
Air Force Systems Command
Griffiss Air Force Base, New York 13441

RADC-TR-79-257 has been reviewed and is approved for publication.

This report has been reviewed by the RADC Public Affairs Office (PA) and is releasable to the National Technical Information Service (NTIS). At NTIS it will be releasable to the general public, including foreign nations.

APPROVED: Roy F. Stratton

ROY F. STRATTON
Project Engineer

APPROVED: David C. Luke

DAVID C. LUKE, Lt Col, USAF
Chief, Reliability & Compatibility Division

FOR THE COMMANDER: John P. Huss

JOHN P. HUSS
Acting Chief, Plans Office

If your address has changed or if you wish to be removed from the RADC mailing list, or if the addressee is no longer employed by your organization, please notify RADC (RBCT), Griffiss AFB NY 13441. This will assist us in maintaining a current mailing list.

Do not return this copy. Retain or destroy.

UNCLASSIFIED

SECURITY CLASSIFICATION OF THIS PAGE (When Data Entered)

REPORT DOCUMENTATION PAGE

READ INSTRUCTIONS BEFORE COMPLETING FORM

1. REPORT NUMBER: RADC-TR-79-257	2. GOVT ACCESSION NO.
3. RECIPIENT'S CATALOG NUMBER	
4. TITLE (and Subtitle): ELECTROMAGNETIC TRANSMISSION THROUGH A FILLED SLIT OF ARBITRARY CROSS SECTION IN A CONDUCTING PLANE OF FINITE THICKNESS	5. TYPE OF REPORT & PERIOD COVERED: Phase Report
	6. PERFORMING ORG. REPORT NUMBER: N/A
7. AUTHOR(s): David T. Auckland, Roger F. Harrington	8. CONTRACT OR GRANT NUMBER(s): F30602-79-C-0011
9. PERFORMING ORGANIZATION NAME AND ADDRESS: Syracuse University, Department of Electrical & Computer Engineering, Syracuse NY 13210	10. PROGRAM ELEMENT, PROJECT, TASK AREA & WORK UNIT NUMBERS: 62702F, 23380317
11. CONTROLLING OFFICE NAME AND ADDRESS: Rome Air Development Center (RBCT), Griffiss AFB NY 13441	12. REPORT DATE: October 1979
	13. NUMBER OF PAGES: 145
14. MONITORING AGENCY NAME & ADDRESS (if different from Controlling Office): Same	15. SECURITY CLASS. (of this report): UNCLASSIFIED
	15a. DECLASSIFICATION/DOWNGRADING SCHEDULE: N/A

16. DISTRIBUTION STATEMENT (of this Report)

Approved for public release; distribution unlimited.

17. DISTRIBUTION STATEMENT (of the abstract entered in Block 20, if different from Report)

Same

18. SUPPLEMENTARY NOTES

RADC Project Engineer: Roy F. Stratton (RBCT)

19. KEY WORDS (Continue on reverse side if necessary and identify by block number)

Apertures	Modal solution	Thick slits
Approximate solutions	Nonmodal solution	
Equivalence principle	Slit impedance	
Equivalent circuit	Slit polarizability	
Filled slits	Slots	

20. ABSTRACT (Continue on reverse side if necessary and identify by block number)

Electromagnetic transmission through a filled slit in a conducting plane of finite thickness is investigated when the slit cross section is an arbitrary shape. A non-modal formulation is developed whereby the original problem is broken up, via the equivalence principle, into three isolated situations. An integral equation is written for each of these situations involving equivalent electric and magnetic currents as unknowns on the closed contour defining the slit cross section. These three integral equations are (Cont'd)

DD FORM 1 JAN 73 1473

UNCLASSIFIED

SECURITY CLASSIFICATION OF THIS PAGE (When Data Entered)

406737

Item 20 (Cont'd)

solved simultaneously and it is shown that they have a unique solution at all frequencies. A modal solution is also developed for the case when the slit cross section can be viewed as a sequence of two-dimensional rectangular cavities, each coupled to the other by an aperture. Results obtained from these two solutions are compared. Some additional slits, which cannot be solved by a modal solution, are investigated by the non-modal solution.

Two approximate solutions are also investigated when the slit cross section is rectangular. For small slit widths w, such that $k_o w << 1$, the transmitted fields can be written in terms of a slit impedance for the TE case, and a slit polarizability for the TM case. An equivalent circuit is developed for the TE case and comparison with the modal solution is made for the slit impedance and transmission coefficient. The equivalent circuit involving the aperture impedance of a flange is shown to accurately determine the transmission characteristics of the slit. One interesting result is that the transmission coefficient becomes quite large (as w becomes small) for some values of the conducting plane thickness d which may be determined from a resonance of the equivalent circuit.

The second approximate solution utilizes the assumption that the field in the slit cross section may be represented by a forward and backward travelling plane wave. This solution yields accurate results for wider slits, and is especially useful when the material filling the slit is dense, i.e., the intrinsic wavelength of the material is much smaller than that of free space.

CONTENTS

LIST OF FIGURES

Figures

Figures Page

Figures Page

LIST OF SYMBOLS

$\underline{L}^e$	Electric field operator for unbounded space.
$\underline{L}^h$	Magnetic field operator for unbounded space.
$\underline{B}^h$	Magnetic field operator for two-dimensional closed conducting box.
$\underline{E}$	Electric field vector.
$\underline{H}$	Magnetic field vector.
$\underline{J}$	Electric current vector.
$\underline{M}$	Magnetic current vector.
$\underline{F}$	Electric vector potential.
$\underline{A}$	Magnetic vector potential.
$\underline{r}$	Vector from origin to field point.
$\underline{r}'$	Vector from origin to source point.
$\underline{0}$	Null vector.
$\hat{\underline{u}}$	Unit vector in u direction.
$\vec{V}$	Column vector.
$\tilde{\vec{V}}$	Transpose of column vector.
$\vec{V}^*$	Complex conjugate of column vector.
[Y]	Matrix.
Y_{mn}	Matrix element, row m, column n.
j	$\sqrt{-1}$.
ω	Radian frequency.
μ	Permeability.
ε	Permittivity.

k	Wavenumber, $\omega\sqrt{\mu\varepsilon}$.
η	Impedance, $\sqrt{\mu/\varepsilon}$.
ϕ^i	Angle of incident plane wave in region a measured from negative x axis.
Z	Slit impedance, ohms.
α_m	Slit polarizability, meters.
ε_p	Neumann's number, $\varepsilon_p = 1$ if $p = 0$ and $\varepsilon_p = 2$ if $p > 0$.
T	Transmission coefficient.
$H_0^{(2)}$	Hankel function, second kind, order zero.
$H_1^{(2)}$	Hankel function, second kind, order one.
$\alpha(z)$	$\int_0^z H_0^{(2)}(u)du$.
$G(\phi)$	Gain pattern function in region c.
$F(\phi)$	Far field pattern function in region c.
Γ	Line in the x-y plane.
ΔC	Straight line segment in the x-y plane. Also used as the length of the line segment.
$A \cup B$	Union of A and B.
$\bigcup_{i=1}^{N} A_i$	$A_1 \cup A_2 \cup \ldots \cup A_N$.
$<\underline{A},\underline{B}>$	Symmetric product of $\underline{A}$ and $\underline{B}$.
$\underline{1}$	Unit dyad, $\underline{1}\,\underline{A} = \underline{A}$.
$\underline{f}$	Triangle basis functions for non-modal formulation.
$\underline{g}$	Pulse basis functions for non-modal formulation.
$\underline{e}$	Basis functions for modal formulation.

Chapter 1

INTRODUCTION

The problem of electromagnetic transmission through apertures in conducting planes of finite thickness has been the object of several investigations. This problem is important because of the need to determine the effects of wall thickness on coupling through slots and holes in waveguides and cavities. Several quasi-static solutions have been developed, which include expanding the field in terms of the characteristic functions of Laplace's equation [1], using asymptotic expansions to solve a set of integral equations [2], and variational methods [3,4]. These solutions are usually valid when the radius of the circular aperture or the width of the slot is small compared to the wavelength. The effects of wall thickness have also been measured for some waveguide coupling problems [5], and for a long slot in a thick screen [6,7,8].

The slit (slot of infinite length) of rectangular cross section in a thick conducting screen is the object of most of the theoretical investigations. The fields in the slit region are usually expanded in terms of the parallel plate waveguide modes, while the fields in the half space regions have various integral representations. Enforcing continuity of the tangential field at the aperture faces, one obtains a coupled set of integral equations. The formulation and solution of these equations make use of a variety of techniques, such as the use of Weber-Schafheitlin discontinuous integrals [9,10], Wiener-Hopf methods

and generalized matrix techniques [11], Fourier integral methods [12,13], Green's function methods [14,15], and the equivalence principle and moment methods [16]. Another procedure is to expand the fields in the half space regions in terms of the characteristic functions of the Helmholtz equation in elliptic cylinder coordinates [17,18]. A doubly infinite set of linear algebraic equations is then obtained for determining the coefficients of expansion.

A slightly more general problem is treated in [19], where the thick ground screen is an infinite slab with finite conductivity. Analytic properties of finite Fourier transforms are used to reduce the problem to the solution of a single variable Fredholm integral equation of the second kind. A slit of arbitrary cross section is treated in [20] whereby the scattered electric field is expressed as an integral over the electric current induced on the infinite conductors. By requiring the total tangential electric field to vanish at a finite number of points on the conducting contours, a system of algebraic equations is obtained which determines the electric current at these points.

Problems of this nature are also of interest in the area of electromagnetic compatibility. If the slit region is filled with a conducting material, it might represent a gasket between two perfectly conducting walls. A different analysis than the above mentioned methods is then possible using approximations and models for the transmission mechanism [21].

This report considers the problem of a filled slit of arbitrary cross section in a thick conducting screen. The formulation presented here is basically a specialization of that given in [22] for a class of aperture coupling problems. The basis of the method rests on the equivalence principle, as it is defined and used in [23,24], which is used to break the problem up into three isolated regions. This isolation is achieved by the use of equivalent electric and magnetic current sources, which radiate in unbounded space and are constrained to give the correct fields in each region. An operator equation is thus obtained for each region in terms of the equivalent sources as the unknowns. These operator equations are solved simultaneously via a Galerkin procedure [25,26] after suitable sets of expansion functions are chosen to represent the unknowns. Some immediate advantages of this formulation are summarized as follows:

1) The necessary equivalent sources exist on a finite two-dimensional contour.
2) These equivalent sources radiate into unbounded, homogeneous space and hence their fields have a simple retarded potential representation.
3) The system of three simultaneous operator equations has a unique solution at all frequencies.
4) The cross section of the slit may be an arbitrary shape and filled with lossy material.

The operator equations are derived in detail in Chapter 2, where an argument for the uniqueness of solution is also given.

Each polarization is handled separately in Chapters 3 and 4. The term transverse electric as used here means that the electric field lies in the plane of the slit cross section, and transverse magnetic means that the magnetic field lies in the plane of the slit cross section.

Once the tangential fields over the aperture faces are known, several transmission characteristics may be computed. These are defined in Chapter 5, where they are written in terms of a measurement vector and as such are referred to as measured quantities. A slit impedance and polarizability are also defined which, when the slit width is electrically small, characterize the slit.

An alternate method of solution is presented in Chapter 6 when the slit cross section is composed of a number of rectangular regions. These are viewed as a sequence of two-dimensional, infinitely long, rectangular cavities, each coupled to the other by an aperture. The method is an extension to that presented in [16], and is referred to here as a modal solution. It has the advantage that each rectangular region may be filled with different material.

When the slit cross section is rectangular, an approximate solution is developed in Chapter 7 based on assumptions concerning the equivalent magnetic current. This approximate solution has the advantage of yielding a greatly simplified numerical solution, accurate when the material filling the slit is dense. A material is said to be dense when the intrinsic wavelength in the material is much smaller than that of free space.

Chapter 2

PROBLEM FORMULATION

2.1. Derivation of Operator Equations

The problem to be considered is shown in Fig. 1, where electromagnetic transmission occurs through a slit of arbitrary cross section in a perfectly conducting plane of finite thickness. The slit cross section is composed of the straight lines Γ_1 and Γ_3, which are the two aperture faces, and the lines Γ_2 and Γ_4, which are arbitrary in their specification. The characteristic dimensions of the slit cross section are shown in Fig. 1. This problem is strictly two-dimensional in that everything is invariant in the z direction. A time dependence of $e^{j\omega t}$ is assumed throughout.

In the original problem, $(\underline{E}^i+\underline{E}^a, \underline{H}^i+\underline{H}^a)$ is the total field in region a, $(\underline{E}^b, \underline{H}^b)$ is the total field in region b, and $(\underline{E}^c, \underline{H}^c)$ is the total field in region c. The field $(\underline{E}^i, \underline{H}^i)$ is that which would exist if the sources $(\underline{J}^i, \underline{M}^i)$ were to radiate into unbounded, homogeneous space with (μ_a, ε_a) everywhere. The equivalence principle [23,24] is used to isolate the three regions by postulating equivalent sources to support the fields in these regions.

The equivalent sources for region a consist of an electric current sheet $\underline{J}^a$ which exists everywhere on the plane at x = 0 and a magnetic current sheet $\underline{M}^1$ which exists only over the aperture face Γ_1. This current distribution radiates into unbounded space with (μ_a, ε_a)

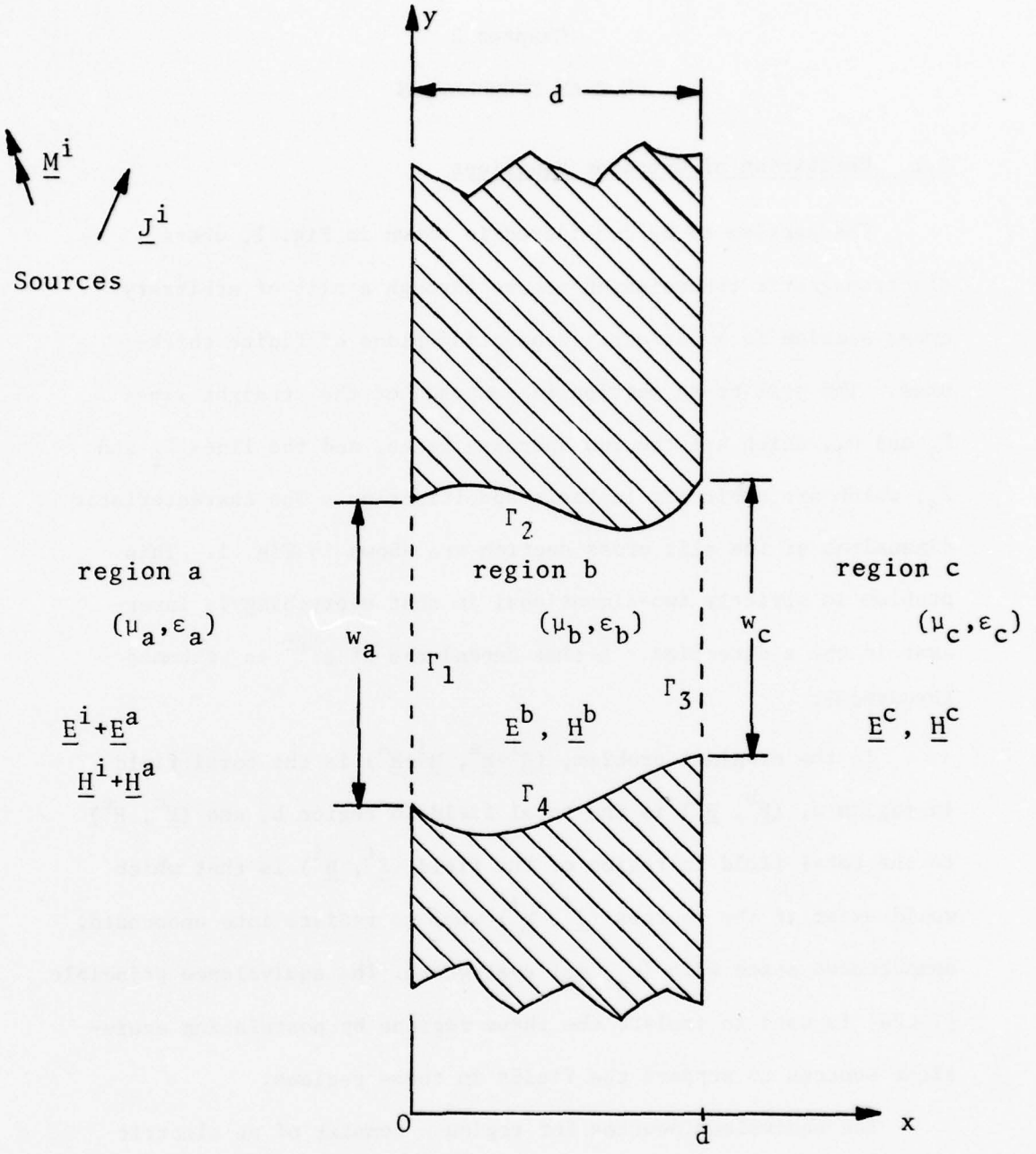

Fig. 1. Original problem: Slit of arbitrary cross section cut in a conducting plane of finite thickness.

everywhere and in the presence of the sources ($\underline{J}^i$, $\underline{M}^i$) to give the fields ($\underline{E}^i + \underline{E}^a$, $\underline{H}^i + \underline{H}^a$) to the left of the x = 0 plane and zero field to the right. This situation is shown in Fig. 2a. The condition that the tangential magnetic field is zero just to the right of the plane at x = 0 is written as

$$\underline{L}_t^{ha}(\underline{J}^a, \underline{M}^1) = - \underline{H}_t^i \tag{2-1}$$

The operator $\underline{L}^{hq}$ gives the magnetic field of sources radiating in unbounded space with (μ_q, ε_q) everywhere. The permittivity ε_q and permeability μ_q are, in general, complex numbers. The index q stands for a, b, or c and the subscript t denotes the tangential component found by the usual $-\hat{\underline{n}} \times \hat{\underline{n}} \times$ operation. This magnetic field operator is defined explicitly in terms of electric and magnetic current sources by the equation [24, p. 130]

$$\hat{\underline{n}} \times \underline{L}^{hq}(\underline{J},\underline{M}) = \pm \frac{1}{2} \underline{J}(\underline{r}) - \frac{1}{4j} \int_C \hat{\underline{n}} \times \underline{J}(\underline{r}') \times \underline{\nabla} H_o^{(2)}(k_q|\underline{r}-\underline{r}'|)dt'$$

$$- \frac{k_q}{4\eta_q} \hat{\underline{n}} \times (\underline{1} + \frac{1}{k_q^2} \underline{\nabla} \underline{\nabla} \cdot) \int_C \underline{M}(\underline{r}') H_o^{(2)}(k_q|\underline{r}-\underline{r}'|)dt' \tag{2-2}$$

Here the domain of the integrals, which is usually given by $\underline{J}$ and $\underline{M}$, is restricted to the contour $C = \bigcup_{i=1}^{4} \Gamma_i$ in anticipation of the fact that, when Eq. (2-1) is enforced at Γ_1, not all of the electric current on the plane x = 0 contributes to the tangential magnetic field there. The minus sign is used when the field point, $\underline{r}$, is on the $-\hat{\underline{n}}$ side of C(q=a or c) and the plus sign is used when q=b. The elemental

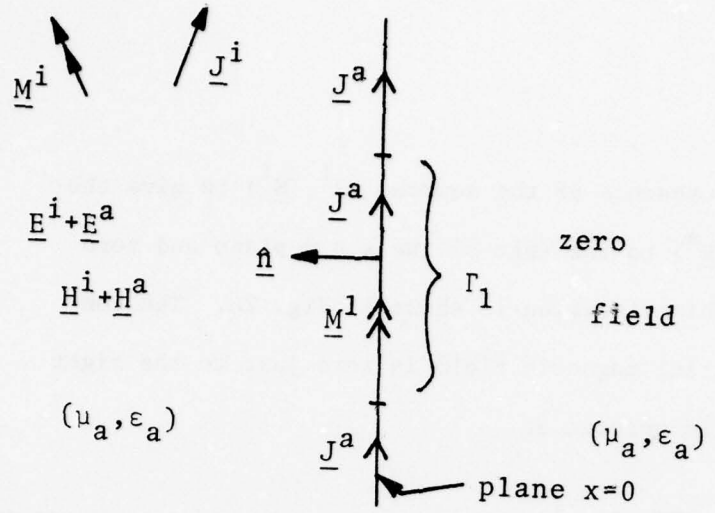

Fig. 2a. Equivalence for region a.

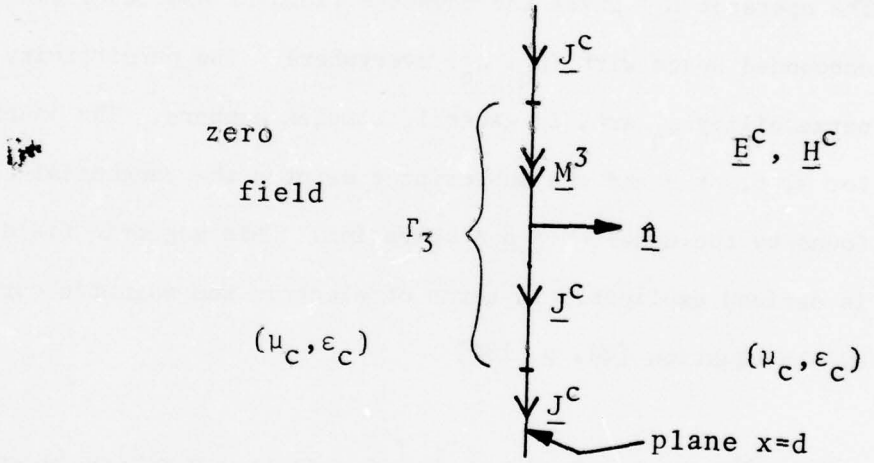

Fig. 2b. Equivalence for region c.

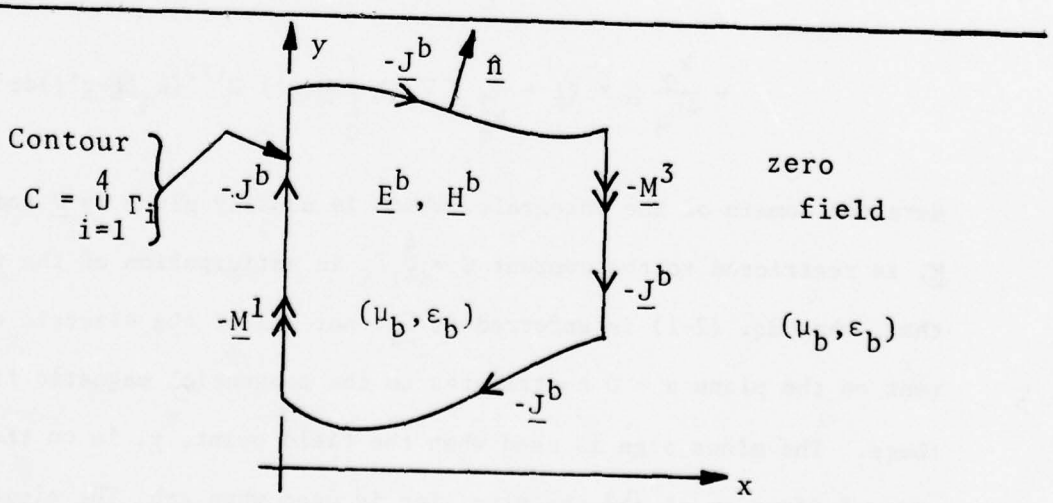

Fig. 2c. Equivalence for region b, $\underline{J}^b = \underline{J}^a$ at Γ_1 and $\underline{J}^b = \underline{J}^c$ at Γ_3.

arc length is dt', $\underline{1}$ is a unit dyad, $k_q = \omega\sqrt{\mu_q \varepsilon_q}$, $\eta_q = \sqrt{\mu_q/\varepsilon_q}$, $H_o^{(2)}$ is the Hankel function of second kind, order zero, and $\underline{r}'$ determines a point on the source distribution.

The equivalent sources for region c are given by an electric current sheet $\underline{J}^c$ which exists everywhere on the plane at x = d and a magnetic current sheet $\underline{M}^3$ which exists only at the aperture face Γ_3. This current distribution radiates into unbounded space with (μ_c, ε_c) everywhere to produce the field $(\underline{E}^c, \underline{H}^c)$ to the right of the plane at x = d and zero field to the left. This situation is shown in Fig. 2b. The condition that the tangential magnetic field is zero just to the left of the plane at x = d is written as

$$\underline{L}_t^{hc}(\underline{J}^c, \underline{M}^3) = \underline{0} \tag{2-3}$$

where $\underline{L}_t^{hc}$ is obtained from Eq. (2-2).

The true solution to the problem in Fig. 1 requires that the tangential electric and magnetic fields be continuous at the aperture faces Γ_1 and Γ_3. Hence the equivalent sources for region b consist of magnetic current sheets $-\underline{M}^1$ on Γ_1 and $-\underline{M}^3$ on Γ_3 along with an electric current $-\underline{J}^b$ which exists on the contour $C \equiv \bigcup_{i=1}^{4} \Gamma_i$, where $\underline{J}^b = \underline{J}^a$ on Γ_1 and $\underline{J}^b = \underline{J}^c$ on Γ_3. This distribution of currents on the contour C radiates into unbounded space with (μ_b, ε_b) everywhere to produce the field $(\underline{E}^b, \underline{H}^b)$ inside C and zero field outside. This situation is shown in Fig. 2c. The condition that the tangential magnetic field be zero just outside the contour C is written as

$$\hat{\underline{n}} \times \underline{L}^{hb}(-\underline{J}^b, -\underline{M}^1 - \underline{M}^3) = \underline{0} \tag{2-4}$$

where $\underline{L}^{hb}$ is obtained from Eq. (2-2). Alternatively, the condition that the total tangential electric field be zero just outside the contour C is written as

$$\underline{L}_t^{eb}(-\underline{J}^b, -\underline{M}^1 -\underline{M}^3) = \underline{0} \tag{2-5}$$

where the operator $\underline{L}^{eq}$ gives the electric field due to sources radiating into unbounded space with (μ_q, ε_q) everywhere and is defined by the equation [24, p. 130]

$$\hat{\underline{n}} \times \underline{L}^{eq}(\underline{J},\underline{M}) = \mp \frac{1}{2} \underline{M}(\underline{r}) + \frac{1}{4j} \int_C \hat{\underline{n}} \times \underline{M}(\underline{r}') \times \underline{\nabla} H_o^{(2)}(k_q|\underline{r}-\underline{r}'|)dt'$$

$$- \frac{k_q \eta_q}{4} \hat{\underline{n}} \times (\underline{1} + \frac{1}{k_q^2} \underline{\nabla} \underline{\nabla} \cdot) \int_C \underline{J}(\underline{r}') H_o^{(2)}(k_q|\underline{r}-\underline{r}'|)dt' \tag{2-6}$$

where the same remarks hold as those following Eq. (2-2) except that the plus sign is used when q = a or c and the minus sign is used when q = b.

An alternative electric field equation could also have been written in place of Eqs. (2-1) or (2-3). This is not done, however, because the electric currents $\underline{J}^a$ and $\underline{J}^c$ over the infinite portions of the planes at x = 0 and x = d contribute to the tangential electric field on Γ_1 and Γ_3 respectively. These electric currents do not contribute to the tangential magnetic field on Γ_1 and Γ_3, and hence do not appear in Eqs. (2-1) and (2-3) when they are enforced on Γ_1 and Γ_3 respectively. The necessary unknown equivalent sources, then, consist of $\underline{M}^1$, $\underline{M}^3$, and $\underline{J}^b$ which occupy a finite domain given by the closed two-dimensional contour C.

2.2. Uniqueness of Solution

The solution to the operator equations (2-1), (2-3), and either (2-4) or (2-5) will be unique if the sets of homogeneous equations consisting of

$$\underline{L}_t^{ha}(\underline{J}^a, \underline{M}^1) = \underline{0} \tag{2-7}$$

and either (2-3) and (2-4) or (2-3) and (2-5) have only the trivial solution. Thus it remains to show that if the sources are removed from the problem in Fig. 1, the fields everywhere will collapse to zero.

Equation (2-7) states that the tangential magnetic field equals zero just to the right of the plane at $x = 0$ due to $\underline{J}^a$ and $\underline{M}^1$ radiating in unbounded space with (μ_a, ε_a) everywhere. This current distribution also creates the fields $(\underline{E}^a, \underline{H}^a)$ everywhere to the left of the plane at $x = 0$. This situation is shown in Fig. 3a. Equations (2-4) and (2-5) state that the tangential electric and magnetic fields are zero just outside C due to $-\underline{M}^1$, $-\underline{M}^3$, and $-\underline{J}^b$ radiating in unbounded space with (μ_b, ε_b) everywhere. This implies that the electromagnetic field everywhere outside C is zero while the field inside C is given by $(\underline{E}^b, \underline{H}^b)$. This situation is shown in Fig. 3b and it is noted that either of Eqs. (2-4) or (2-5) is sufficient to produce this situation. Equation (2-3) states that the tangential magnetic field equals zero just to the left of the plane at $x = d$ due to $\underline{J}^c$ and $\underline{M}^3$ radiating in unbounded space (μ_c, ε_c) everywhere. This current distribution also creates the fields $(\underline{E}^c, \underline{H}^c)$ everywhere to the right of the plane at $x = d$. This situation is shown in Fig. 3c.

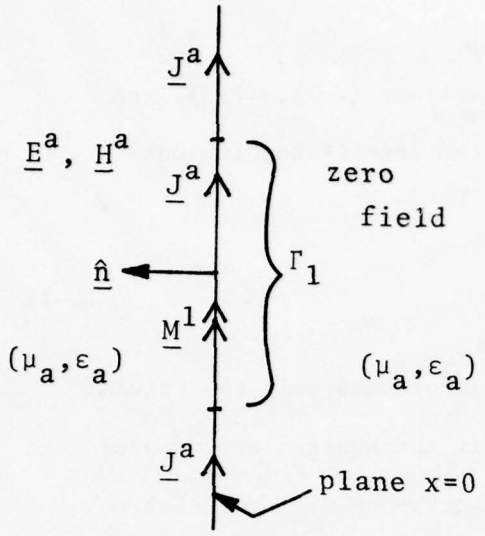

Fig. 3a. Situation of Eq.(2-7), $\underline{J}^a = \underline{J}^b$ at Γ_1.

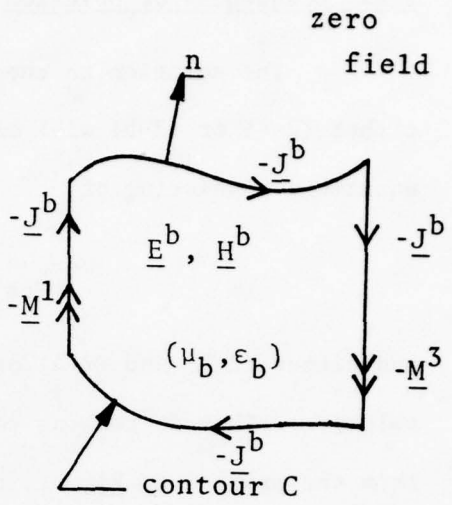

Fig. 3b. Situation of Eqs.(2-4) and (2-5), $-\underline{J}^b = -\underline{J}^a$ on Γ_1 and $-\underline{J}^b = -\underline{J}^c$ on Γ_3.

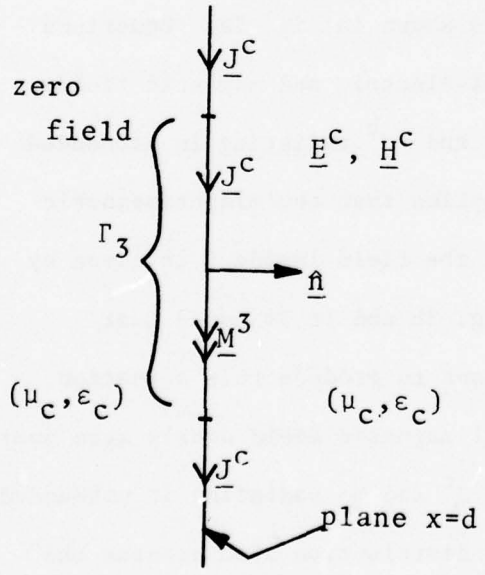

Fig. 3c. Situation of Eq.(2-3), $\underline{J}^c = \underline{J}^b$ at Γ_3.

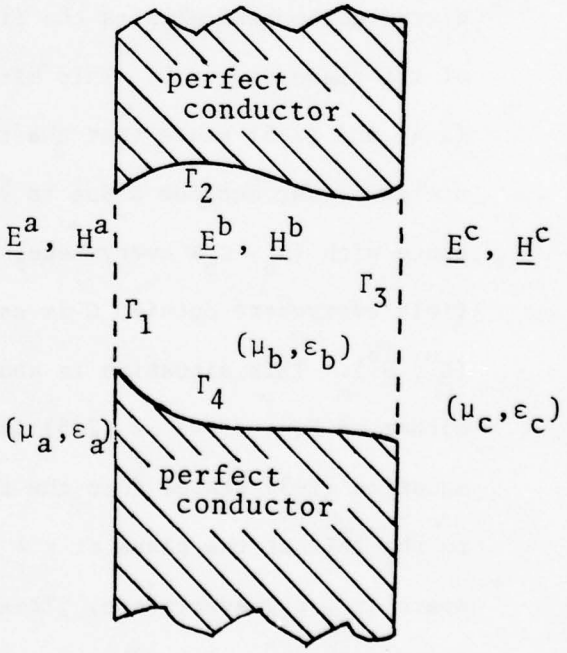

Fig. 3d. Composite situation.

Now the composite situation shown in Fig. 3d is considered where the fields of Figs. 3a - 3c have been superposed. From Fig. 3a, the tangential component of $\underline{E}^a$ is zero everywhere at x = 0 except on Γ_1 and from Fig. 3c, the tangential component of $\underline{E}^c$ is zero everywhere at x = d except on Γ_3. From Fig. 3b, the tangential component of $\underline{E}^b$ is zero at the perfectly conducting contours Γ_2 and Γ_4. Figures 3a and 3b indicate that there are no equivalent sources at Γ_1 in Fig. 3d and Figures 3b and 3c indicate that there are no equivalent sources at Γ_3 in Fig. 3d. The conclusion is that the tangential electric field is zero everywhere on the boundaries of the perfect conductors in the composite situation of Fig. 3d and also that the region outside the perfect conductors is source free. Thus the fields in Figs. 3a-3c are collapsed to the null field and hence the solution to Eqs. (2-1), (2-3), and either (2-4) or (2-5) is unique.

2.3. Specification of Slit Cross Section, Basis Functions, and Symmetric Product

The contour C which determines the slit cross section is approximated by a number of straight line segments each of length ΔC_n for integers $n=1,2,\ldots,N_5-1$. This is shown in Fig. 4. The integers N_i, i=1,2,3,4, or 5 are assigned to the beginning and end points of each Γ_i with $N_1 \equiv 1$ so that each Γ_i is broken up into $N_{i+1} - N_i$ segments. Each segment ΔC_n has a transverse directed normal $\hat{\underline{n}}_n$ and tangent $\hat{\underline{t}}_n$ such that

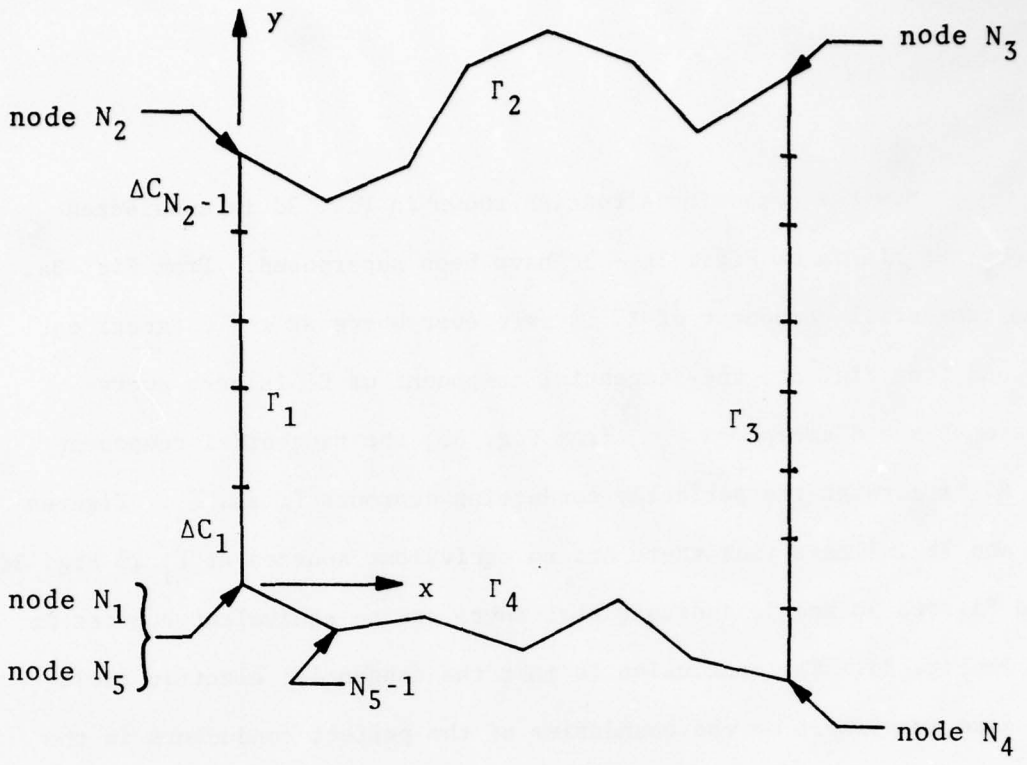

Fig. 4. Contour C approximated by N_5-1 straight line segments.

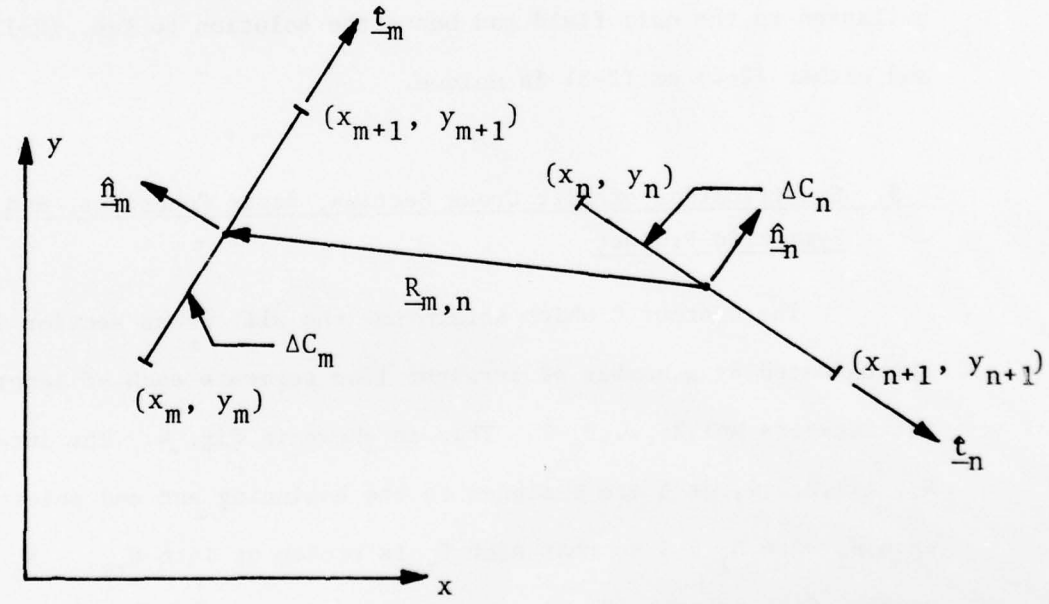

Fig. 5. Typical segments ΔC_m and ΔC_n. $\underline{R}_{m,n}$ is defined as a vector from the midpoint of ΔC_n to the midpoint of ΔC_m.

$$\hat{t}_n \times \hat{n}_n = \hat{z} \tag{2-8}$$

It is useful to introduce the parameter t which represents the arc length along C from the origin to any point on C. Thus the subscripted values of t are given by

$$t_n = \sum_{i=1}^{n-1} \Delta C_i \tag{2-9}$$

for n=2,3,..., N_5 and $t_1 \equiv 0$. Two typical straight line segments are shown in Fig. 5 where the vector $\underline{R}_{m,n}$ is also defined.

For each polarization, both transverse ($\hat{t}$) and longitudinal ($\hat{z}$) directed current sources are present. The transverse currents have a charge associated with them and it is desirable, though not necessary, that their representation be differentiable. The z directed currents have no such requirements but sometimes become unbounded at edges. The longitudinal expansion functions, then, should not be constrained to be continuous at edges. For the sake of simplicity, the edge condition [27,28] will not be built in a-priori into the representation of the unknown currents. With these considerations in mind, then, two different sets of expansion functions are defined as

$$\underline{f}_m(t) = \begin{cases} \dfrac{t - t_{m-1}}{t_m - t_{m-1}} \hat{t}_{m-1} & \text{for } t_{m-1} \leq t \leq t_m \\ \dfrac{t - t_{m+1}}{t_m - t_{m+1}} \hat{t}_m & \text{for } t_m \leq t \leq t_{m+1} \\ 0 & \text{for t elsewhere} \end{cases} \tag{2-10}$$

and

$$\underline{g}_m(t) = \begin{cases} 1\ \hat{\underline{z}} & \text{for } t_m \leq t \leq t_{m+1} \\ 0 & \text{for } t \text{ elsewhere} \end{cases} \tag{2-11}$$

for $m=1,2,\ldots, N_5-1$ and with $t_o \equiv t_{N_5-1}$.

Lastly, in order to carry out the method of moments procedure, it is necessary to define a symmetric product as

$$\langle \underline{A}, \underline{B} \rangle = \int_C \underline{A} \cdot \underline{B}\ dt \tag{2-12}$$

where $\underline{A}$ and $\underline{B}$ are vector functions defined on the two dimensional contour C.

2.4. Reduction of Operator Equations to Matrix Equations

The method of moments [25] is applied somewhat mechanically to solve either one of two possible sets of simultaneous operator equations. These consist of the sets (2-1), (2-3), and (2-4) or (2-1), (2-3), and (2-5). The two different polarizations are considered separately in Chapters 3 and 4. The first step is to assume that the unknown currents can be represented by a linear combination of vector basis functions defined on the two-dimensional contour C. These may be chosen from the sets defined in Section 2.3. Thus the equivalent currents are represented in general by

$$\underline{M}^1 = \sum_n V_n^1\ \underline{\alpha}_{1n}(t) \tag{2-13}$$

$$\underline{M}^3 = \sum_n V_n^3\ \underline{\alpha}_{3n}(t) \tag{2-14}$$

$$\underline{J}^b = \sum_n I_n\ \underline{\beta}_n(t) \tag{2-15}$$

where V_n^1, V_n^3, and I_n are unknown complex coefficients to be determined. The functions $\underline{\alpha}_1$, $\underline{\alpha}_3$, $\underline{\beta}$ are vector basis functions defined on Γ_1, Γ_3, and C respectively and will be chosen from the sets (2-10) and (2-11) depending on the polarization considered.

The next step is to substitute Eqs. (2-13) - (2-15) into the operator equations and "test" each equation on that portion of the contour C over which it is valid. This is done by taking the symmetric product of the operator equation with "testing" functions defined on the contour C. It is desirable to choose testing functions which are in the range of the operator. The operator equations have been written in such a way as to allow the use of the basis functions for the testing procedure. This is computationally convenient in that several matrices become symmetric. Thus Eq. (2-1) is tested with $\underline{\alpha}_{1m}$ at Γ_1, Eq. (2-3) is tested with $\underline{\alpha}_{3m}$ at Γ_3, and Eqs. (2-4) and (2-5) are tested all along C with $\underline{\beta}_m$. This procedure results in two possible sets of simultaneous equations which are written in matrix form as

$$\begin{bmatrix} [Y^a] & [0] & [U^1] \\ [0] & [Y^c] & [U^3] \\ [Y^{h1}] & [Y^{h3}] & [T^h] \end{bmatrix} \begin{bmatrix} \vec{V}^1 \\ \vec{V}^3 \\ \eta_o \vec{I} \end{bmatrix} = \begin{bmatrix} \vec{I}^i \\ \vec{0} \\ \vec{0} \end{bmatrix} \tag{2-16}$$

or

$$\begin{bmatrix} [Y^a] & [0] & [U^1] \\ [0] & [Y^c] & [U^3] \\ [Y^{e1}] & [Y^{e3}] & [T^e] \end{bmatrix} \begin{bmatrix} \vec{V}^1 \\ \vec{V}^3 \\ \eta_o \vec{I} \end{bmatrix} = \begin{bmatrix} \vec{I}^i \\ \vec{0} \\ \vec{0} \end{bmatrix} \tag{2-17}$$

The matrix [0] stands for a matrix of zeros and $\vec{0}$ stands for a column vector of zeros. As shown earlier, either (2-16) or (2-17) provide a

unique solution to the original problem. The matrix elements are given by the general formulas:

$$Y^{a}_{mn} = - k_o \eta_o \langle \underline{\alpha}_{1m}, \underline{L}^{ha}_{t}(\underline{0}, \underline{\alpha}_{1n}) \rangle \tag{2-18}$$

$$Y^{c}_{mn} = - k_o \eta_o \langle \underline{\alpha}_{3m}, \underline{L}^{hc}_{t}(\underline{0}, \underline{\alpha}_{3n}) \rangle \tag{2-19}$$

$$U^{1}_{mn} = - \frac{k_o}{2} \langle \underline{\alpha}_{1m}, \hat{\underline{n}} \times \underline{\beta}_{n} \rangle \tag{2-20}$$

$$U^{3}_{mn} = - \frac{k_o}{2} \langle \underline{\alpha}_{3m}, \hat{\underline{n}} \times \underline{\beta}_{n} \rangle \tag{2-21}$$

$$Y^{h1}_{mn} = - k_o \eta_o \langle \underline{\beta}_{m}, \hat{\underline{n}} \times \underline{L}^{hb}(\underline{0}, \underline{\alpha}_{1n}) \rangle \tag{2-22}$$

$$Y^{h3}_{mn} = - k_o \eta_o \langle \underline{\beta}_{m}, \hat{\underline{n}} \times \underline{L}^{hb}(\underline{0}, \underline{\alpha}_{3n}) \rangle \tag{2-23}$$

$$T^{h}_{mn} = - k_o \langle \underline{\beta}_{m}, \hat{\underline{n}} \times \underline{L}^{hb}(\underline{\beta}_{n}, \underline{0}) \rangle \tag{2-24}$$

$$Y^{e1}_{mn} = - k_o \langle \underline{\beta}_{m}, \underline{L}^{eb}_{t}(\underline{0}, \underline{\alpha}_{1n}) \rangle \tag{2-25}$$

$$Y^{e3}_{mn} = - k_o \langle \underline{\beta}_{m}, \underline{L}^{eb}_{t}(\underline{0}, \underline{\alpha}_{3n}) \rangle \tag{2-26}$$

$$T^{e}_{mn} = - \frac{k_o}{\eta_o} \langle \underline{\beta}_{m}, \underline{L}^{eb}_{t}(\underline{\beta}_{n}, \underline{0}) \rangle \tag{2-27}$$

The linearity of the operators $\underline{L}^{eq}$ and $\underline{L}^{hq}$ has been used in the above. Scaling has also been done with k_o, the wavenumber of free space, and η_o, the impedance of free space, so that the computed matrix quantities are dimensionless. The minus signs are kept in (2-18)-(2-27) so that

the Y matrices may be identified as the usual admittance matrices obtained in the network analogue. The non-zero elements of the excitation vector are given by

$$I_m^i = k_o \eta_o \langle \underline{\alpha}_{1m}, \underline{H}_t^i \rangle \tag{2-28}$$

If Eq. (2-16) is partitioned and the vector $\eta_o \vec{I}$ is eliminated, one obtains

$$\begin{bmatrix} [Y^a - U^1[T^h]^{-1}Y^{h1}] & [-U^1[T^h]^{-1}Y^{h3}] \\ [-U^3[T^h]^{-1}Y^{h1}] & [Y^c - U^3[T^h]^{-1}Y^{h3}] \end{bmatrix} \begin{bmatrix} \vec{V}^1 \\ \vec{V}^3 \end{bmatrix} = \begin{bmatrix} \vec{I}^i \\ \vec{0} \end{bmatrix} \tag{2-29}$$

assuming that the inverse $[T^h]^{-1}$ *exists*. A similar set of equations may be obtained from Eq. (2-17) under the condition that $[T^e]^{-1}$ exists. These inverse operators do not exist at all frequencies, however, since $[T^h]$ and $[T^e]$ arise from the magnetic and electric field formulation of scattering by a closed perfectly conducting contour. These operators become ill-behaved at certain resonant frequencies. Equation (2-29) and its counterpart, obtained by partitioning Eq. (2-17), do not have a unique solution at all frequencies. They do, however, have the convenient network coupling representation as shown in Fig. 6.

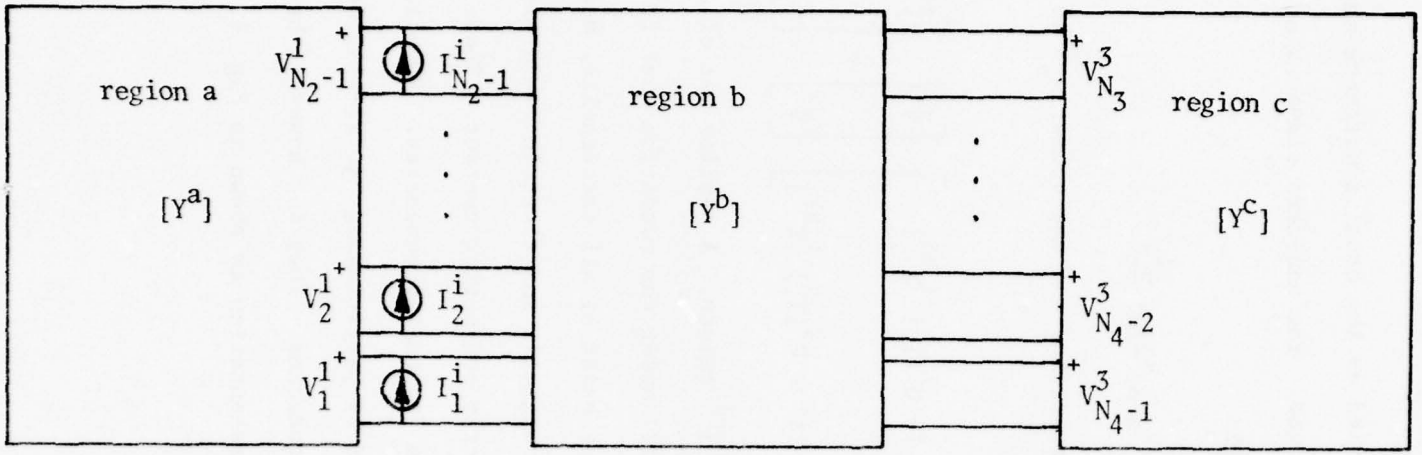

Fig. 6. Network coupling interpretation of partitioned matrix equations.

Chapter 3

TRANSVERSE ELECTRIC (TE) CASE

3.1. Expansion of the Equivalent Currents

For the TE polarization, there is only a z component of magnetic field and transverse components of electric field. The equivalent magnetic currents are z directed and satisfy no boundary conditions on Γ_1 and Γ_3. The equivalent electric currents are transverse directed and are continuous all along the contour C. With this in mind, the functions of Eq. (2-11) are chosen for $\underline{\alpha}_1$ and $\underline{\alpha}_3$ of (2-13) and (2-14) and the functions of Eq. (2-10) are chosen for $\underline{\beta}$ of (2-15). The unknown currents are then expanded as

$$\underline{M}^1 = \sum_{n=1}^{N_2-1} V_n^1 \, \underline{g}_n(t) \tag{3-1}$$

$$\underline{M}^3 = \sum_{n=N_3}^{N_4-1} V_n^3 \, \underline{g}_n(t) \tag{3-2}$$

and

$$\underline{J}^b = \sum_{n=1}^{N_5-1} I_n \, \underline{f}_n(t) \tag{3-3}$$

The formulas for the matrix elements of (2-16) and (2-17) may now be obtained from Eqs. (2-18) - (2-28). They are given as follows where the ranges of the indices m and n are specified:

$$Y_{mn}^a = - k_o \eta_o \langle \underline{g}_m, \underline{L}_t^{ha}(\underline{0}, \underline{g}_n) \rangle \qquad \begin{matrix} 1 \le m \le N_2-1 \\ 1 \le n \le N_2-1 \end{matrix} \tag{3-4}$$

$$Y_{mn}^c = - k_o \eta_o \langle \underline{g}_m, \underline{L}_t^{hc}(\underline{0}, \underline{g}_n) \rangle \qquad \begin{matrix} N_3 \le m \le N_4-1 \\ N_3 \le n \le N_4-1 \end{matrix} \tag{3-5}$$

$$U^1_{mn} = -\frac{k_o}{2} \langle \underline{g}_m, \hat{\underline{n}} \times \underline{f}_n \rangle \qquad \begin{matrix} 1 \le m \le N_2-1 \\ 1 \le n \le N_5-1 \end{matrix} \qquad (3\text{-}6)$$

$$U^3_{mn} = -\frac{k_o}{2} \langle \underline{g}_m, \hat{\underline{n}} \times \underline{f}_n \rangle \qquad \begin{matrix} N_3 \le m \le N_4-1 \\ 1 \le n \le N_5-1 \end{matrix} \qquad (3\text{-}7)$$

$$Y^{h1}_{mn} = -k_o \eta_o \langle \underline{f}_m, \hat{\underline{n}} \times \underline{L}^{hb}(\underline{0}, \underline{g}_n) \rangle \qquad \begin{matrix} 1 \le m \le N_5-1 \\ 1 \le n \le N_2-1 \end{matrix} \qquad (3\text{-}8)$$

$$Y^{h3}_{mn} = -k_o \eta_o \langle \underline{f}_m, \hat{\underline{n}} \times \underline{L}^{hb}(\underline{0}, \underline{g}_n) \rangle \qquad \begin{matrix} 1 \le m \le N_5-1 \\ N_3 \le n \le N_4-1 \end{matrix} \qquad (3\text{-}9)$$

$$T^h_{mn} = -k_o \langle \underline{f}_m, \hat{\underline{n}} \times \underline{L}^{hb}(\underline{f}_n, \underline{0}) \rangle \qquad \begin{matrix} 1 \le m \le N_5-1 \\ 1 \le n \le N_5-1 \end{matrix} \qquad (3\text{-}10)$$

$$Y^{e1}_{mn} = -k_o \langle \underline{f}_m, \underline{L}^{eb}_t(\underline{0}, \underline{g}_n) \rangle \qquad \begin{matrix} 1 \le m \le N_5-1 \\ 1 \le n \le N_2-1 \end{matrix} \qquad (3\text{-}11)$$

$$Y^{e3}_{mn} = -k_o \langle \underline{f}_m, \underline{L}^{eb}_t(\underline{0}, \underline{g}_n) \rangle \qquad \begin{matrix} 1 \le m \le N_5-1 \\ N_3 \le n \le N_4-1 \end{matrix} \qquad (3\text{-}12)$$

$$T^e_{mn} = -\frac{k_o}{\eta_o} \langle \underline{f}_m, \underline{L}^{eb}_t(\underline{f}_n, \underline{0}) \rangle \qquad \begin{matrix} 1 \le m \le N_5-1 \\ 1 \le n \le N_5-1 \end{matrix} \qquad (3\text{-}13)$$

The non-zero elements of the excitation vector are given by

$$I^i_m = k_o \eta_o \langle \underline{g}_m, \underline{H}^i_t \rangle \qquad 1 \le m \le N_2-1 \qquad (3\text{-}14)$$

3.2. Formulas for TE Matrix Elements

Equations (3-4) - (3-13) define the elements of the matrices in Eqs. (2-16) and (2-17). Explicit formulas will be derived here for these symmetric products using the definitions of the operators given by Eqs. (2-2) and (2-6) and the expansion functions (2-10) and (2-11). Equations (3-4) and (3-5) may be computed by examining the inner product

$$P_1 = - k_o \eta_o \langle \underline{g}_m, \underline{L}_t^{ha}(\underline{0}, \underline{g}_n) \rangle$$

$$= - \frac{k_o \eta_o k_a}{4\eta_a} \int_{t_m}^{t_{m+1}} \underline{g}_m(t) \cdot \hat{\underline{n}} \times \hat{\underline{n}} \times \int_{t_n}^{t_{n+1}} \underline{g}_n(t') H_o^{(2)}(k_a |\underline{r}_m(t) - \underline{r}_n(t)|) dt' dt \qquad (3\text{-}15)$$

where $\underline{r}_m(t)$ denotes a vector from the origin to a point on ΔC_m for $m=1,2,\ldots,N_5-1$. Using the variables $u = \frac{2}{\Delta C_m} t$, $u' = \frac{2}{\Delta C_n} t'$, and $\underline{R}_{m,n}$ defined in Fig. 5, one may write Eq. (3-15) as

$$P_1 = \begin{cases} \dfrac{k_o \eta_o}{4 k_a \eta_a} \dfrac{\gamma_m \gamma_n}{4} \displaystyle\int_{-1}^{1} \int_{-1}^{1} H_o^{(2)}(|\frac{\gamma_m}{2} u \hat{\underline{t}}_m - \frac{\gamma_n}{2} u' \hat{\underline{t}}_n + k_a \underline{R}_{m,n}|) du' du & \text{if } m \neq n \\ \dfrac{k_o \eta_o}{4 k_a \eta_a} \dfrac{\gamma_m}{2} \displaystyle\int_{-1}^{1} [\alpha(\frac{\gamma_m}{2}(u+1)) + \alpha(\frac{\gamma_m}{2}(1-u))] du & \text{if } m = n \end{cases} \qquad (3\text{-}16)$$

where $\gamma_m = k_a \Delta C_m$, $\gamma_n = k_a \Delta C_n$, and the function α is defined by

$$\alpha(z) = \int_0^z H_o^{(2)}(v) dv \qquad (3\text{-}17)$$

This function may be computed using Struve functions [29-11.1.7]. The integrals in (3-16) may be approximated readily by Gaussian quadrature

formulae as outlined in the Appendix. Equation (3-5) is given by an identical result where subscript c replaces a.

Equations (3-6) and (3-7) are straightforward and one may easily obtain

$$P_2 = -\frac{k_o}{2} \langle \underline{g}_m, \hat{n} \times \underline{f}_n \rangle$$

$$= \begin{cases} \dfrac{k_o \Delta C_m}{4} & \text{for } m = n-1 \text{ or } m = n \\ 0 & \text{for } m \text{ otherwise} \end{cases} \tag{3-18}$$

Equations (3-8) and (3-9) are similar to (3-15) as can be seen from the following symmetric product:

$$P_3 = -k_o \eta_o \langle \underline{f}_m, \hat{n} \times \underline{L}^{hb}(\underline{0}, \underline{g}_n) \rangle$$

$$= \frac{k_o \eta_o k_b}{4\eta_b} \left\{ \int_{t_{m-1}}^{t_m} \int_{t_n}^{t_{n+1}} \frac{t - t_{m-1}}{t_m - t_{m-1}} H_o^{(2)}(k_b |\underline{r}_{m-1}(t) - \underline{r}_n(t')|) dt' dt \right.$$

$$\left. + \int_{t_m}^{t_{m+1}} \int_{t_n}^{t_{n+1}} \frac{t - t_{m+1}}{t_m - t_{m+1}} H_o^{(2)}(k_b |\underline{r}_m(t) - \underline{r}_n(t')|) dt' dt \right\} \tag{3-19}$$

Using an appropriate change of variables in each integral and $\gamma_m = k_b \Delta C_m$, one may write

$$P_3 = \frac{k_o \eta_o}{k_b \eta_b} (S_1 + S_2) \tag{3-20}$$

where S_1 and S_2 are given by

$$S_1 = \begin{cases} \dfrac{\gamma_{m-1}\gamma_n}{16} \displaystyle\int_{-1}^{1}\int_{-1}^{1} \left(\frac{u}{2}+\frac{1}{2}\right) H_o^{(2)}\left(\left|\frac{\gamma_{m-1}}{2}\, u\, \hat{\underline{t}}_{m-1} - \frac{\gamma_n}{2}\, u'\hat{\underline{t}}_n + k_b \underline{R}_{m-1,n}\right|\right) du'du & \text{if } m-1 \neq n \\ \dfrac{\gamma_{m-1}}{8} \displaystyle\int_{-1}^{1} \left(\frac{u}{2}+\frac{1}{2}\right)\left[\alpha\left(\frac{\gamma_n}{2}(u+1)\right) + \alpha\left(\frac{\gamma_n}{2}(1-u)\right)\right] du & \text{if } m-1 = n \end{cases} \tag{3-21}$$

$$S_2 = \begin{cases} \dfrac{\gamma_m \gamma_n}{16} \displaystyle\int_{-1}^{1}\int_{-1}^{1} \left(\frac{-u}{2}+\frac{1}{2}\right) H_o^{(2)}\left(\left|\frac{\gamma_m}{2}\, u\, \hat{\underline{t}}_m - \frac{\gamma_n}{2}\, u'\hat{\underline{t}}_n + k_b \underline{R}_{m,n}\right|\right) du'du & \text{if } m \neq n \\ \dfrac{\gamma_m}{8} \displaystyle\int_{-1}^{1} \left(\frac{-u}{2}+\frac{1}{2}\right)\left[\alpha\left(\frac{\gamma_n}{2}(u+1)\right) + \alpha\left(\frac{\gamma_n}{2}(1-u)\right)\right] du & \text{if } m = n \end{cases} \tag{3-22}$$

For Eq. (3-10), the magnetic field due to a transverse directed electric current is needed and using (2-2) with $\underline{M} = 0$, one obtains

$$P_4 = -k_o \langle \underline{f}_m, \hat{\underline{n}} \times \underline{L}^{hb}(\underline{f}_n, \underline{0}) \rangle$$

$$= -\frac{k_o}{2} \int_{t_{m-1}}^{t_{m+1}} \underline{f}_m(t) \cdot \underline{f}_n(t)\, dt$$

$$+ \frac{k_o}{4j} \int_{t_{m-1}}^{t_{m+1}} \underline{f}_m(t) \cdot \int_{t_{n-1}}^{t_{n+1}} \hat{\underline{n}} \times \underline{f}_n(t') \times \underline{\nabla} H_o^{(2)}(k_b|\underline{r}-\underline{r}'|)\, dt'dt \tag{3-23}$$

where $\underline{r}$ is a vector from the origin to a point on $\Delta C_{m-1} \cup \Delta C_m$ and $\underline{r}'$ is a vector from the origin to a point on $\Delta C_{n-1} \cup \Delta C_n$. The above

integral is broken up into four parts and the symmetric product is written as

$$P_4 = \frac{k_o}{k_b} [S_4(m-1,n-1,1,1) + S_4(m-1,n,1,-1) + S_4(m,n-1,-1,1) + S_4(m,n,-1,-1)] \quad (3\text{-}24)$$

The function S_4 is defined by

$$S_4(m,n,p,q) = \begin{cases} -\frac{\gamma_m \gamma_n}{16j} \int_{-1}^{1} \int_{-1}^{1} (p\,\frac{u}{2} + \frac{1}{2})(q\,\frac{u}{2} + \frac{1}{2})\,\phi(m,n)\,du'du & \text{if } m \neq n \\ -\frac{\gamma_m}{4}\,(\frac{1}{2} + \frac{pq}{6}) & \text{if } m=n \end{cases} \quad (3\text{-}25)$$

where

$$\phi(m,n) = \frac{\hat{n}_n \cdot \hat{R}_{m,n}}{|\hat{R}_{m,n}|} H_1^{(2)}(|\hat{R}_{m,n}|) \quad (3\text{-}26)$$

and

$$\hat{R}_{m,n} = k_b R_{m,n} + \frac{\gamma_m}{2} u\hat{t}_m - \frac{\gamma_n}{2} u'\hat{t}_n \quad (3\text{-}27)$$

A similar transformation of variables as was done for Eq. (3-19) has been used as well as the identity

$$\nabla H_o^{(2)}(k_b|r-r'|) = \frac{-k_b(r-r')}{|r-r'|} H_1^{(2)}(k_b|r-r'|) \quad (3\text{-}28)$$

Equations (3-11) and (3-12) are computed using the electric field operator defined in Eq. (2-6), from which one obtains

$$P_5 = - k_o \langle \underline{f}_m, \underline{L}_t^{eb}(\underline{0}, \underline{g}_n) \rangle$$

$$= - \frac{k_o}{2} \int_{t_{m-1}}^{t_{m+1}} \underline{f}_m(t) \cdot \hat{\underline{n}} \times \underline{g}_n(t) dt$$

$$+ \frac{k_o}{4j} \int_{t_{m-1}}^{t_{m+1}} \underline{f}_m(t) \cdot \hat{\underline{n}} \times \int_{t_n}^{t_{n+1}} \hat{\underline{n}} \times \underline{g}_n(t') \times \underline{\nabla} H_o^{(2)}(k_b |\underline{r}-\underline{r}'|) dt' dt \tag{3-29}$$

where $\underline{r}$ is a vector from the origin to a point on $\Delta C_{m-1} \cup \Delta C_m$ and $\underline{r}'$ is a vector from the origin to a point on ΔC_n. Using the same transformation as for Eq. (3-19), one obtains

$$P_5 = \frac{k_o}{k_b} (S_1 + S_2) \tag{3-30}$$

where S_1 and S_2 are defined by

$$S_1 = \begin{cases} -\frac{\gamma_{m-1}}{4} & \text{if } m-1 = n \\ -\frac{1}{4j} \frac{\gamma_{m-1}\gamma_n}{4} \int_{-1}^{1} \int_{-1}^{1} (\frac{u}{2} + \frac{1}{2}) \phi(m-1,n) du' du & \text{if } m-1 \neq n \end{cases} \tag{3-31}$$

$$S_2 = \begin{cases} -\frac{\gamma_m}{4} & \text{if } m = n \\ -\frac{1}{4j} \frac{\gamma_m\gamma_n}{4} \int_{-1}^{1} \int_{-1}^{1} (\frac{-u}{2} + \frac{1}{2}) \phi(m,n) du' du & \text{if } m \neq n \end{cases} \tag{3-32}$$

and

$$\phi(m,n) = \frac{\hat{\underline{n}}_m \cdot \hat{\underline{R}}_{m,n}}{|\hat{\underline{R}}_{m,n}|} H_1^{(2)}(|\hat{\underline{R}}_{m,n}|) \tag{3-33}$$

where $\hat{\underline{R}}_{m,n}$ is defined in Eq. (3-27).

Finally, to obtain Eq. (3-13), one must compute the following symmetric product:

$$P_6 = -\frac{k_o}{\eta_o} \langle \underline{f}_m, \underline{L}_t^{eb}(\underline{f}_n, \underline{0}) \rangle$$

$$= -\frac{k_o k_b \eta_b}{4\eta_o} \int_{t_{m-1}}^{t_{m+1}} \underline{f}_m(t) \cdot \hat{\underline{n}} \times \hat{\underline{n}} \times (\underline{1} + \frac{1}{k_b^2} \underline{\nabla}\,\underline{\nabla}\,\cdot) \int_{t_{n-1}}^{t_{n+1}} \underline{f}_n(t') H_o^{(2)}(k_b|\underline{r}-\underline{r}'|)dt'dt \tag{3-34}$$

where $\underline{r}$ is a vector from the origin to a point on $\Delta C_{m-1} \cup \Delta C_m$ and $\underline{r}'$ is a vector from the origin to a point on $\Delta C_{n-1} \cup \Delta C_n$. The technique of integration by parts is applied twice to the term containing the $\underline{\nabla}\,\underline{\nabla}\,\cdot$ operation and the result is given by:

$$P_6 = \frac{k_o k_b \eta_b}{4\eta_o} \int_{t_{m-1}}^{t_{m+1}} \int_{t_{n-1}}^{t_{n+1}} [\underline{f}_m(t) \cdot \underline{f}_n(t') - \frac{1}{k_b^2} \frac{df_m(t)}{dt} \frac{df_n(t')}{dt'}] H_o^{(2)}(k_b|\underline{r}-\underline{r}'|)dt'dt \tag{3-35}$$

This integral is broken up into four parts and after similar transformations as used in (3-19), one obtains

$$P_6 = \frac{k_o \eta_b}{k_b \eta_o} \{S_6(m-1, n-1, 1, 1) + S_6(m-1, n, 1, -1)$$

$$+ S_6(m, n-1, -1, 1) + S_6(m, n, -1, -1)\} \tag{3-36}$$

where the function S_6 is defined by

$$S_6(m,n,p,q) = \begin{cases} \dfrac{\gamma_m\gamma_n}{16} \displaystyle\int_{-1}^{1}\int_{-1}^{1} \left[\left(\frac{pu}{2}+\frac{1}{2}\right)\left(\frac{qu'}{2}+\frac{1}{2}\right)\hat{t}_m \cdot \hat{t}_n - \frac{p}{\gamma_m}\frac{q}{\gamma_n}\right] \\ \qquad \cdot H_o^{(2)}\left(\left|\frac{\gamma_m}{2}u\,\hat{t}_m - \frac{\gamma_n}{2}u'\hat{t}_n + k_b R_{m,n}\right|\right)du'du \\ \qquad\qquad \text{if } m \neq n \\ \dfrac{\gamma_m}{8}\displaystyle\int_{-1}^{1} \left\{\left[\left(\frac{pu}{2}+\frac{1}{2}\right)\left(\frac{qu}{2}+\frac{1}{2}\right) - \frac{pq}{\gamma_m^2}\right]\left[\alpha\left(\frac{\gamma_m}{2}(u+1)\right)\right. \right. \\ \qquad \left. + \alpha\left(\frac{\gamma_m}{2}(1-u)\right)\right] + q\left(\frac{pu}{2}+\frac{1}{2}\right)\left[\left(\frac{1}{2}-\frac{u}{2}\right)\right. \\ \qquad \left. \left. \cdot H_1^{(2)}\left(\frac{\gamma_m}{2}(1-u)\right) - \left(\frac{1}{2}+\frac{u}{2}\right)H_1^{(2)}\left(\frac{\gamma_m}{2}(1+u)\right)\right]\right\}du \\ \qquad\qquad \text{if } m = n \end{cases} \tag{3-37}$$

In the above formula for S_6, the identity (3-17) was used as well as [29, 11.3.20 and 11.3.24]

$$\int_0^z u\,H_o^{(2)}(u)du = z\,H_1^{(2)}(z) - \frac{2j}{\pi} \tag{3-38}$$

3.3. Formulas for TE Excitation Vector

The elements of the non-zero excitation vector are given by Eq. (3-14). The incident magnetic field is z directed and is adjusted so that the incident electric field is equal to unity and has zero phase at the center of aperture face Γ_1 with respect to the coordinate system in Fig. 4. Plane wave and line source excitations are considered separately. For plane wave excitation, the incident magnetic field is given by

$$H_z^i = \frac{1}{\eta_a} e^{-jk_a[x \cos \phi^i - (y - \frac{w_a}{2})\sin \phi^i]} \tag{3-39}$$

where the angle of incidence ϕ^i is measured from the negative x axis. Substitution of this into Eq. (3-14) yields

$$I_m^i = k_a \Delta C_m \frac{\eta_o k_o}{\eta_a k_a} e^{jk_a(t_m + \frac{\Delta C_m}{2} - \frac{w_a}{2})\sin \phi^i} \frac{\sin(\frac{k_a \Delta C_m}{2} \sin \phi^i)}{(\frac{k_a \Delta C_m}{2} \sin \phi^i)} \tag{3-40}$$

If a magnetic line source of strength K^i volts is placed at the coordinates (x_s, y_s) in region a then the incident magnetic field at the point (x,y) is given by

$$H_z^i = \frac{j}{\eta_a} \frac{H_o^{(2)}(k_a\sqrt{(x - x_s)^2 + (y - y_s)^2})}{H_1^{(2)}(k_a\sqrt{x_s^2 + (\frac{w_a}{2} - y_s)^2})} \tag{3-41}$$

where K^i has been adjusted to

$$K^i = - \frac{4j}{k_a H_1^{(2)}(k_a\sqrt{x_s^2 + (\frac{w_a}{2} - y_s)^2})} \tag{3-42}$$

Substitution of Eq. (3-41) into (3-14) yields

$$I_m^i = j \frac{k_o \eta_o}{k_a \eta_a} \frac{k_a \Delta C_m}{2} \int_{-1}^{1} \frac{H_o^{(2)}(k_a\sqrt{x_s^2 + (\frac{\Delta C_m}{2} u + t_m + \frac{\Delta C_m}{2} - y_s)^2}) \, du}{H_1^{(2)}(k_a\sqrt{x_s^2 + (\frac{w_a}{2} - y_s)^2})} \tag{3-43}$$

Chapter 4

TRANSVERSE MAGNETIC (TM) CASE

4.1. Expansion of the Equivalent Currents

For the TM polarization, there is only a z component of electric field and transverse components of magnetic field. The equivalent magnetic currents are transverse directed and must satisfy the boundary condition that they are zero at the ends of Γ_1 and Γ_3. The equivalent electric currents are z directed and satisfy no boundary conditions on the contour C. In fact, it is expected that $\underline{J}^b$ becomes unbounded at the ends of Γ_2 and Γ_4 when region b is lossless since it is the actual electric current induced on these surfaces in the original problem. With this in mind, the functions of Eq. (2-10) are chosen for the $\underline{\alpha}_1$ and $\underline{\alpha}_3$ of (2-13) and (2-14) while the functions of Eq. (2-11) are chosen for $\underline{\beta}$ of (2-15). The unknown currents are thus expanded as

$$\underline{M}^1 = \sum_{n=2}^{N_2-1} V_n^1 \, \underline{f}_n(t) \tag{4-1}$$

$$\underline{M}^3 = \sum_{n=N_3+1}^{N_4-1} V_n^3 \, \underline{f}_n(t) \tag{4-2}$$

$$\underline{J}^b = \sum_{n=1}^{N_5-1} I_n \, \underline{g}_n(t) \tag{4-3}$$

The formulas for the matrix elements of Eqs. (2-16) and (2-17) are obtainable from Eqs. (2-18)-(2-28). They are given as follows where the ranges of the indices m and n are now specified:

$$Y^a_{mn} = - k_o \eta_o \langle \underline{f}_m, \underline{L}^{ha}_t(\underline{0}, \underline{f}_n) \rangle \qquad \begin{matrix} 2 \le m \le N_2-1 \\ 2 \le n \le N_2-1 \end{matrix} \qquad (4\text{-}4)$$

$$Y^c_{mn} = - k_o \eta_o \langle \underline{f}_m, \underline{L}^{hc}_t(\underline{0}, \underline{f}_n) \rangle \qquad \begin{matrix} N_3 + 1 \le m \le N_4-1 \\ N_3 + 1 \le n \le N_4-1 \end{matrix} \qquad (4\text{-}5)$$

$$U^1_{mn} = - \frac{k_o}{2} \langle \underline{f}_m, \hat{n} \times \underline{g}_n \rangle \qquad \begin{matrix} 2 \le m \le N_2-1 \\ 1 \le n \le N_5-1 \end{matrix} \qquad (4\text{-}6)$$

$$U^3_{mn} = - \frac{k_o}{2} \langle \underline{f}_m, \hat{n} \times \underline{g}_n \rangle \qquad \begin{matrix} N_3 + 1 \le m \le N_4-1 \\ 1 \le n \le N_5-1 \end{matrix} \qquad (4\text{-}7)$$

$$Y^{h1}_{mn} = - k_o \eta_o \langle \underline{g}_m, \hat{n} \times \underline{L}^{hb}(0, \underline{f}_n) \rangle \qquad \begin{matrix} 1 \le m \le N_5-1 \\ 2 \le n \le N_2-1 \end{matrix} \qquad (4\text{-}8)$$

$$Y^{h3}_{mn} = - k_o \eta_o \langle \underline{g}_m, \hat{n} \times \underline{L}^{hb}(\underline{0}, \underline{f}_n) \rangle \qquad \begin{matrix} 1 \le m \le N_5-1 \\ N_3 + 1 \le n \le N_4-1 \end{matrix} \qquad (4\text{-}9)$$

$$T^h_{mn} = - k_o \langle \underline{g}_m, \hat{n} \times \underline{L}^{hb}(\underline{g}_n, \underline{0}) \rangle \qquad \begin{matrix} 1 \le m \le N_5-1 \\ 1 \le n \le N_5-1 \end{matrix} \qquad (4\text{-}10)$$

$$Y^{e1}_{mn} = - k_o \langle \underline{g}_m, \underline{L}^{eb}_t(\underline{0}, \underline{f}_n) \rangle \qquad \begin{matrix} 1 \le m \le N_5-1 \\ 2 \le n \le N_2-1 \end{matrix} \qquad (4\text{-}11)$$

$$Y^{e3}_{mn} = - k_o \langle \underline{g}_m, \underline{L}^{eb}_t(\underline{0}, \underline{f}_n) \rangle \qquad \begin{matrix} 1 \le m \le N_5-1 \\ N_3 + 1 \le n \le N_4-1 \end{matrix} \qquad (4\text{-}12)$$

$$T^e_{mn} = - \frac{k_o}{\eta_o} \langle \underline{g}_m, \underline{L}^{eb}_t(\underline{g}_n, \underline{0}) \rangle \qquad \begin{matrix} 1 \le m \le N_5-1 \\ 1 \le n \le N_5-1 \end{matrix} \qquad (4\text{-}13)$$

The non-zero elements of the excitation vector are given by

$$I_m^i = k_o \eta_o \langle \underline{f}_m, \underline{H}_t^i \rangle \qquad 2 \leq m \leq N_2 - 1 \tag{4-14}$$

4.2. Formulas for TM Matrix Elements

Equations (4-4) - (4-13) define the elements of the matrices in Eqs. (2-16) and (2-17). Explicit formulas will be derived here for these symmetric products using the definitions of the operators given by Eqs. (2-2) and (2-6) and the expansion functions (2-10) and (2-11).

For Eqs. (4-4) and (4-5) it is necessary to know the magnetic field due to a transverse directed magnetic current. This is obtained by duality from the electric field due to a transverse electric current which was used in Eq. (3-13) for the TE case. Thus one may write

$$\begin{aligned} Q_1 &= - k_o \eta_o \langle \underline{f}_m, \underline{L}_t^{ha}(\underline{0}, \underline{f}_n) \rangle \\ &= \frac{k_o \eta_o}{k_a \eta_a} \{ S_6(m-1, n-1, 1, 1) + S_6(m-1, n, 1, -1) \\ &\qquad + S_6(m, n-1, -1, 1) + S_6(m, n, -1, -1) \} \end{aligned} \tag{4-15}$$

where the function S_6 is defined in Eq. (3-37) and k_a replaces k_b.

Equations (4-6) and (4-7) are straightforward and one may easily write

$$Q_2 = -\frac{k_o}{2} \langle \underline{f}_m, \hat{n} \times \underline{g}_n \rangle$$

$$= \begin{cases} -\frac{k_o \Delta C_n}{4} & \text{for } m-1 = n \text{ or } m = n \\ 0 & \text{for } m \text{ otherwise} \end{cases} \qquad (4\text{-}16)$$

Equations (4-8) and (4-9) require the magnetic field due to a transverse directed magnetic current. Thus the inner product is written as

$$Q_3 = -k_o \eta_o \langle \underline{g}_m, \hat{n} \times \underline{L}^{hb}(0, \underline{f}_n) \rangle$$

$$= \frac{k_b k_o \eta_o}{4\eta_b} \int_{t_m}^{t_{m+1}} \underline{g}_m \cdot \hat{n} \times \int_{t_{n-1}}^{t_{n+1}} \underline{f}_n(t') H_o^{(2)}(k_b |\underline{r}-\underline{r}'|) dt' dt$$

$$+ \frac{k_o \eta_o}{4 k_b \eta_b} \int_{t_m}^{t_{m+1}} \underline{g}_m \cdot \hat{n} \times \nabla \nabla \cdot \int_{t_{n-1}}^{t_{n+1}} \underline{f}_n(t') H_o^{(2)}(k_b |\underline{r}-\underline{r}'|) dt' dt \qquad (4\text{-}17)$$

where $\underline{r}$ is a vector from the origin to a point on ΔC_m and $\underline{r}'$ is a vector from the origin to a point on $\Delta C_{n-1} \cup \Delta C_n$. After some manipulation, one may write the above in the form

$$Q_3 = \frac{k_o \eta_o}{k_b \eta_b} \sum_{i=1}^{6} S_i \qquad (4\text{-}18)$$

where each S_i is defined by

$$S_1 = \begin{cases} -\frac{\gamma_m\gamma_{n-1}}{16}\int_{-1}^{1}\int_{-1}^{1}(\hat{t}_m\cdot\hat{t}_{n-1})(\frac{u'}{2}+\frac{1}{2})H_o^{(2)}(|k_{b\underline{R}_{m,n-1}}+\frac{\gamma_m}{2}u\,\hat{t}_m \\ \qquad -\frac{\gamma_{n-1}}{2}u'\,\hat{t}_{n-1}|)du'du \\ \qquad\qquad \text{if } m\neq n-1 \\ -\frac{\gamma_m}{8}\int_{-1}^{1}\{(\frac{u}{2}+\frac{1}{2})[\alpha(\frac{\gamma_m}{2}(u+1))+\alpha(\frac{\gamma_m}{2}(1-u))] \\ \qquad +(\frac{1}{2}-\frac{u}{2})H_1^{(2)}(\frac{\gamma_m}{2}(1-u))-(\frac{1}{2}+\frac{u}{2})H_1^{(2)}(\frac{\gamma_m}{2}(1+u))\}du \\ \qquad\qquad \text{if } m=n-1 \end{cases} \tag{4-19}$$

$$S_2 = \begin{cases} -\frac{\gamma_m\gamma_n}{16}\int_{-1}^{1}\int_{-1}^{1}(\hat{t}_m\cdot\hat{t}_n)(-\frac{u'}{2}+\frac{1}{2})H_o^{(2)}(|k_{b\underline{R}_{m,n}}+\frac{\gamma_m}{2}u\,\hat{t}_m \\ \qquad -\frac{\gamma_n}{2}u'\,\hat{t}_n|)du'du \\ \qquad\qquad \text{if } m\neq n \\ -\frac{\gamma_m}{8}\int_{-1}^{1}\{(-\frac{u}{2}+\frac{1}{2})[\alpha(\frac{\gamma_m}{2}(1+u))+\alpha(\frac{\gamma_m}{2}(1-u))] \\ \qquad +(\frac{1}{2}+\frac{u}{2})H_1^{(2)}(\frac{\gamma_m}{2}(1+u))-(\frac{1}{2}-\frac{u}{2})H_1^{(2)}(\frac{\gamma_m}{2}(1-u))\}du \\ \qquad\qquad \text{if } m=n \end{cases} \tag{4-20}$$

$$S_3 = \begin{cases} \frac{1}{8}\int_{-1}^{1}H_o^{(2)}(|k_{b\underline{R}_{m,n-1}}+\frac{\gamma_m}{2}\hat{t}_m-\frac{\gamma_{n-1}}{2}u'\,\hat{t}_{n-1}|)du' \\ \qquad\qquad \text{if } m\neq n-1 \text{ or } n-2 \\ \frac{1}{4\gamma_{n-1}}\alpha(\gamma_{n-1}) \qquad \text{if } m=n-1 \text{ or } n-2 \end{cases} \tag{4-21}$$

$$S_4 = \begin{cases} -\frac{1}{8}\int_{-1}^{1} H_o^{(2)}(|k_b \underline{R}_{m,n-1} - \frac{\gamma_m}{2}\hat{\underline{t}}_m - \frac{\gamma_{n-1}}{2} u' \hat{\underline{t}}_{n-1}|)du' & \text{if } m \neq n \text{ or } n-1 \\ -\frac{1}{4\gamma_{n-1}}\alpha(\gamma_{n-1}) & \text{if } m = n \text{ or } n-1 \end{cases} \quad (4\text{-}22)$$

$$S_5 = \begin{cases} -\frac{1}{8}\int_{-1}^{1} H_o^{(2)}(|k_b \underline{R}_{m,n} + \frac{\gamma_m}{2}\hat{\underline{t}}_m - \frac{\gamma_n}{2} u' \hat{\underline{t}}_n|)du' & \text{if } m \neq n \text{ or } n-1 \\ -\frac{1}{4\gamma_n}\alpha(\gamma_n) & \text{if } m = n \text{ or } n-1 \end{cases} \quad (4\text{-}23)$$

$$S_6 = \begin{cases} \frac{1}{8}\int_{-1}^{1} H_o^{(2)}(|k_b \underline{R}_{m,n} - \frac{\gamma_m}{2}\hat{\underline{t}}_m - \frac{\gamma_n}{2} u' \hat{\underline{t}}_n|)du' & \text{if } m \neq n \text{ or } n+1 \\ \frac{1}{4\gamma_n}\alpha(\gamma_n) & \text{if } m = n \text{ or } n+1 \end{cases} \quad (4\text{-}24)$$

In the above, $\gamma_m = k_b \Delta C_m$.

For Eq. (4-10), the magnetic field due to a z directed electric current is necessary and one obtains

$$Q_4 = - k_o \langle \underline{g}_m, \hat{n} \times \underline{L}^{hb}(\underline{g}_n, \underline{0}) \rangle$$

$$= - k_o \int_{t_m}^{t_{m+1}} \frac{1}{2} \underline{g}_m \cdot \underline{g}_n \, dt$$

$$- \frac{k_o k_b}{4j} \int_{t_m}^{t_{m+1}} \underline{g}_m \cdot \int_{t_n}^{t_{n+1}} \hat{n} \times \underline{g}_n \times \frac{(\underline{r}-\underline{r}')}{|\underline{r}-\underline{r}'|} H_1^{(2)}(k_b|\underline{r}-\underline{r}'|) dt' dt \qquad (4\text{-}25)$$

where $\underline{r}$ and $\underline{r}'$ are vectors from the origin to points on ΔC_m and ΔC_n respectively. The above is written in the form

$$Q_4 = \begin{cases} - \frac{k_o}{2} \Delta C_m & \text{if } m = n \\ - \frac{k_o}{k_b} \frac{1}{4j} \frac{\gamma_m \gamma_n}{4} \int_{-1}^{1} \int_{-1}^{1} \frac{\hat{n} \cdot \hat{R}_{m,n}}{|\hat{R}_{m,n}|} H_1^{(2)}(|\hat{R}_{m,n}|) du' du & \text{if } m \neq n \end{cases} \qquad (4\text{-}26)$$

where $\gamma_m = k_b \Delta C_m$ and $\hat{R}_{m,n}$ is defined by Eq. (3-27).

For Eqs. (4-11) and (4-12) it is necessary to know the electric field due to a transverse magnetic current. Thus

$$Q_5 = - k_o \langle \underline{g}_m, \underline{L}_t^{eb}(\underline{0}, \underline{f}_n) \rangle$$

$$= - \frac{k_o}{2} \int_{t_m}^{t_{m+1}} \underline{g}_m \cdot \hat{n} \times \underline{f}_n \, dt$$

$$- \frac{k_o}{4j} \int_{t_m}^{t_{m+1}} \underline{g}_m(t) \cdot \hat{n} \times \int_{t_{n-1}}^{t_{n+1}} \hat{n} \times \underline{f}_n(t') \times \nabla H_o^{(2)}(k_b|\underline{r}-\underline{r}'|) dt' dt \qquad (4\text{-}27)$$

where $\underline{r}$ is a vector from the origin to a point on ΔC_m and $\underline{r}'$ is a vector from the origin to a point on $\Delta C_{n-1} \cup \Delta C_n$. This equation is very similar to Eq. (3-29) and after some manipulation, one obtains

$$Q_5 = \frac{k_o}{k_b} (S_1 + S_2) \tag{4-28}$$

where S_1 and S_2 are defined by

$$S_1 = \begin{cases} \dfrac{\gamma_m}{4} & \text{if } m = n-1 \\ \dfrac{1}{4j} \dfrac{\gamma_m \gamma_{n-1}}{4} \displaystyle\int_{-1}^{1} \int_{-1}^{1} \left(\frac{u'}{2} + \frac{1}{2}\right) \phi(m,n-1)du'du & \text{if } m \neq n-1 \end{cases} \tag{4-29}$$

$$S_2 = \begin{cases} \dfrac{\gamma_m}{4} & \text{if } m = n \\ \dfrac{1}{4j} \dfrac{\gamma_m \gamma_n}{4} \displaystyle\int_{-1}^{1} \int_{-1}^{1} \left(-\frac{u'}{2} + \frac{1}{2}\right) \phi(m,n)du'du & \text{if } m \neq n \end{cases} \tag{4-30}$$

and $\phi(m,n)$ is defined in Eq. (3-26). In the above, $\gamma_m = k_b \Delta C_m$.

Lastly, for Eq. (4-13), it is necessary to have the electric field due to a z directed electric current. This is found simply from the magnetic field due to a z directed magnetic current used in Eq. (3-15). Hence one easily obtains

$$\begin{aligned} Q_6 &= -\frac{k_o}{\eta_o} \langle \underline{g}_m, \underline{L}_t^{eb}(\underline{g}_n, \underline{0}) \rangle \\ &= \frac{1}{\eta_o^2} P_1 \end{aligned} \tag{4-31}$$

where P_1 is defined by Eq. (3-16).

4.3. Formulas for TM Excitation Vector

The elements of the non-zero excitation vector are given by Eq. (4-14). The incident electric field is z directed and is adjusted so that it is equal to unity and has zero phase at the center of aperture face Γ_1 with respect to the coordinate system in Fig. 4. Plane wave and line source excitations are considered separately.

For plane wave excitation, the incident magnetic field has a component tangential to Γ_1 given by

$$H_y^i = -\frac{\cos\phi^i}{\eta_a} e^{-jk_a[x\cos\phi^i - (y - \frac{w_a}{2})\sin\phi^i]} \tag{4-32}$$

where the angle of incidence ϕ^i is measured from the negative x axis. Substituting this into Eq. (4-18), one obtains

$$I_m^i = -\frac{k_o\eta_o}{k_a\eta_a}\frac{\cos\phi^i}{j\sin\phi^i} e^{jk_a(t_m - \frac{w_a}{2})\sin\phi^i} \left[\frac{e^{-jk_a\Delta C_{m-1}\sin\phi^i} - 1}{jk_a\Delta C_{m-1}\sin\phi^i}\right.$$

$$\left. + \frac{e^{jk_a\Delta C_m\sin\phi^i} - 1}{jk_a\Delta C_m\sin\phi^i}\right] \tag{4-33}$$

If an electric line source of strength I^i amps is placed at the coordinates (x_s, y_s) in region a, then the tangential component of magnetic field at Γ_1 is given by

$$H_y^i = \frac{x_s H_1^{(2)}(k_a\sqrt{x_s^2 + (y - y_s)^2})}{j\eta_a\sqrt{x_s^2 + (y - y_s)^2}\; H_o^{(2)}(k_a\sqrt{x_s^2 + (\frac{w_a}{2} - y_s)^2})} \tag{4-34}$$

where I^i has been adjusted to

$$I^i = \frac{-4}{k_a \eta_a H_o^{(2)}\left(k_a \sqrt{x_s^2 + \left(\frac{w_a}{2}\right)^2}\right)} \tag{4-35}$$

Substituting Eq. (4-34) into (4-14), one obtains

$$I_m^i = \frac{k_o \eta_o}{k_a \eta_a} \frac{x_s}{jH_o^{(2)}\left(k_a \sqrt{x_s^2 + \left(\frac{w_a}{2} - y_s\right)^2}\right)}$$

$$\cdot \left\{ \frac{k_a \Delta C_{m-1}}{2} \int_{-1}^{1} \frac{\left(\frac{v}{2} + \frac{1}{2}\right) H_1^{(2)}\left(k_a \sqrt{x_s^2 + \left(\frac{\Delta C_{m-1}}{2}(v+1) + t_{m-1} - y_s\right)^2}\right)}{\sqrt{x_s^2 + \left(\frac{\Delta C_{m-1}}{2}(v+1) + t_{m-1} - y_s\right)^2}} dv \right.$$

$$\left. + \frac{k_a \Delta C_m}{2} \int_{-1}^{1} \frac{\left(-\frac{v}{2} + \frac{1}{2}\right) H_1^{(2)}\left(k_a \sqrt{x_s^2 + \left(\frac{\Delta C_m}{2}(v+1) + t_m - y_s\right)^2}\right)}{\sqrt{x_s^2 + \left(\frac{\Delta C_m}{2}(v+1) + t_m - y_s\right)^2}} dv \right\} \tag{4-36}$$

Chapter 5

MEASURED QUANTITIES

Once the magnetic currents on the aperture faces are determined, several transmission characteristics of the slit may then be computed. In each following section, the TE case is treated first, followed by the TM case.

5.1. Measurement Vector

For the TE case the magnetic current sheet at Γ_3 is z directed, hence, to measure the magnetic field $\underline{H}^c$ at a point in region c as shown in Fig. 7, a magnetic line source $K^\ell \hat{\underline{z}}$ is placed at the measurement point. From reciprocity one obtains

$$\underline{H}^c \cdot K^\ell \hat{\underline{z}} = \int_{\Gamma_3} \underline{H}^\ell \cdot \underline{M}^3 \, dy \tag{5-1}$$

where $\underline{H}^\ell$ is the magnetic field due to $K^\ell \hat{\underline{z}}$ radiating in the presence of a complete conductor and $\underline{H}^c$ is the magnetic field of currents $\underline{M}^3$ radiating in the presence of a complete conductor. After using Eq. (3-2) for $\underline{M}^3$, Eq. (5-1) becomes

$$\begin{aligned} H_z^c K^\ell &= \int_{\Gamma_3} \sum_{n=N_3}^{N_4-1} V_n^3 \, \underline{g}_n(t) \cdot \underline{H}^\ell dt \\ &= -\frac{K^\ell k_c}{2\eta_c} \sum_{n=N_3}^{N_4-1} V_n^3 \int_{-\frac{w_c}{2}}^{\frac{w_c}{2}} g_n(y) H_o^{(2)}(k_c |y\hat{\underline{y}} - \underline{r}_m|) dy \end{aligned} \tag{5-2}$$

Here the coordinate origin is now in the center of Γ_3 and the above equation may be written in matrix form as

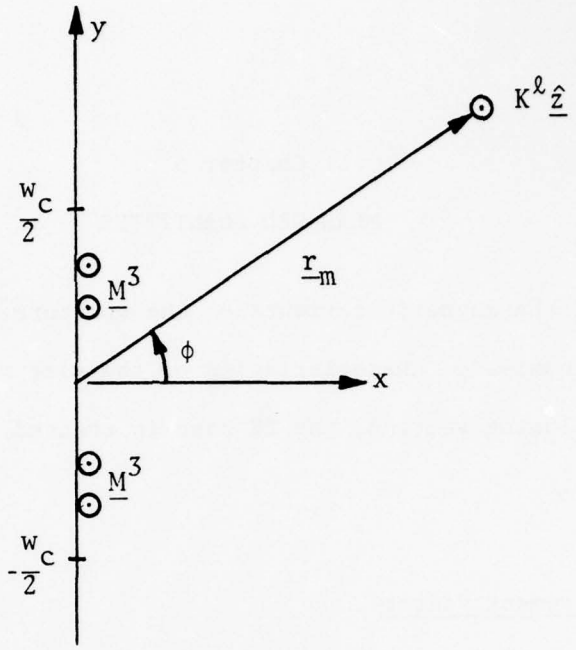

Fig. 7. Measurement of $\underline{H}^c$ at $\underline{r}_m$, TE case.

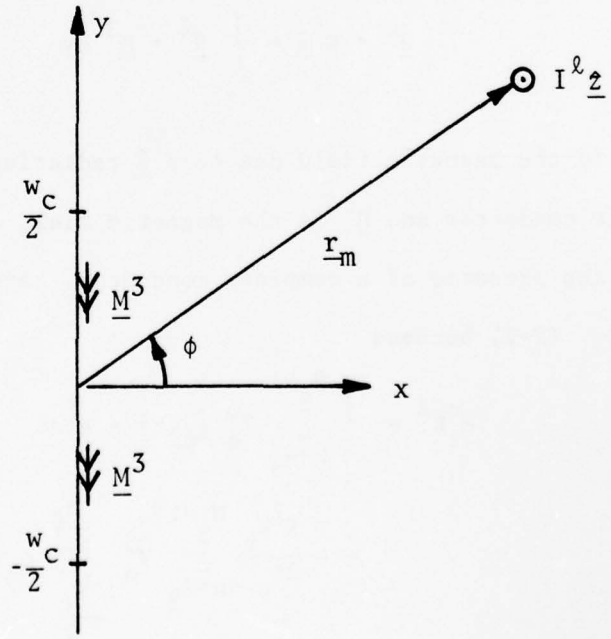

Fig. 8. Measurement of $\underline{H}^c$ at $\underline{r}_m$, TM case.

$$H_z^c = \frac{1}{\eta_c}\sqrt{\frac{jk_c}{2\pi r_m}}\; e^{-jk_c r_m}\; \tilde{\vec{I}}^e\, \vec{V}^3 \tag{5-3}$$

where the tilde (~) denotes transpose and $\vec{I}^e$ is a TE measurement vector whose elements are defined as

$$I_n^e = -\sqrt{\frac{\pi k_c r_m}{2j}}\, e^{jk_c r_m} \int_{-\frac{w_c}{2}}^{\frac{w_c}{2}} g_n(y) H_o^{(2)}(k_c|y\hat{y} - \underline{r}_m|)dy \tag{5-4}$$

for $n = N_3, N_3+1, \ldots, N_4-1$. If $r_m >> \lambda_c$ so that far-field measurements are of interest, the large argument approximation to the Hankel function is used in Eq. (5-4) to obtain

$$\begin{aligned} I_n^{ef} &= -\int_{-w_c/2}^{w_c/2} g_n(y) e^{jk_c y \sin\phi}\, dy \\ &= -\Delta C_n\, e^{jk_c(h_n + \frac{\Delta C_n}{2})\sin\phi}\, \frac{\sin\left(\frac{k_c \Delta C_n}{2}\sin\phi\right)}{\left(\frac{k_c \Delta C_n}{2}\sin\phi\right)} \end{aligned} \tag{5-5}$$

where $h_n = \frac{w_c}{2} - \sum_{i=N_3}^{n} \Delta C_i$ for $n = N_3, N_3+1, \ldots, N_4-1$. This can be conveniently written in terms of the excitation vector of Eq. (3-40).

For the TM case, the magnetic current sheet at Γ_3 is y directed, hence the electric field $\underline{E}^c$ in region c is measured by placing an electric line source $I^{\ell}\hat{\underline{z}}$ at the measurement point as shown in Fig. 8. Again from reciprocity, one obtains

$$\underline{E}^c \cdot I^{\ell}\hat{\underline{z}} = \int_{\Gamma_3} \underline{H}^{\ell} \cdot \underline{M}^3\, dy \tag{5-6}$$

Equation (4-2) is substituted for $\underline{M}^3$ and the above is rewritten as

$$E_z^c I^\ell = \int_{\Gamma_3} \sum_{n=N_3+1}^{N_4-1} V_n^3 \underline{f}_n(t) \cdot \underline{H}^\ell dt \tag{5-7}$$

where use has been made of the fact that $\underline{f}_n(t)$ on Γ_3 is $-\hat{\underline{y}}$ directed. Using the y component of $\underline{H}^\ell$ in the above, one obtains

$$E_z^c I^\ell = -\frac{k_c I^\ell}{2j} x_m \sum_{n=N_3+1}^{N_4-1} V_n^3 \int_{-\frac{w_c}{2}}^{\frac{w_c}{2}} f_n(y) \frac{H_1^{(2)}(k_c|y\hat{\underline{y}} - \underline{r}_m|)dy}{\sqrt{x_m^2 + (y - y_m)^2}} \tag{5-8}$$

where $\underline{r}_m = x_m \hat{\underline{x}} + y_m \hat{\underline{y}}$. An expression for E_z^c may now be written in matrix form as

$$E_z^c = \sqrt{\frac{jk_c}{2\pi r_m}}\, e^{-jk_c r_m}\, \tilde{\vec{I}}^m\, \vec{V}^3 \tag{5-9}$$

where $\vec{I}^m$ is the TM measurement vector whose elements are given by

$$I_n^m = -\frac{x_m}{j}\sqrt{\frac{\pi k_c r_m}{2j}}\, e^{jk_c r_m} \int_{-\frac{w_c}{2}}^{\frac{w_c}{2}} f_n(y) \frac{H_1^{(2)}(k_c|y\hat{\underline{y}} - \underline{r}_m|)dy}{\sqrt{x_m^2 + (y - y_m)^2}} \tag{5-10}$$

for $n = N_3+1, N_3+2, \ldots, N_4-1$. If $r_m >> \lambda_c$ for far field measurements, Eq. (5-10) becomes

$$I_n^{mf} = \mp \cos\phi \int_{-\frac{w_c}{2}}^{\frac{w_c}{2}} f_n(y)\, e^{jk_c y \sin\phi}\, dy$$

$$= \cos\phi \frac{2\Delta C_n\, e^{jk_c(h_n - \frac{\Delta C_n}{2})\sin\phi}}{j(k_c \Delta C_n \sin\phi)^2} \sin\left(\frac{k_c \Delta C_n}{2} \sin\phi\right)$$

$$- \cos\phi \frac{2\Delta C_{n-1}\, e^{jk_c(h_n + \frac{\Delta C_{n-1}}{2})\sin\phi}}{j(k_c \Delta C_{n-1} \sin\phi)^2} \sin\left(\frac{k_c \Delta C_{n-1}}{2} \sin\phi\right) \qquad (5\text{-}11)$$

where $h_n = \frac{w_c}{2} - \sum_{i=N_3+1}^{n} \Delta C_{i-1}$ for $n=N_3+1,\ N_3+2,\ldots,N_4-1$. If each $\Delta C_n = \Delta C$ on Γ_3, then (5-11) becomes

$$I_n^{mf} = -\cos\phi\, \Delta C\, e^{jk_c h_n \sin\phi} \left[\frac{\sin\left(\frac{k_c \Delta C}{2} \sin\phi\right)}{\left(\frac{k_c \Delta C \sin\phi}{2}\right)}\right]^2 \qquad (5\text{-}12)$$

5.2. Transmission Coefficient

The transmission coefficient of the slit is defined by the ratio

$$T = \frac{P_{t3}}{P_{iN}} \qquad (5\text{-}13)$$

where P_{t3} is the time average power transmitted through the aperture face Γ_3 and P_{iN} is the time average power intercepted by the aperture face Γ_1 when the source is normally incident. If the time average power transmitted through aperture face Γ_1 is denoted by P_{t1}, then when the slit

is filled with a lossless medium, P_{t1} must equal P_{t3}. This may be used as a check on the numerical solution when the imaginary parts of the complex power through Γ_1 and Γ_3 are not significantly different.

Consider the TE case first. A magnetic line source is placed at $(x_s, \frac{w_a}{2})$ in region a to produce an incident field. The slit intercepts a fraction of the incident power. This fraction is given by

$$P_{iN} = (\frac{\theta}{2\pi}) \frac{k_a}{4\eta_a} |K^i|^2 = \frac{\theta k_a}{8\pi\eta_a} |K^i|^2 \tag{5-14}$$

where $\theta = 2 \tan^{-1} (\frac{w_a}{2x_s})$ and K^i is the strength of the magnetic line source. A normally incident plane wave in region a produces an intercepted time average power given by ($|E^i| = 1$ volt/meter)

$$P_{iN} = w_a \eta_a |H_z^i|^2 = \frac{w_a}{\eta_a} \tag{5-15}$$

To compute the time average power into region c, the real part of the Poynting vector flux at Γ_3 is integrated along Γ_3. This gives the formula

$$P_{t3} = \frac{2}{k_o \eta_o} \tilde{\vec{V}}^3 [Y^c]^* \vec{V}^3 \tag{5-16}$$

This is the usual equation for power flow into a network represented by an admittance matrix $[2Y^c]$ except for the factor of $1/k_o\eta_o$. This factor appears because of the factor $- k_o\eta_o$ in Eq. (2-19). Another method for finding P_{t3} is to integrate the Poynting vector flux over the far field in region c. This gives

$$P_{t3} = \mathrm{Re} \int_{-\pi/2}^{\pi/2} E^c \times H^{c*} \cdot \hat{\underline{r}}\, r d\phi$$

$$= \frac{k_c}{\eta_c 2\pi} \int_{-\pi/2}^{\pi/2} \left| \tilde{\vec{I}}^{ef} \vec{V}^3 \right|^2 d\phi \qquad (5\text{-}17)$$

For the TM case, an electric line source is placed at $(x_s, \frac{w_a}{2})$ in region a. The fraction of the time average power intercepted by the slit is given by

$$P_{iN} = \left(\frac{\theta}{2\pi}\right) \frac{k_a \eta_a}{4} |I^i|^2 = \frac{\theta k_a \eta_a}{8\pi} |I^i|^2 \qquad (5\text{-}18)$$

where I^i is the strength of the electric line source and θ is the same as before. A normally incident plane wave gives

$$P_{iN} = \frac{w_a}{\eta_a} |E_z^i|^2 = \frac{w_a}{\eta_a} \qquad (5\text{-}19)$$

The time average power P_{t3} for the TM case is given by Eqs. (5-16) and (5-17) but with TM quantities used.

5.3. Power Gain and Normalized Field Pattern

The power gain function is defined as the ratio of the radiation intensity in a given direction to the radiation intensity which would exist if the transmitted power were to radiate uniformly over half space. This gives, for the TE case

$$G(\phi) = \lim_{r_m \to \infty} \frac{\pi r_m \eta_c |H_z^c|^2}{P_t} = \frac{k_c}{2\eta_c P_t} \left| \tilde{\vec{I}}^{ef} \vec{V}^3 \right|^2 \qquad (5\text{-}20)$$

and for the TM case,

$$G(\phi) = \lim_{r_m \to \infty} \frac{\pi r_m}{\eta_c P_t} |E_z^c|^2 = \frac{k_c}{2\eta_c P_t} |\tilde{\vec{I}}^{mf} \vec{V}^3|^2 \qquad (5\text{-}21)$$

If the medium in region c is lossy, the term "radiation intensity" does not apply. Here it is desirable to define a directive gain as the ratio of the time average power density produced at a certain range in a certain direction to the uniformly radiated time average power density at that range.

The normalized field pattern is another quantity of interest and is computed in the far field by

$$F^e(\phi) = \frac{|H_z^c(\phi)|}{|H_z^c|_{max}} = \frac{|\tilde{\vec{I}}^{ef} \vec{V}^3|}{|\tilde{\vec{I}}^{ef} \vec{V}^3|_{max}} \qquad (5\text{-}22)$$

for the TE case, and by

$$F^m(\phi) = \frac{|E_z^c(\phi)|}{|E_z^c|_{max}} = \frac{|\tilde{\vec{I}}^{mf} \vec{V}^3|}{|\tilde{\vec{I}}^{mf} \vec{V}^3|_{max}} \qquad (5\text{-}23)$$

for the TM case. The denominator denotes the maximum value of field magnitude measured in region c.

5.4. Slit Impedance and Polarizability

Since the fields in region c arise from a magnetic current $\underline{M}^3$ radiating in the presence of a complete conductor at x = d, the magnetic vector potential for these fields may be written as

$$\underline{F} = \frac{1}{2j} \int_{-\frac{w_c}{2}}^{\frac{w_c}{2}} \underline{M}^3(y') \, H_o^{(2)}(k_c|\underline{r} - y'\hat{\underline{y}}|)dy' \qquad (5\text{-}24)$$

where the coordinates of Figures 7 and 8 are used and $\underline{r}$ replaces $\underline{r}_m$ as the field point. The following assumptions are made:

a) $w_a = w_c = w$.

b) $k_c y' << 1$ for $y' \in [-\frac{w}{2}, \frac{w}{2}]$.

c) The field point $\underline{r}$ is such that $|\underline{r}| >> y'$.

d) The incident field is constant on Γ_1.

The Hankel function in Eq. (5-24) is now approximated by [24, Appendix D]

$$H_o^{(2)}(k_c|\underline{r} - y'\hat{\underline{y}}|) \to \sqrt{\frac{2j}{\pi k_c r}} \left(1 + \frac{1}{2}\frac{y'}{r}\sin\phi\right)(1 + jky'\sin\phi)e^{-jk_c r} \qquad (5\text{-}25)$$

Neglecting terms of order y'^2 and higher, one can write the magnetic vector potential as

$$\underline{F} \approx \frac{e^{-jk_c r}}{\sqrt{2\pi jk_c r}} \int_{-\frac{w}{2}}^{\frac{w}{2}} \underline{M}^3(y')dy' + \frac{jk_c e^{-jk_c r} \sin\phi}{\sqrt{2\pi jk_c r}} \int_{-\frac{w}{2}}^{\frac{w}{2}} \underline{M}^3(y')y'\left(1 + \frac{1}{2jk_c r}\right)dy' \qquad (5\text{-}26)$$

The first term in the above equation is dominant, and hence will be considered in the following discussion for each polarization.

For the TE case, the magnetic field in region c is given by

$$H_z^c = -\frac{jk_c}{\eta_c} F_z = -\frac{1}{\eta_c}\sqrt{\frac{jk_c}{2\pi r}}\, e^{-jk_c r} \int_{-\frac{w}{2}}^{\frac{w}{2}} M_z^3(y')dy' \tag{5-27}$$

A slit impedance Z is defined by the equation

$$\int_{-\frac{w}{2}}^{\frac{w}{2}} M_z^3(y')dy' = Z(H_{z1}^{isc}\, w) \tag{5-28}$$

where H_{z1}^{isc} is the short circuit incident magnetic field evaluated at the center of Γ_1. This is obtained by letting the sources in region a radiate in the presence of a complete conducting plane at x = 0. The magnetic field H_z^c is now written in the form

$$H_z^c = -\frac{Zw}{\eta_c}\sqrt{\frac{jk_c}{2\pi r}}\, e^{-jk_c r}\, H_{z1}^{isc} \tag{5-29}$$

which may be compared to the measurement vector formula given in Eq. (5-3).

For the TM case, the electric field in region c is given by

$$E_z^c = -\hat{z} \cdot \nabla \times \underline{F} \approx -\cos\phi\sqrt{\frac{jk_c}{2\pi r}}\, e^{-jk_c r} \int_{-\frac{w}{2}}^{\frac{w}{2}} M_y^3(y')dy' \tag{5-30}$$

If ρ_m is the magnetic charge density associated with the transverse directed magnetic current then

$$\int_{-\frac{w}{2}}^{\frac{w}{2}} M_y^3(y')dy' = -\int_{-\frac{w}{2}}^{\frac{w}{2}} y'(\underline{\nabla}' \cdot \underline{M}^3)dy'$$

$$= j\omega \int_{-\frac{w}{2}}^{\frac{w}{2}} y'\rho_m dy'$$

$$= j\omega\mu_c \, p_{my} \tag{5-31}$$

where the continuity equation

$$\underline{\nabla}' \cdot \underline{M}^3 = -j\omega\rho_m \tag{5-32}$$

has been used and a magnetic dipole moment $\underline{p}_m$ is defined by

$$\underline{p}_m = \frac{1}{j\omega\mu_c} \int_{-\frac{w}{2}}^{\frac{w}{2}} \underline{M}^3(y')dy' \tag{5-33}$$

A slit polarizability α_m is now defined in terms of the y component of Eq. (5-33) by the equation

$$p_{my} = \alpha_m(wH_{y1}^{isc}) \tag{5-34}$$

where again H_{y1}^{isc} is the tangential component of the short circuit incident magnetic field evaluated at the center of Γ_1. The electric field is expressed in terms of this polarizability as

$$E_z^c = \frac{k_c w\eta_c \cos\phi}{2} \sqrt{\frac{jk_c}{2\pi r}} e^{-jk_c r} \alpha_m H_{y1}^{isc} \tag{5-35}$$

which also may be compared to the measurement vector formula given by Eq. (5-9). In the preceeding discussion, Z has the dimension of ohms and α_m has the dimension of length.

Chapter 6

MODAL SOLUTION

6.1. Problem Formulation

The discussion thus far has been concerned with slits of arbitrary cross section. If the slit has a rectangular cross section, the equivalence principle may be used to break the problem up into three isolated regions [16]. The fields in region b then have a modal representation, which is not necessarily the case when the slit cross section is an arbitrary shape.

In this chapter, a special case of slit cross section is considered which allows region b to be considered as a sequence of two-dimensional rectangular cavities each coupled to another by an aperture. One such possible configuration is shown in Fig. 9. Each cavity may be filled with different material. In general, region b will consist of Q such rectangular sub-regions. The q^{th} rectangular sub-region is specified by dimensions as shown in Fig. 10. The equivalence principle is applied as in [16], so that each aperture face Γ_q, for q = 1,2,..., Q + 1, is replaced by a perfect electric conductor with a magnetic current sheet residing on each side. These magnetic current sheets are chosen to assure continuity of the tangential component of electric field at each Γ_q in the original problem.

The original problem has now been broken up into Q + 2 isolated regions, each with postulated equivalent sources. The total field in

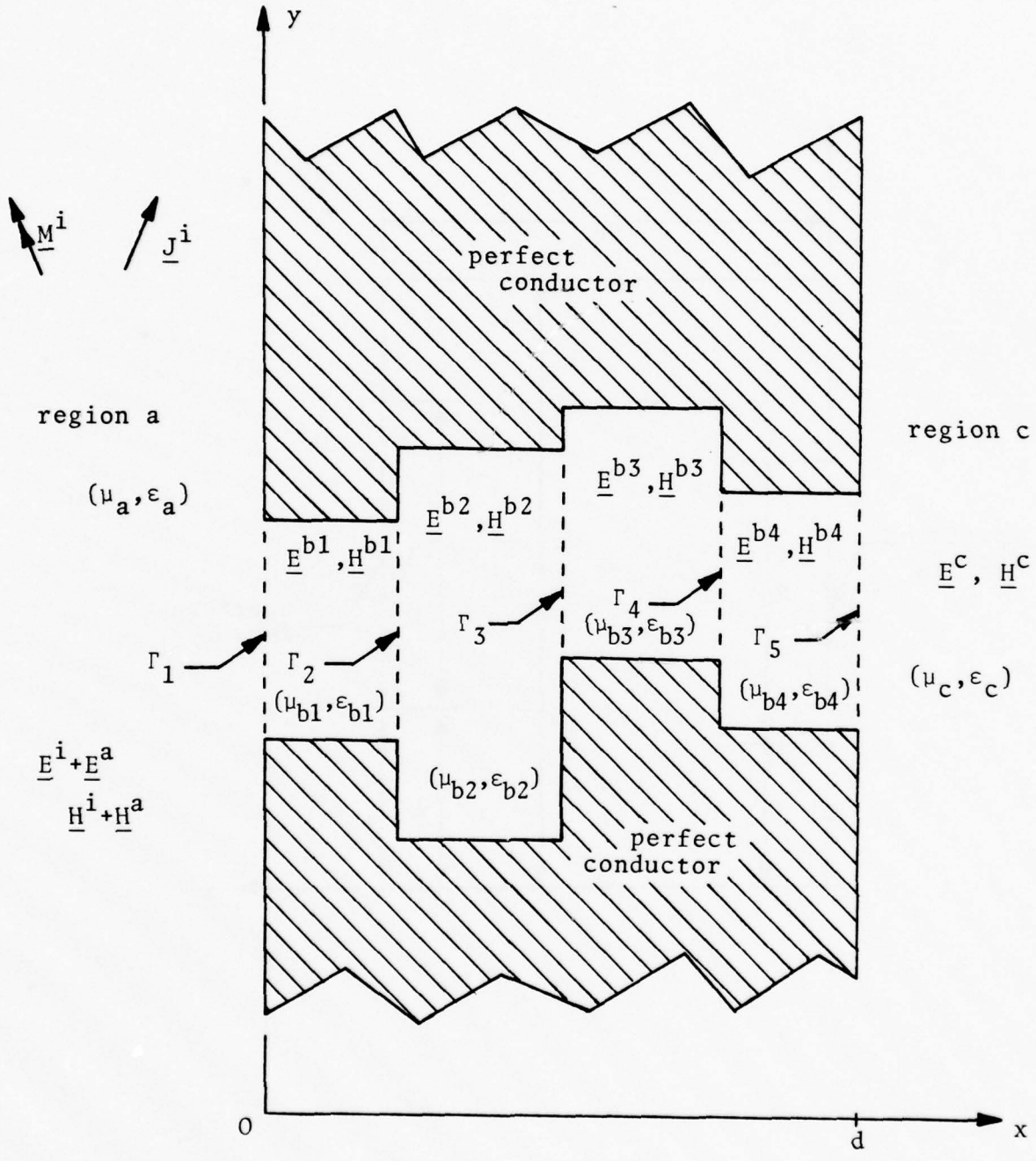

Fig. 9. The slit cross section, region b, as a sequence of two-dimensional rectangular cavities. Q = 4

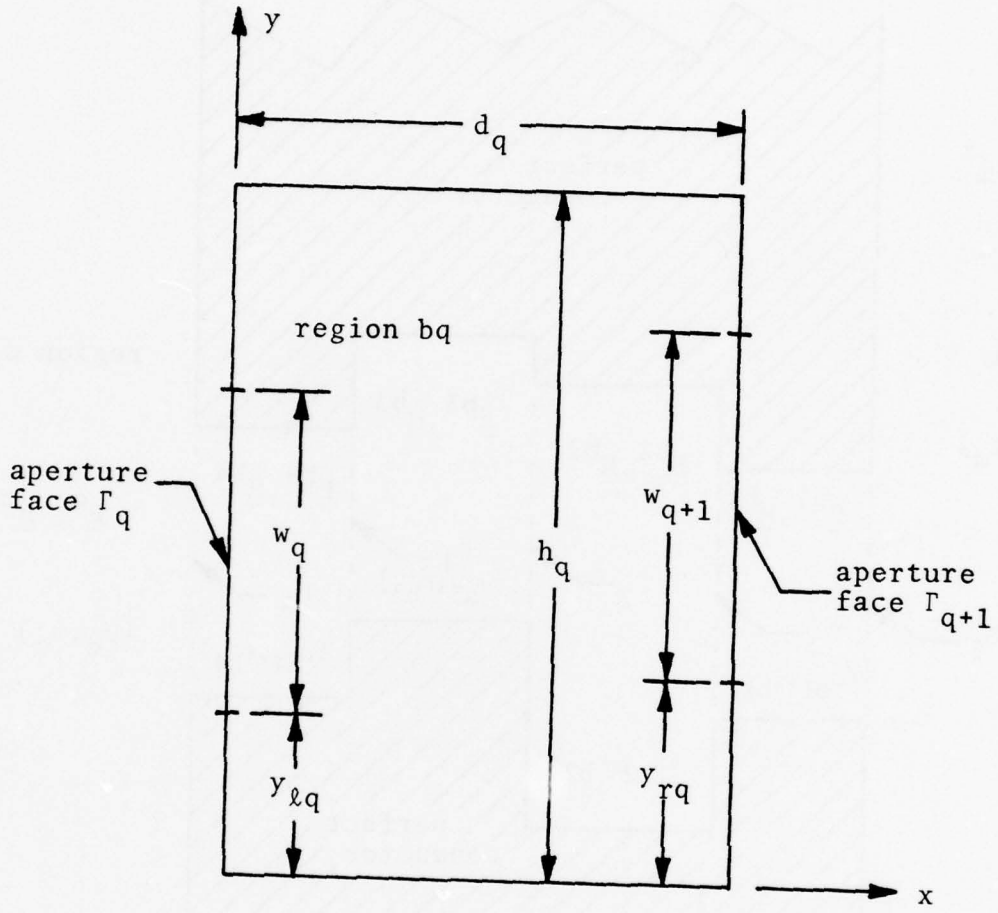

Fig. 10. The q^{th} rectangular cavity of region b.

region a is $(\underline{E}^i + \underline{E}^a, \underline{H}^i + \underline{H}^a)$, where $(\underline{E}^i, \underline{H}^i)$ is due to sources $(\underline{J}^i, \underline{M}^i)$ radiating in front of a complete conductor at x = 0 and $(\underline{E}^a, \underline{H}^a)$ is due to magnetic current sheet $\underline{M}_1$ at Γ_1 radiating in front of a complete conductor at x = 0. The magnetic current sheet $\underline{M}_1$ is given by

$$\underline{M}_1 = \hat{\underline{x}} \times \underline{E}^a \qquad \text{at } \Gamma_1 \tag{6-1}$$

The total field in each sub-region bq of region b is $(\underline{E}^{bq}, \underline{H}^{bq})$ due to magnetic currents $-\underline{M}_q$ at Γ_q and $\underline{M}_{q+1}$ at Γ_{q+1} radiating inside a closed, two-dimensional, conducting box filled with material of permeability μ_{bq} and permittivity ε_{bq}. These magnetic currents are given by

$$\underline{M}_q = \hat{\underline{x}} \times \underline{E}^{bq} \qquad \text{at } \Gamma_q \tag{6-2}$$

$$\underline{M}_{q+1} = \hat{\underline{x}} \times \underline{E}^{bq} \qquad \text{at } \Gamma_{q+1} \tag{6-3}$$

The total field in region c is $(\underline{E}^c, \underline{H}^c)$ due to the equivalent magnetic current sheet $-\underline{M}_{Q+1}$ at Γ_{Q+1} radiating in front of a complete conductor at x = d. This magnetic current sheet is given by

$$\underline{M}_{Q+1} = \hat{\underline{x}} \times \underline{E}^c \qquad \text{at } \Gamma_{Q+1} \tag{6-4}$$

The preceding equivalent magnetic current sheets must also be determined so as to assure continuity of the tangential component of magnetic field at each aperture face in the original problem. Thus the following equations are written:

$$2\underline{L}_{t1}^{ha}(\underline{0},\ \underline{M}_1) + \underline{B}_{t1}^{1h,1}(\underline{M}_1) - \underline{B}_{t1}^{1h,2}(\underline{M}_2) = -\underline{H}_{t1}^{i} \qquad \text{at } \Gamma_1$$

$$-\underline{B}_{t2}^{1h,1}(\underline{M}_1) + \underline{B}_{t2}^{1h,2}(\underline{M}_2) + \underline{B}_{t2}^{2h,2}(\underline{M}_2) - \underline{B}_{t2}^{2h,3}(\underline{M}_3) = \underline{0} \qquad \text{at } \Gamma_2$$

$$\vdots \qquad (6\text{-}5)$$

$$-\underline{B}_{tQ}^{Q-1h,Q-1}(\underline{M}_{Q-1}) + \underline{B}_{tQ}^{Q-1h,Q}(\underline{M}_Q) + \underline{B}_{tQ}^{Qh,Q}(\underline{M}_Q) - \underline{B}_{tQ}^{Qh,Q+1}(\underline{M}_{Q+1}) = \underline{0} \qquad \text{at } \Gamma_Q$$

$$-\underline{B}_{tQ+1}^{Qh,Q}(\underline{M}_Q) + \underline{B}_{tQ+1}^{Qh,Q+1}(\underline{M}_{Q+1}) + 2\underline{L}_{tQ+1}^{hc}(\underline{0},\ \underline{M}_{Q+1}) = \underline{0} \qquad \text{at } \Gamma_{Q+1}$$

The operators $\underline{L}_t^{ha}$ and $\underline{L}_t^{hc}$ are defined by Eq. (2-2) and $\underline{H}_t^i$ is the tangential component of the magnetic field due to sources $(\underline{J}^i,\ \underline{M}^i)$ radiating in the half space filled with $(\mu_a,\ \varepsilon_a)$ in the presence of a complete conductor at x = 0. The factors of 2 in Eqs. (6-5) come from the images of the magnetic current sources. The operator $\underline{B}_{tq}^{mh,n}$ gives the tangential component of magnetic field at Γ_q due to a magnetic current sheet at Γ_n radiating inside the two-dimensional cavity bm. The superscript h denotes magnetic field operator.

Using the method of moments procedure, one can reduce Eqs. (6-5) to a system of matrix equations. Each aperture face Γ_q is divided into N_q segments of constant length Δ_q. It is assumed that the equivalent magnetic current sheets may be expanded as a linear combination of basis functions defined on each domain Γ_q. This is written as

$$\underline{M}_q = \sum_{n=1}^{N_q} V_{q,n}\, \underline{e}_{q,n}(y) \qquad \text{on } \Gamma_q \tag{6-6}$$

for $q = 1,2,\ldots, Q+1$. The coefficients $V_{q,n}$ are complex scalars to be determined and the functions $\underline{e}_{q,n}$ will be specified for each polarization. The testing functions are chosen to be the same as those used for expansion and a suitable symmetric product is defined by

$$\langle \underline{A}_q, \underline{B}_q \rangle = \int_{\substack{Q \\ \cup \\ q=1}} \underline{A}_q \cdot \underline{B}_q \, dy \tag{6-7}$$

where $\underline{A}_q$ and $\underline{B}_q$ are vector functions defined on Γ_q.

Equation (6-6) is substituted into Eqs. (6-5) for the unknown magnetic currents. The symmetric product of the q^{th} equation of (6-5) is then taken with $\underline{e}_{q,m}$ for $m = 1,2,\ldots, N_q$ and $q = 1,2,\ldots, Q+1$. The result is a system of linear equations which is written in matrix form as

$$\begin{bmatrix} Y^a + Y_{11}^{b1} & Y_{12}^{b1} & & & & & 0 & & \\ Y_{21}^{b1} & Y_{22}^{b1} + Y_{11}^{b2} & Y_{12}^{b2} & & & & & & \\ & \ddots & \ddots & \ddots & & & & & \\ & & \ddots & \ddots & \ddots & & & & \\ & & & \ddots & \ddots & \ddots & & & \\ & & & & \ddots & \ddots & \ddots & & \\ & & & & & Y_{21}^{bQ-1} & Y_{22}^{bQ-1} + Y_{11}^{bQ} & Y_{12}^{bQ} & \\ & 0 & & & & & Y_{21}^{bQ} & Y_{22}^{bQ} + Y^c & \end{bmatrix} \begin{bmatrix} \vec{V}_1 \\ \vec{V}_2 \\ \vdots \\ \vdots \\ \vdots \\ \vec{V}_Q \\ \vec{V}_{Q+1} \end{bmatrix} = \begin{bmatrix} \vec{I}^i \\ \vec{0} \\ \vdots \\ \vdots \\ \vdots \\ \vec{0} \\ \vec{0} \end{bmatrix} \tag{6-8}$$

where $\vec{V}_q$ are column vectors containing the coefficients $V_{q,1}, V_{q,2}, \ldots, V_{q,N_q}$.

The matrix in Eq. (6-8) is block tridiagonal. Each submatrix has elements given by the formulas:

$$Y^a_{mn} = - k_o \eta_o \langle \underline{e}_{1,m}, 2\underline{L}^{ha}_t(\underline{0}, \underline{e}_{1,n}) \rangle \tag{6-9}$$

$$(Y^{bq}_{11})_{mn} = - k_o \eta_o \langle \underline{e}_{q,m}, \underline{B}^{qh,q}_{tq}(\underline{e}_{q,n}) \rangle \tag{6-10}$$

$$(Y^{bq}_{12})_{mn} = k_o \eta_o \langle \underline{e}_{q,m}, \underline{B}^{qh,q+1}_{tq}(\underline{e}_{q+1,n}) \rangle \tag{6-11}$$

$$(Y^{bq}_{21})_{mn} = k_o \eta_o \langle \underline{e}_{q+1,m}, \underline{B}^{qh,q}_{tq+1}(\underline{e}_{q,n}) \rangle \tag{6-12}$$

$$(Y^{bq}_{22})_{mn} = - k_o \eta_o \langle \underline{e}_{q+1,m}, \underline{B}^{qh,q+1}_{tq+1}(\underline{e}_{q+1,n}) \rangle \tag{6-13}$$

$$Y^c_{mn} = - k_o \eta_o \langle \underline{e}_{Q+1,m}, 2\underline{L}^{hc}_{tQ+1}(\underline{0}, \underline{e}_{Q+1,n}) \rangle \tag{6-14}$$

where the factor $-k_o \eta_o$ has been multiplied through Eqs. (6-5). The non-zero elements of the excitation column are given by

$$I^i_m = k_o \eta_o \langle \underline{e}_{1,m}, 2\underline{H}^i_{t1} \rangle \tag{6-15}$$

The ranges of the indices m and n are determined after the specification of the expansion functions.

The original problem may be viewed as Q+2 cascaded networks. Each network represents an isolated region and has a characteristic admittance matrix which depends only upon the properties of the region which the network represents. Due to the choice of expansion functions made in the next two sections, it will be seen that the sub-matrices of the composite matrix in Eq. (6-8) have the following properties:

1) $[Y^a]$ and $[Y^c]$ are symmetric Toeplitz matrices, hence only one column of each need be computed.

2) Y_{11}^{bq} and Y_{22}^{bq} are symmetric matrices.

3) $(Y_{12}^{bq})_{mn} = (Y_{21}^{bq})_{nm}$.

The matrix of coefficients in Eq. (6-8) is block-tridiagonal and symmetric, hence special computational and storage procedures are used.

6.2. TE Case

For this polarization, the equivalent magnetic current sheets are z directed. Thus expansion functions for the aperture faces Γ_q and Γ_{q+1} are chosen as

$$\underline{e}_{q,n}(y) = \begin{cases} 1\hat{\underline{z}} & (n-1)\,\Delta_q \leq y - y_{\ell q} \leq n\Delta_q \\ 0 & y \text{ elsewhere} \end{cases} \tag{6-16.1}$$

for $n = 1,2,\ldots, N_q$ and

$$\underline{e}_{q+1,n}(y) = \begin{cases} 1\hat{\underline{z}} & (n-1)\,\Delta_{q+1} \leq y - y_{rq} \leq n\,\Delta_{q+1} \\ 0 & y \text{ elsewhere} \end{cases} \tag{6-16.2}$$

for $n = 1,2,\ldots, N_{q+1}$. Also, in the above, $\Delta_q = w_q/N_q$ for $q = 1,2,\ldots,Q+1$. Equations (6-16) are written with respect to the coordinate system shown in Fig. 10. Figure 11 shows the order in which the functions $\underline{e}_{q,n}$ appear on aperture face Γ_q.

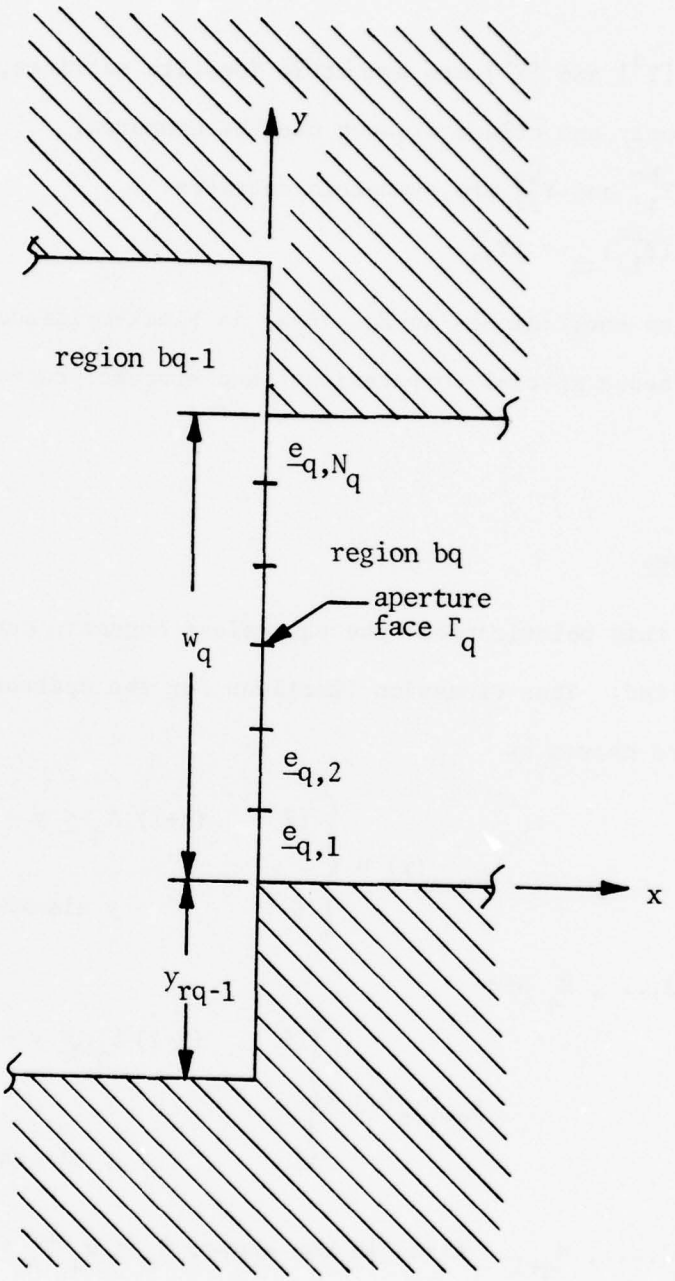

Fig. 11. Order in which functions $\underline{e}_{q,n}$ appear on aperture face Γ_q for TE case.

The elements of $[Y^a]$ are determined from a specialization of Eq. (3-15) to Γ_1. Hence, one may easily obtain the formula

$$Y^a_{mn} = \begin{cases} \dfrac{k_o \eta_o}{2 k_a \eta_a} \dfrac{\gamma^2}{4} \displaystyle\int_{-1}^{1} \int_{-1}^{1} H_o^{(2)}(\gamma \left| \frac{u}{2} - \frac{u'}{2} + (m-n) \right|) du' du & \text{if } m \neq n \\ \dfrac{k_o \eta_o}{2 k_a \eta_a} \dfrac{\gamma}{2} \displaystyle\int_{-1}^{1} [\alpha(\frac{\gamma}{2}(u+1)) + \alpha(\frac{\gamma}{2}(1-u))] du & \text{if } m = n \end{cases} \tag{6-17}$$

where $\gamma = k_a \Delta_1$ and the function α is defined by Eq. (3-17). The matrix $[Y^c]$ is determined from (6-17) where $\gamma = k_c \Delta_{Q+1}$, k_c replaces k_a, and η_c replaces η_a.

To compute Eqs. (6-10) - (6-13), TE fields must be constructed inside a two-dimensional perfectly conducting cavity. To do this, an electric vector potential $\underline{F}^{bq} = \psi^{bq} \hat{z}$ is chosen for each region bq. The fields in each region are obtained by

$$\underline{E}^{bq} = - \nabla \times \underline{F}^{bq} = - \hat{x} \frac{\partial \psi^{bq}}{\partial y} + \hat{y} \frac{\partial \psi^{bq}}{\partial x} \tag{6-18}$$

$$\underline{H}^{bq} = - \frac{j k_{bq}}{\eta_{bq}} \underline{F}^{bq} \tag{6-19}$$

where $k_{bq} = \omega \sqrt{\mu_{bq} \varepsilon_{bq}}$ and $\eta_{bq} = \sqrt{\mu_{bq} / \varepsilon_{bq}}$. Each scalar function ψ^{bq} satisfies the equation

$$\frac{\partial^2 \psi^{bq}}{\partial x^2} + \frac{\partial^2 \psi^{bq}}{\partial y^2} + k_{bq}^2 \psi^{bq} = 0 \tag{6-20}$$

everywhere in region bq except where the sources are. Considering the magnetic current sources $\underline{e}_{q,n}$ at Γ_q and $\underline{e}_{q+1,n}$ at Γ_{q+1} separately, one may solve Eq. (6-20) with the appropriate boundary conditions on the cavity walls. The resulting magnetic field operators are then defined by

$$\underline{B}_z^{qh,q}(\underline{e}_{q,n}) = \hat{\underline{z}} \frac{jk_{bq}}{h_q \eta_{bq}} \sum_{p=0}^{\infty} \frac{\varepsilon_p \cos k_{xp}^q (x - d_q)}{k_{xp}^q \sin k_{xp}^q d_q} \cos \frac{p\pi y}{h_q}$$

$$\cdot \int_0^{h_q} e_{q,n}(y') \cos \frac{p\pi y'}{h_q} \, dy' \qquad (6\text{-}21)$$

and

$$\underline{B}_z^{qh,q+1}(\underline{e}_{q+1,n}) = \hat{\underline{z}} \frac{jk_{bq}}{h_q \eta_{bq}} \sum_{p=0}^{\infty} \frac{\varepsilon_p \cos k_{xp}^q x}{k_{xp}^q \sin k_{xp}^q d_q} \cos \frac{p\pi y}{h_q}$$

$$\cdot \int_0^{h_q} e_{q+1,n}(y') \cos \frac{p\pi y'}{h_q} \, dy' \qquad (6\text{-}22)$$

where the subscript t has been replaced by z. The second subscript on $\underline{B}$ will be either $q(x = 0)$ or $q+1(x = d_q)$. In the above, $\varepsilon_p = 1$ for $p = 0$, $\varepsilon_p = 2$ for $p \neq 0$, and

$$(k_{xp}^q)^2 = k_{bq}^2 - (\frac{p\pi}{h_q})^2 \qquad (6\text{-}23)$$

Thus, for Eqs. (6-10) and (6-13), one may obtain

$$(Y_{11}^{bq})_{mn} = -\frac{j\eta_o}{\eta_{bq}} (k_o \Delta_q) \frac{\Delta q}{h_q} \sum_{p=0}^{\infty} \frac{\varepsilon_p \cot k_{xp}^q d_q}{\sqrt{1 - (\frac{p\pi}{k_{bq} h_q})^2}} \left[\frac{\sin \frac{p\pi\Delta_q}{2h_q}}{\frac{p\pi\Delta_q}{2h_q}} \right]^2$$

$$\cdot \cos \frac{p\pi}{h_q} [y_{\ell q} + (m - .5)\Delta_q] \cos \frac{p\pi}{h_q} [y_{\ell q} + (n - .5)\Delta_q] \tag{6-24}$$

for $1 \leq m \leq N_q$, $1 \leq n \leq N_q$, and

$$(Y_{22}^{bq})_{mn} = -\frac{j\eta_o}{\eta_{bq}} (k_o \Delta_{q+1}) \frac{\Delta_{q+1}}{h_q} \sum_{p=0}^{\infty} \frac{\varepsilon_p \cot k_{xp}^q d_q}{\sqrt{1 - (\frac{p\pi}{k_{bq} h_q})^2}} \left[\frac{\sin \frac{p\pi\Delta_{q+1}}{2h_q}}{\frac{p\pi\Delta_{q+1}}{2h_q}} \right]^2$$

$$\cdot \cos \frac{p\pi}{h_q} [y_{rq} + (m - .5)\Delta_{q+1}] \cos \frac{p\pi}{h_q} [y_{rq} + (n - .5)\Delta_{q+1}] \tag{6-25}$$

for $1 \leq m \leq N_{q+1}$, $1 \leq n \leq N_{q+1}$. The formula for Eq. (6-11) is given by

$$(Y_{12}^{bq})_{mn} = \frac{j\eta_o}{\eta_{bq}} (k_o \Delta_{q+1}) \frac{\Delta_q}{h_q} \sum_{p=0}^{\infty} \frac{\varepsilon_p \csc k_{xp}^q d_q}{\sqrt{1 - (\frac{p\pi}{k_{bq} h_q})^2}} \left[\frac{\sin \frac{p\pi\Delta_{q+1}}{2h_q}}{\frac{p\pi\Delta_{q+1}}{2h_q}} \right]$$

$$\cdot \left[\frac{\sin \frac{p\pi\Delta_q}{2h_q}}{\frac{p\pi\Delta_q}{2h_q}} \right] \cos \frac{p\pi}{h_q} [y_{\ell q} + (m - .5)\Delta_q]$$

$$\cdot \cos \frac{p\pi}{h_q} [y_{rq} + (n - .5)\Delta_{q+1}] \tag{6-26}$$

for $1 \leq m \leq N_q$, $1 \leq n \leq N_{q+1}$. The formula for Eq. (6-12) is easily seen to be

$$(Y_{21}^{bq})_{mn} = (Y_{12}^{bq})_{nm} \tag{6-27}$$

for $1 \leq m \leq N_{q+1}$, $1 \leq n \leq N_q$.

The non-zero elements of the excitation column vector are obtained as in Section 3.3. Thus for an incident plane wave, Eq. (3-40) becomes

$$I_m^i = \frac{2k_o\eta_o}{k_a\eta_a}(k_a\Delta_1)\, e^{jk_a[(m-.5)\Delta_1 - \frac{w_1}{2}]\sin\phi^i} \cdot \frac{\sin(\frac{k_a\Delta_1}{2}\sin\phi^i)}{\frac{k_a\Delta_1}{2}\sin\phi^i} \tag{6-28}$$

The formula for line source incidence may be obtained by a specialization of Eq. (3-43).

6.3. TM Case

For this polarization, the equivalent magnetic current sheets are y directed. Thus expansion functions for the aperture faces Γ_q and Γ_{q+1} are chosen as

$$\underline{e}_{q,n}(y) = \begin{cases} (\frac{y - y_{\ell q}}{\Delta_q} + 1 - n)\hat{y} & (n-1)\Delta_q \leq y - y_{\ell q} \leq n\Delta_q \\ (\frac{y_{\ell q} - y}{\Delta_q} + 1 + n)\hat{y} & n\Delta_q \leq y - y_{\ell q} \leq (n+1)\Delta_q \\ 0 & y \text{ elsewhere} \end{cases} \tag{6-29.1}$$

for $n = 1,2,\ldots, N_q-1$ and

$$\underline{e}_{q+1,n}(y) = \begin{cases} \left(\dfrac{y - y_{rq}}{\Delta_{q+1}} + 1-n\right)\hat{\underline{y}} & (n-1)\Delta_{q+1} \leq y - y_{rq} \leq n\Delta_{q+1} \\ \left(\dfrac{y_{rq} - y}{\Delta_{q+1}} + 1+n\right)\hat{\underline{y}} & n\Delta_{q+1} \leq y - y_{rq} \leq (n+1)\Delta_{q+1} \\ 0 & y \text{ elsewhere} \end{cases} \tag{6-29.2}$$

for $n = 1,2,\ldots, N_{q+1}-1$. In the above, $\Delta_q = w_q/N_q$ for $q = 1,2,\ldots, N_q-1$. Equations (6-29) are written with respect to the coordinate system shown in Fig. 10. Figure 12 shows the order in which the functions $\underline{e}_{q,n}$ appear on aperture face Γ_q.

The elements of $[Y^a]$ are determined from a specialization of Eq. (4-15) to Γ_1. This is written as

$$Y^a_{mn} = \frac{k_o \eta_o}{k_a \eta_a} \{S(m-1, n-1, 1, 1) + S(m-1, n, 1, -1) + S(m, n-1, -1, 1) + S(m, n, -1, -1)\} \tag{6-30}$$

for $1 \leq m \leq N_1$, $1 \leq n \leq N_1$ and S is defined by

$$S(m,n,p,q) = \begin{cases} \dfrac{\gamma^2}{8} \displaystyle\int_{-1}^{1}\int_{-1}^{1} \left[\left(\frac{pu}{2} + \frac{1}{2}\right)\left(\frac{qu'}{2} + \frac{1}{2}\right) - \frac{pq}{\gamma^2}\right] H_o^{(2)}\left(\gamma\left|\frac{u}{2} - \frac{u'}{2} + (m-n)\right|\right) du'du \\ \qquad\qquad \text{if } m \neq n \\ \dfrac{\gamma}{4} \displaystyle\int_{-1}^{1} \left\{\left[\left(\frac{pu}{2} + \frac{1}{2}\right)\left(\frac{qu}{2} + \frac{1}{2}\right) - \frac{pq}{\gamma^2}\right]\left[\alpha\left(\frac{\gamma}{2}(u+1)\right) + \alpha\left(\frac{\gamma}{2}(1-u)\right)\right] + q\left(\frac{pu}{2} + \frac{1}{2}\right)\left[\left(\frac{1}{2} - \frac{u}{2}\right)\right.\right. \\ \qquad \left.\left. \cdot H_1^{(2)}\left(\frac{\gamma}{2}(1-u)\right) - \left(\frac{1}{2} + \frac{u}{2}\right) H_1^{(2)}\left(\frac{\gamma}{2}(1+u)\right)\right]\right\} du \\ \qquad\qquad \text{if } m = n \end{cases} \tag{6-31}$$

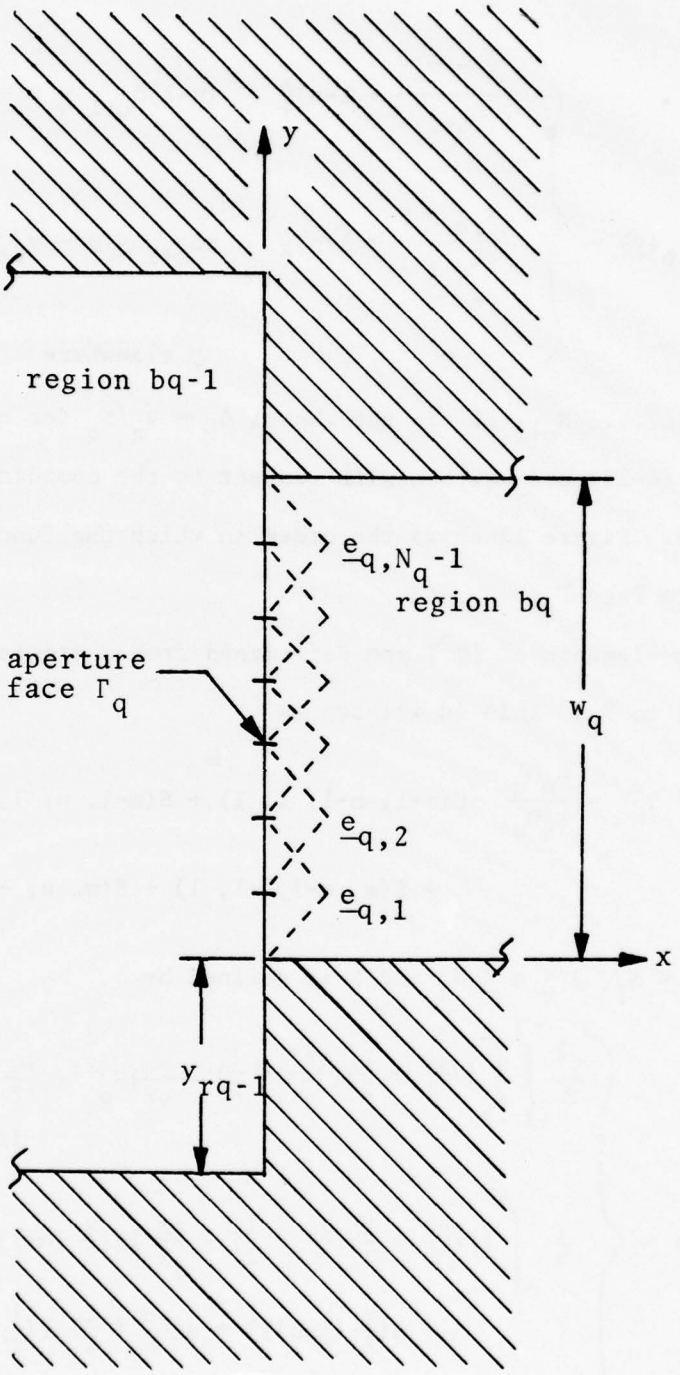

Fig. 12. Order in which functions $\underline{e}_{q,n}$ appear on aperture face Γ_q for TM case.

where $\gamma = k_a \Delta_1$ and the function α is defined by Eq. (3-17). The matrix $[Y^c]$ is determined from Eq. (6-30) where $\gamma = k_c \Delta_{Q+1}$, k_c replaces k_a, and η_c replaces η_a.

To compute Eqs. (6-10) - (6-13), TM fields must be constructed inside a two-dimensional perfectly conducting cavity. To do this, an electric vector potential $\underline{A}^{bq} = \psi^{bq}\hat{z}$ is chosen for each region bq. The fields in each region are obtained by

$$\underline{E}^{bq} = - jk_{bq}\eta_{bq}\,\underline{A}^{bq} \tag{6-32}$$

$$\underline{H}^{bq} = \underline{\nabla} \times \underline{A}^{bq} = \hat{x}\,\frac{\partial \psi^{bq}}{\partial y} - \hat{y}\,\frac{\partial \psi^{bq}}{\partial x} \tag{6-33}$$

Each scalar function ψ^{bq} satisfies Eq. (6-20) everywhere in region bq except where the sources are. Considering the magnetic current sources $\underline{e}_{q,n}$ at Γ_q and $\underline{e}_{q+1,n}$ at Γ_{q+1} separately, one may solve Eq. (6-20) with the appropriate boundary conditions on the cavity walls. The resulting y components of the magnetic field operators are defined by

$$\underline{B}_y^{qh,q}(\underline{e}_{q,n}) = \hat{y}\,\frac{2j}{k_{bq}\eta_{bq}h_q} \sum_{p=1}^{\infty} \frac{k_{xp}^q \cos k_{xp}^q (x - d_q)}{\sin k_{xp}^q d_q} \cdot \sin \frac{p\pi y}{h_q} \int_0^{h_q} e_{q,n}(y') \sin \frac{p\pi y'}{h_q}\, dy' \tag{6-34}$$

and

$$\underline{B}_y^{qh,q+1}(\underline{e}_{q+1,n}) = \hat{y}\,\frac{2j}{k_{bq}\eta_{bq}h_q} \sum_{p=1}^{\infty} \frac{k_{xp}^q \cos k_{xp}^q x}{\sin k_{xp}^q d_q} \sin \frac{p\pi y}{h_q} \cdot \int_0^{h_q} e_{q+1,n}(y') \sin \frac{p\pi y'}{h_q}\, dy' \tag{6-35}$$

where the subscript t has been replaced by y. The second subscript will be either q(x=0) or q+1(x=d_q). Equation (6-23) also holds for k_{xp}. Thus, for Eqs. (6-10) and (6-13), one may obtain

$$(Y_{11}^{bq})_{mn} = -\frac{2j\eta_o}{\eta_{bq}} (k_o\Delta_q)\frac{\Delta_q}{h_q} \sum_{p=1}^{\infty}\sqrt{1 - (\frac{p\pi}{k_{bq}h_q})^2} \cot k_{xp}^q d_q$$

$$\cdot \left[\frac{\sin \frac{p\pi\Delta_q}{2h_q}}{\frac{p\pi\Delta_q}{2h_q}}\right]^4 \sin \frac{p\pi}{h_q} (y_{\ell q} + m\Delta_q)$$

$$\cdot \sin \frac{p\pi}{h_q} (y_{\ell q} + n\Delta_q) \qquad (6\text{-}36)$$

for $1 \le m \le N_q - 1$, $1 \le n \le N_q - 1$, and

$$(Y_{22}^{bq})_{mn} = -\frac{2j\eta_o}{\eta_{bq}} (k_o\Delta_{q+1}) \frac{\Delta_{q+1}}{h_q} \sum_{p=1}^{\infty} \sqrt{1 - (\frac{p\pi}{k_{bq}h_q})^2} \cot k_{xp}^q d_q$$

$$\cdot \left[\frac{\sin \frac{p\pi\Delta_{q+1}}{2h_q}}{\frac{p\pi\Delta_{q+1}}{2h_q}}\right]^4 \sin \frac{p\pi}{h_q} (y_{rq} + m\Delta_{q+1}) \sin \frac{p\pi}{h_q} (y_{rq} + n\Delta_{q+1}) \qquad (6\text{-}37)$$

for $1 \le m \le N_{q+1} - 1$, $1 \le n \le N_{q+1} - 1$. The formula for Eq. (6-11) is given by

$$(Y_{12}^{bq})_{mn} = \frac{2j\eta_o}{\eta_{bq}} (k_o \Delta_{q+1}) \frac{\Delta_q}{h_q} \sum_{p=1}^{\infty} \sqrt{1 - \left(\frac{p\pi}{k_{bq} h_q}\right)^2} \csc k_{xp}^q d_q$$

$$\cdot \left[\frac{\sin \frac{p\pi\Delta_q}{2h_q}}{\frac{p\pi\Delta_q}{2h_q}} \right]^2 \left[\frac{\sin \frac{p\pi\Delta_{q+1}}{2h_q}}{\frac{p\pi\Delta_{q+1}}{2h_q}} \right]^2 \sin \frac{p\pi}{h_q} (y_{\ell q} + m\Delta_q)$$

$$\cdot \sin \frac{p\pi}{h_q} (y_{rq} + n\Delta_{q+1}) \qquad (6\text{-}38)$$

for $1 \leq m \leq N_q - 1$, $1 \leq n \leq N_{q+1} - 1$. The formula for Eq. (6-12) is easily seen to be

$$(Y_{21}^{bq})_{mn} = (Y_{12}^{bq})_{nm} \qquad (6\text{-}39)$$

for $1 \leq m \leq N_{q+1} - 1$, $1 \leq n \leq N_q - 1$.

The non-zero elements of the excitation column vector are obtained as in Section 4.3. Thus for an incident plane wave, Eq. (4-33) becomes

$$I_m^i = - \frac{2k_o\eta_o}{k_a\eta_a} (k_a\Delta_1) \cos \phi^i \, e^{jk_a(m\Delta_1 - \frac{w_1}{2})} \sin \phi^i$$

$$\cdot \left[\frac{\sin \left(\frac{k_a\Delta_1}{2} \sin \phi^i\right)}{\frac{k_a\Delta_1}{2} \sin \phi^i} \right]^2 \qquad (6\text{-}40)$$

A formula for line source incidence may be obtained by a specialization of Eq. (4-36).

Chapter 7

APPROXIMATE SOLUTION TO SLIT OF RECTANGULAR CROSS SECTION

7.1. Problem Specialization

In this chapter, a slit of rectangular cross section is considered as shown in Fig. 13. This is a special case of the more general problem considered in Chapter 6 and Eqs. (6-8) become

$$\begin{bmatrix} Y^a + Y^b_{11} & Y^b_{12} \\ Y^b_{21} & Y^b_{22} + Y^c \end{bmatrix} \begin{bmatrix} \vec{V}^1 \\ \vec{V}^2 \end{bmatrix} = \begin{bmatrix} \vec{I}^i \\ \vec{0} \end{bmatrix} \tag{7-1}$$

since region b is represented by one rectangular region. This region has the composite admittance matrix representation $[Y^b]$ denoted by

$$[Y^b] = \begin{bmatrix} Y^b_{11} & Y^b_{12} \\ Y^b_{21} & Y^b_{22} \end{bmatrix} \tag{7-2}$$

where

$$(Y^b_{11})_{mn} = - k_o \eta_o \langle \underline{e}_{1m}, \underline{B}^{1h,1}_{t1}(\underline{e}_{1n}) \rangle \tag{7-3}$$

$$(Y^b_{21})_{mn} = k_o \eta_o \langle \underline{e}_{2m}, \underline{B}^{1h,1}_{t2}(\underline{e}_{1n}) \rangle \tag{7-4}$$

$$(Y^b_{12})_{mn} = (Y^b_{21})_{mn} \tag{7-5}$$

$$(Y^b_{22})_{mn} = (Y^b_{11})_{mn} \tag{7-6}$$

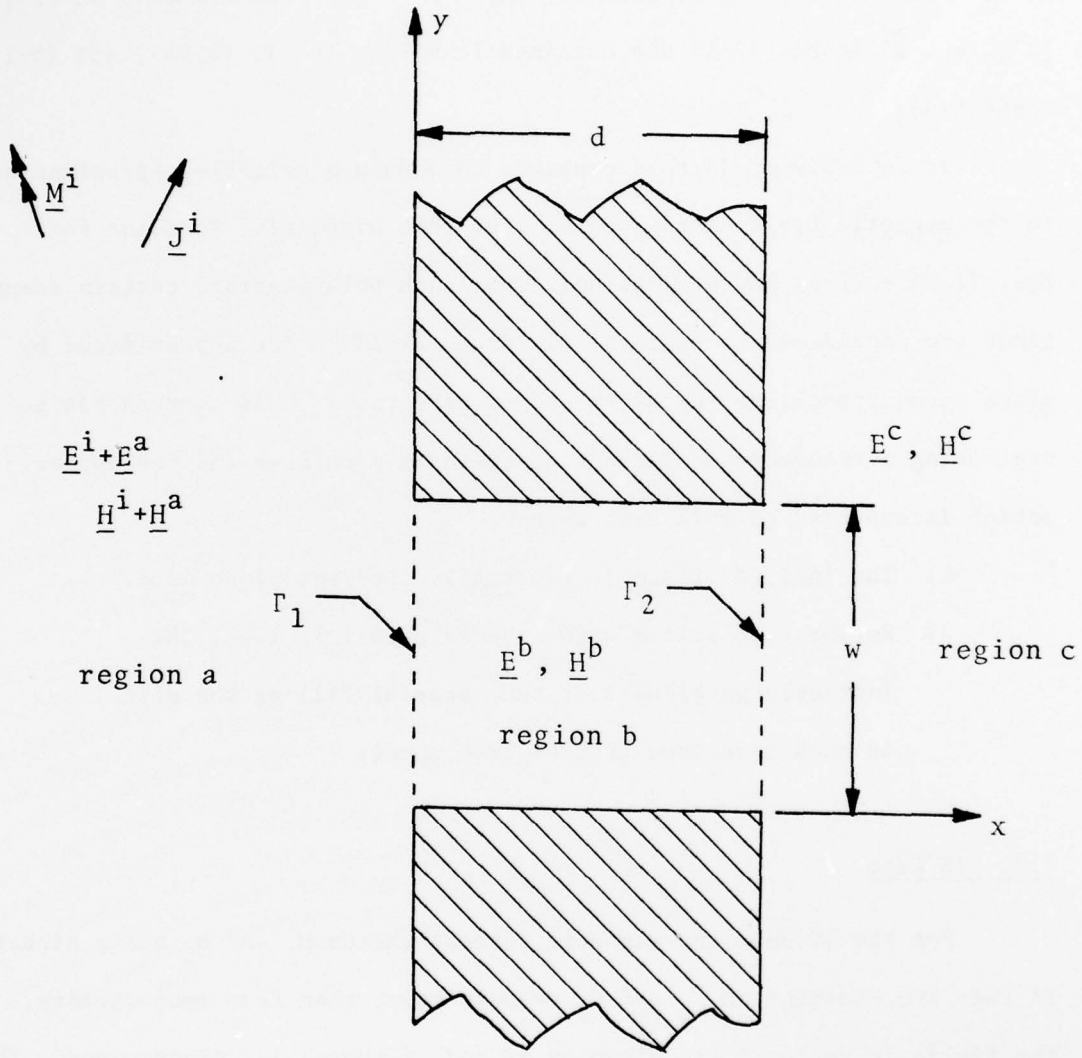

Fig. 13. Slit with rectangular cross section.

Equations (7-3) and (7-4) come from the specialization of Eqs. (6-10) and (6-12) and the last two come from the fact that each aperture face is divided into N subsections each of length $\Delta = w/N$. The elements of $[Y^a]$, $[Y^c]$, and $\vec{I}^i$ in Eq. (7-1) are obtained from Eqs. (6-9), (6-14), and (6-15) respectively.

It is desired, in this chapter, to obtain a suitable approximation to the magnetic field inside region b so that simplified formulas for Eqs. (7-3) - (7-6) may be obtained. For each polarization, certain assumptions are considered so that the fields in region b are approximated by plane waves travelling in the $+\underline{\hat{x}}$ and $-\underline{\hat{x}}$ direction. This corresponds to neglecting a transverse component of field in each case and the approximation is expected to work best when:

1) The incident field is a normally incident plane wave.
2) Region b is filled with a dense material, i.e., the intrinsic wavelength of the material filling the slit is much less than that of free space.

7.2. TE Case

For the TE case the magnetic current sheets $\underline{M}_1$ and $\underline{M}_2$ are z directed. If they are constant on Γ_1 and Γ_2 respectively, then from image theory, the fields in region b are given by $+\underline{\hat{x}}$ and $-\underline{\hat{x}}$ travelling plane waves. The currents $\underline{M}_1$ and $\underline{M}_2$ become unbounded at the ends of Γ_1 and Γ_2 but this is a very localized phenomenon, particularly when region b is a dense material. Thus if $w >> \lambda_b$, the magnetic currents should be constant enough to neglect the x component of electric field.

These remarks lead to the assumption for the z directed magnetic field as

$$H_z^b = A\, e^{-jk_b x} + B\, e^{jk_b x} \tag{7-7}$$

where A and B are constants. Computing E_y^b from Eq. (7-7) and satisfying the boundary conditions at x = 0 and x = d, one obtains

$$\underline{B}_z^{1h,1}(\underline{e}_{1n}) = \begin{cases} \hat{z}\,\dfrac{j}{\eta_b}\,\dfrac{\cos k_b(x-d)}{\sin k_b d} & \text{if } (n-1)\Delta \le y \le n\Delta \\ 0 & \text{if } y \text{ is elsewhere} \end{cases} \tag{7-8}$$

where $\underline{e}_{1n}$ is defined by Eqs. (6-16). Thus Eqs. (7-3) and (7-4) take the simple form of

$$(Y_{11}^b)_{mn} = -\,jk_o\Delta\,\frac{\eta_o}{\eta_b}\cot k_b d\;\delta_{mn} \tag{7-9}$$

and

$$(Y_{21}^b)_{mn} = \;jk_o\Delta\,\frac{\eta_o}{\eta_b}\csc k_b d\;\delta_{mn} \tag{7-10}$$

where $\delta_{mn} = 1$ if m = n and $\delta_{mn} = 0$ for $m \neq n$.

These equations may be obtained by an alternative method. Since E_x is assumed negligible, conducting planes may be placed at $y = n\Delta$ for n = 1,2,..., N, so that each magnetic current expansion function radiates inside the closed conducting box $0 \le x \le d$, $(n-1)\Delta \le y \le n\Delta$. Specializing Eqs. (6-21) and (6-22) to this problem, one obtains Eq. (7-8). The p = 0 term is the only non-zero term.

7.3. TM Case

For this polarization, the magnetic current sheets are y directed and even if $\underline{M}_1$ and $\underline{M}_2$ are assumed constant over Γ_1 and Γ_2, the field inside region b is not represented exactly by a plane wave. If one considers the constant magnetic current distribution $\underline{M}_1 = K\,\hat{\underline{y}}$ radiating inside the closed conducting box $0 \leq x \leq d$, $0 \leq y \leq w$, then one may express the fields inside the box as

$$E_z = -\frac{2K}{\pi} \sum_{p=1}^{\infty} \frac{1}{p} \frac{\sin\left(\sqrt{1 - \left(\frac{p\pi}{k_b w}\right)^2}\, k_b (x-d)\right)}{\sin\sqrt{1 - \left(\frac{p\pi}{k_b w}\right)^2}} \sin\frac{p\pi y}{w} \tag{7-11}$$

$$H_x = -\frac{4K}{jk_b \eta_b w} \sum_{p=1}^{\infty} \frac{\sin\left(\sqrt{1 - \left(\frac{p\pi}{k_b w}\right)^2}\, k_b (x-d)\right)}{\sin\sqrt{1 - \left(\frac{p\pi}{k_b w}\right)^2} k_b d} \cos\frac{p\pi y}{w} \tag{7-12}$$

$$H_y = -\frac{4K}{j\eta_b} \sum_{p=1}^{\infty} \sqrt{\left(\frac{1}{p\pi}\right)^2 - \left(\frac{1}{k_b w}\right)^2} \frac{\cos\sqrt{1 - \left(\frac{p\pi}{k_b w}\right)^2}\, k_b (x-d)}{\sin\sqrt{1 - \left(\frac{p\pi}{k_b w}\right)^2}\, k_b d} \sin\frac{p\pi y}{w} \tag{7-13}$$

Since H_x has no average value on $0 \leq y \leq w$, and if $k_b w >> 1$, it is reasonable that one could neglect H_x as compared to E_z and H_y.

If only E_z and H_y are considered in region b, then, one may proceed with the plane wave assumption as before to obtain

$$\underline{B}_y^{1h,1}(\underline{e}_{1n}) = j \frac{\underline{e}_{1n}(y)}{\eta_b} \frac{\cos k_b (x-d)}{\sin k_b d} \qquad (n-1) \leq y \leq (n+1)\Delta \tag{7-14}$$

where $\underline{e}_{1n}$ is given by Eqs. (6-29). Thus for Eqs. (7-3) and (7-4), one obtains

$$(Y_{11}^b)_{mn} = - jk_o\Delta \frac{\eta_o}{\eta_b} \cot k_b d \; \gamma_{mn} \tag{7-15}$$

and

$$(Y_{21}^b)_{mn} = \quad jk_o\Delta \frac{\eta_o}{\eta_b} \csc k_b d \; \gamma_{mn} \tag{7-16}$$

where

$$\gamma_{mn} = \begin{cases} \frac{1}{6} & \text{if} \quad |m - n| = 1 \\ \frac{2}{3} & \text{if} \quad m = n \\ 0 & \text{otherwise} \end{cases} \tag{7-17}$$

Alternatively, since $E_x = 0$, and $E_z = 0$ at $y = (n-1)\Delta$ and $y = (n+1)\Delta$ for each expansion function $\underline{e}_{1n}$, conducting planes may be placed at the ends of each $\underline{e}_{1n}$ so that each $\underline{e}_{1n}$ radiates inside the closed conducting box $(n-1)\Delta \leq y \leq (n+1)\Delta$. Specializing Eqs. (6-34) and (6-35) to this problem, one obtains

$$\underline{B}_y^{1h,1}(\underline{e}_{1n}) = \frac{j8}{k_b \eta_b} \sum_{\substack{p=1 \\ p \text{ odd}}}^{\infty} \frac{k_{xp} \cos k_{xp}(x-d)}{(p\pi)^2 \sin k_{xp} d} \sin \frac{p\pi y}{2\Delta} \sin \frac{p\pi}{2} \tag{7-18}$$

where $k_{xp}^2 = k_b^2 - (\frac{p\pi}{2\Delta})^2$. Keeping only the $p = 1$ term, one obtains for Eqs. (7-3) and (7-4) the following formulas

$$(Y_{11}^b)_{mn} = - jk_o\Delta \frac{\eta_o}{\eta_b} \beta \cot \beta k_b d \quad \gamma_{mn} \tag{7-19}$$

$$(Y_{21}^b)_{mn} = jk_o\Delta \frac{\eta_o}{\eta_b} \beta \csc \beta k_b d \quad \gamma_{mn} \tag{7-20}$$

where

$$\beta = \sqrt{1 - \left(\frac{\pi}{2k_b\Delta}\right)^2}$$

and

$$\gamma_{mn} = \begin{cases} \frac{8}{\pi^2}\left(\frac{2}{\pi}\left(1 - \frac{2}{\pi}\right)\right) & \text{if } |m-n| = 1 \\ \left(\frac{8}{\pi^2}\right)^2 & \text{if } m = n \\ 0 & \text{otherwise} \end{cases} \qquad (7\text{-}21)$$

Chapter 8

NUMERICAL RESULTS AND DISCUSSION

8.1. Modal and Non-Modal Results

Some representative computations are presented here for filled slits of various cross sections. The cross section shapes and their dimensions are shown in Figs. 14-16. A comparison will first be made between the results obtained from the non-modal solution of Chapters 1 to 4 and the modal solution of Chapter 6. The quantities to be compared are the magnetic current on the aperture faces Γ_1 and Γ_3 and the electric current on the contour C defining the slit cross section. This electric current, which appears as an unknown in the non-modal solution, is computed in the modal solution by first solving for the magnetic currents. Then, using parallel plate guide modes, the tangential magnetic field due to these magnetic currents radiating inside a closed two-dimensional conducting box is computed just inside the contour C. This corresponds directly to the electric current unknown in the non-modal solution. The magnitudes of the electric current times η_o and the magnetic current are plotted as a function of their position on the contour C (cf. Fig. 4). Horizontal and vertical lines are used to denote quantities expanded by pulses while straight lines connect the points given by the triangle expansion functions. Each line Γ_i comprising the contour C is broken up into $N_{i+1} - N_i$ straight line segments which are shown scaled in the figures. The excitation consists

of a plane wave incident from the left of the slits at an angle ϕ^i measured with respect to the negative x axis.

The first example to be considered is a slit of rectangular cross section of width $w = 0.8\lambda_o$ and thickness $d = 0.2\lambda_o$ (λ_o being the wavelength in free space). Regions a, b, and c are always assumed to be free space unless otherwise specified. Excellent agreement is noted between the two solutions for the TE case when $\varepsilon_b = \varepsilon_o$ in Figs. 17 and 18 and when $\varepsilon_b = 5\varepsilon_o$ in Figs. 19 and 20. A numerical check is made on the solution, if region b is lossless, by testing to see if conservation of power flow holds at the two aperture faces. Thus the real parts of the Poynting vector flux at Γ_1, denoted by P_{t1}, and Γ_3, denoted by P_{t3}, are computed. They are compared by the number ΔP defined as

$$\Delta P = 100 \left| \frac{P_{t1} - P_{t3}}{(P_{t1} + P_{t3})/2} \right| \% \qquad (8\text{-}1)$$

which should be as small as possible. This number is computed readily in the non-modal solution and is given, when appropriate, in the figure captions of the computed examples. Cases for which the computation (8-1) is not reliable is when the slit is cut off in the TM case and the imaginary part of the Poynting vector flux is much greater than the real part.

Two TM cases of the previous example are shown in Figs. 21 and 22 where agreement between the magnetic currents is again excellent. The noticeable difference between the two solutions occurs in the electric current at the ends of the illuminated aperture face Γ_1. An analysis

of the field near the edges following the procedure of Meixner [28] shows that the magnetic current should approach zero with an infinite slope right at the ends of Γ_1. Also, the electric current should become singular at these points. An explanation as to why the computed non-modal TM electric current doesn't behave as expected at the ends of the aperture face lies in the fact that the edge behavior of the magnetic current is not represented adequately by the triangle expansion functions. They constrain the magnetic current to approach zero linearly at the ends of the aperture. The modal computation of this electric current, however, always gives a zero value of electric current at y = 0 and y = w because of the nature of the modal expansion. This modal computation converges non-uniformly to the electric current at these points.

To illustrate a more detailed behavior of the aperture fields, a smaller slit ($w = 0.2\lambda_o$, $d = 0.2\lambda_o$) is considered where the number of unknowns is the same as in the previous example. In Figs. 23-26, for the TE case, the agreement in the electric current from the two solutions is still excellent. For the magnetic current, however, a slight oscillation is present in both solutions, the greater variation being noticed in the non-modal results. For a slit of this size, it is not expected from physical considerations that the true solution would have any oscillatory behavior. It is thus concluded that this anomaly is a characteristic of the numerical solution even though the numerical values for ΔP are small. The TM cases for this example are shown in Figs. 27-29 where the modal electric current was

computed at 50 points along each line Γ_i of C. Results from both of the solutions compare well except for $\underline{J}^b$ at each aperture face Γ_1 and Γ_3. The oscillatory behavior in the electric current from the modal solution is due to the triangular representation of the magnetic current which has a pulse representation of magnetic charge. This results in a logarithmic singularity in the y component of magnetic field at each break point of the triangles and hence accounts for the difficulty in computing the electric currents on Γ_1 and Γ_3 by parallel plate guide modes. The agreement between electric currents on Γ_2 and Γ_4 is quite good and the expected behavior at the edges is observed. For the x component of magnetic field, the modal series converges quite rapidly. The effects of increasing the dielectric constant in region b until there is a propagating TM mode are also noticed in Figs. 27-29.

The preceding results for slits of rectangular cross sections, which have received extensive consideration in the literature, gives one an idea of how these two different solutions compare for this simple cross section. As a further check, the modal and non-modal solutions for the slit cross section of Fig. 15 are compared. Here we have a cross section composed of two rectangular regions which may be solved readily by either method. For the TE case shown in Figs. 30 and 31, excellent agreement is obtained for all quantities computed. Slight oscillations are again noticed in the results for the magnetic currents. Some loss is added to the material filling region b ($\varepsilon_b = (1-j)\varepsilon_o$) in Figs. 32 and 33 which corresponds to a

conductivity of 0.017 siemens/meter. Agreement between the two solutions is again quite good. The TM results for this example are shown in Figs. 34-37 where the magnetic currents from the two solutions are seen to agree quite closely. There is more discrepancy between the electric currents where the largest differences occur right at the corner of the cross section on line Γ_2. To improve this, more expansion functions are needed on Γ_2 since the introduction of an edge there causes tremendous changes in the fields close to the edge.

Allowing for a few discrepancies at some points on the contour C, agreement between the computed quantities in the previous examples is, in general, quite good. In fact, as far as the transmitted fields in region c are concerned, there is negligible difference between the two solutions for a given problem. Figures 38-41 show some plots of transmission coefficient versus plane wave angle of incidence (as measured from the negative x-axis) for some of the previously considered slits.

The primary advantage of the non-modal solution is that it may be used to solve slits whose cross sections cannot be broken up exactly into rectangular sub-regions. Figures 16a-h show some slits of various cross sections, some of which are similar. Figures 42 and 43 show the effects on the radiation patterns in region c if the cross section is changed so that some of the conducting plane pushes into the rectangular cross section. These perturbed cross

sections are shown in Figs. 16b,c, and e. The overall effect is to shift the patterns slightly upward in the TE case while almost no effect is noticed in the TM case. If the rectangular cross section is changed so that some of the conducting plane material is carved out, thus making region b bigger, a much more noticeable upward shifting of the pattern is noticed in Fig. 44. There is again a negligible change in the TM slit patterns for those cases. Lastly, Fig. 45 shows the patterns for the slits of Figs. 16d, f and g when the plane wave is incident at an angle of 45°.

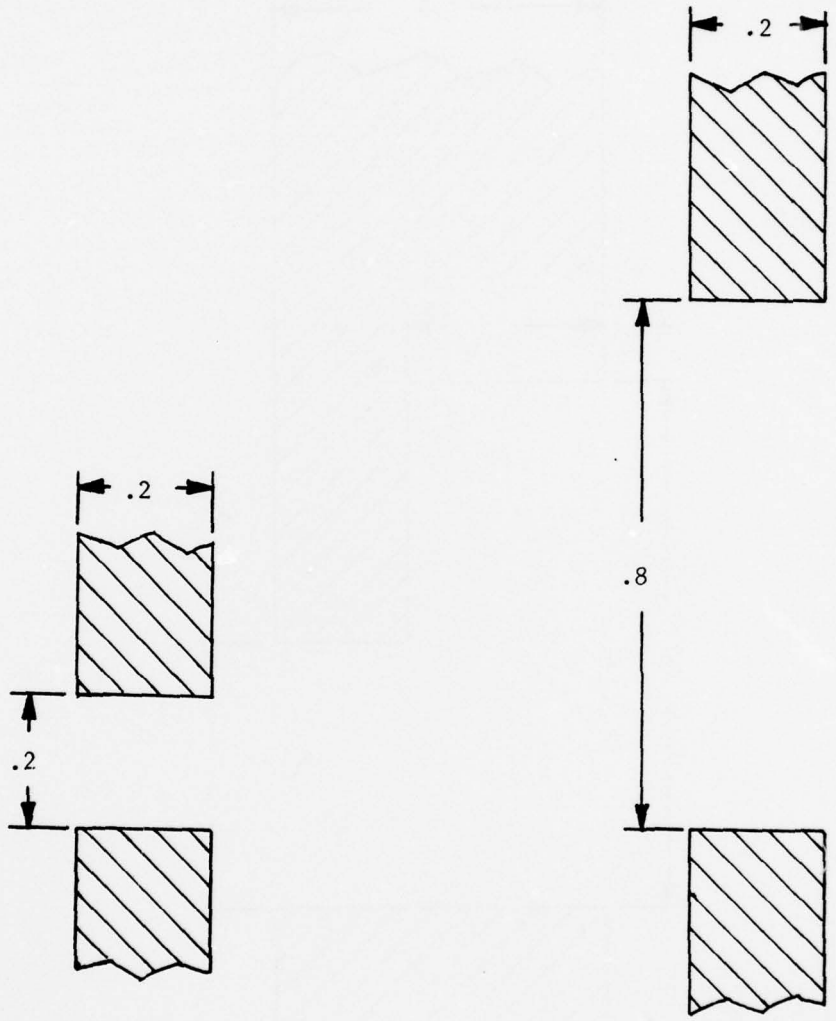

Fig. 14. Slits of a rectangular cross section. Dimensions are in units of λ_o.

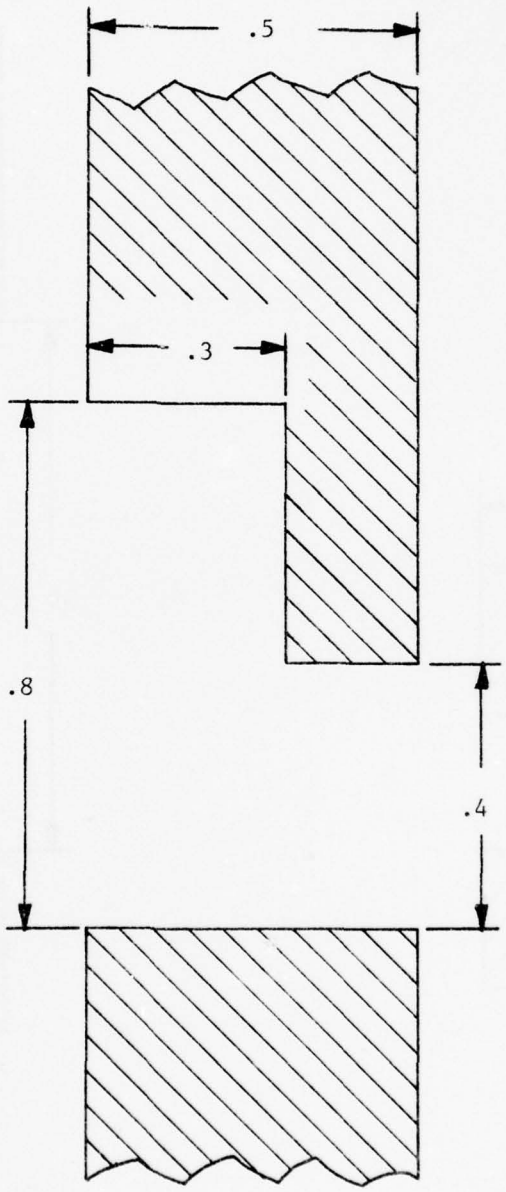

Fig. 15. Slit cross section made up of two rectangular regions. Dimensions are in units of λ_o.

AD-A078 477 SYRACUSE UNIV NY DEPT OF ELECTRICAL AND COMPUTER EN--ETC F/G 20/3
ELECTROMAGNETIC TRANSMISSION THROUGH A FILLED SLIT OF ARBITRARY--ETC(U)
OCT 79 D T AUCKLAND , R F HARRINGTON F30602-79-C-0011

UNCLASSIFIED RADC-TR-79-257 NL

2 OF 2
ADA
078477

END
DATE
FILMED
1 -80
DDC

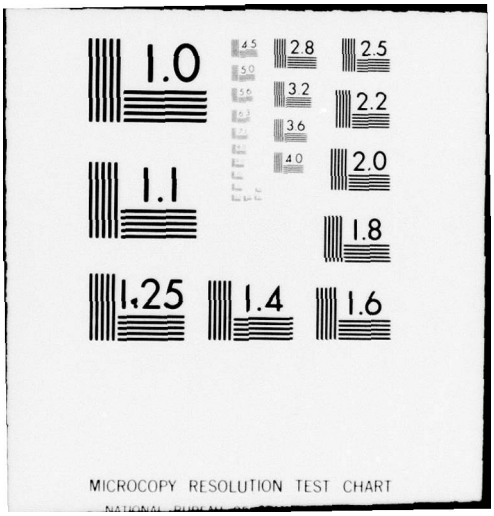
1.0
1.1
1.25
1.4
1.6
1.8
2.0
2.2
2.5
2.8
3.2
3.6
4.0
4.5
5.0
MICROCOPY RESOLUTION TEST CHART

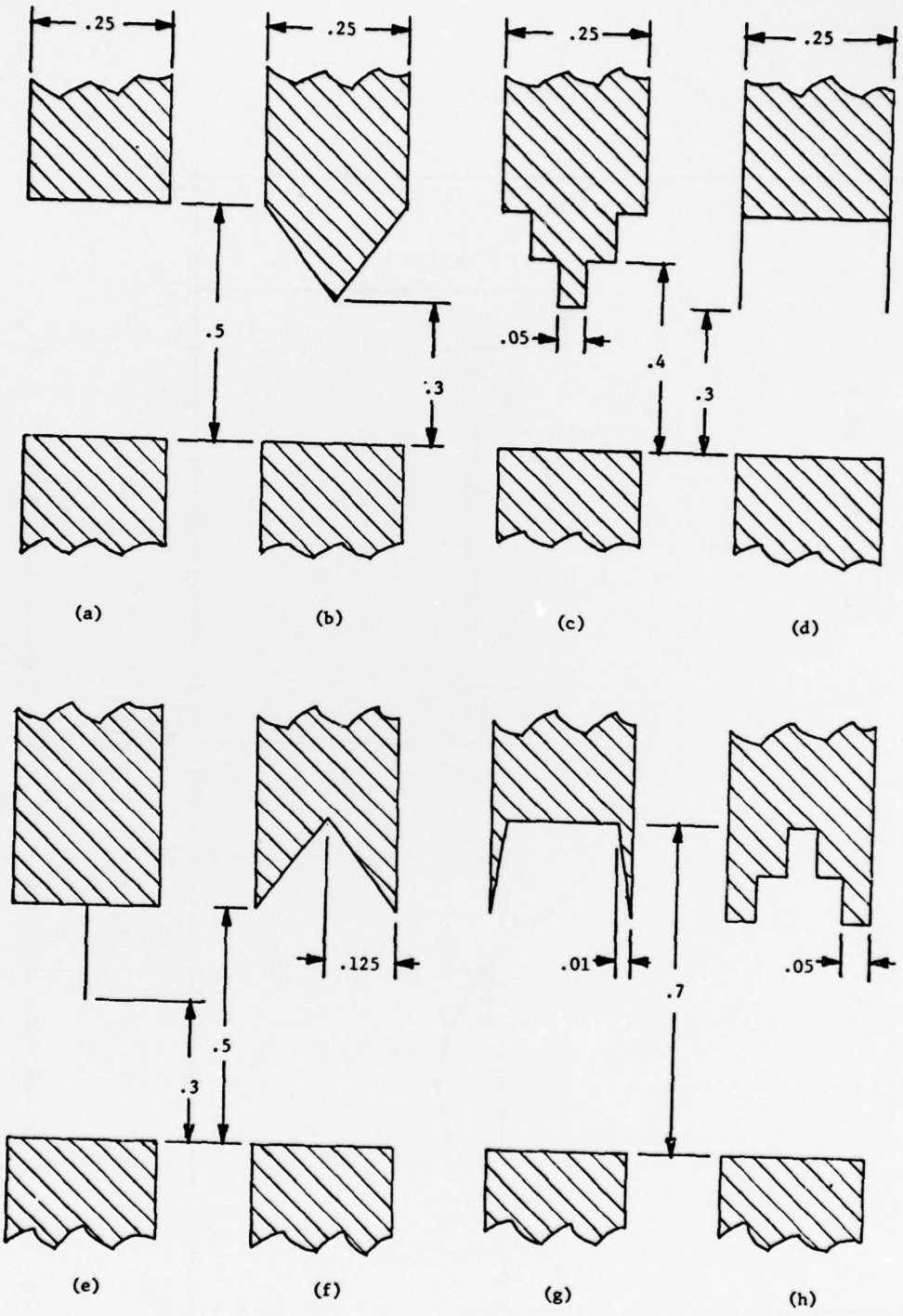

Fig. 16. Slits of various cross section shapes. Dimensions are in units of λ_o.

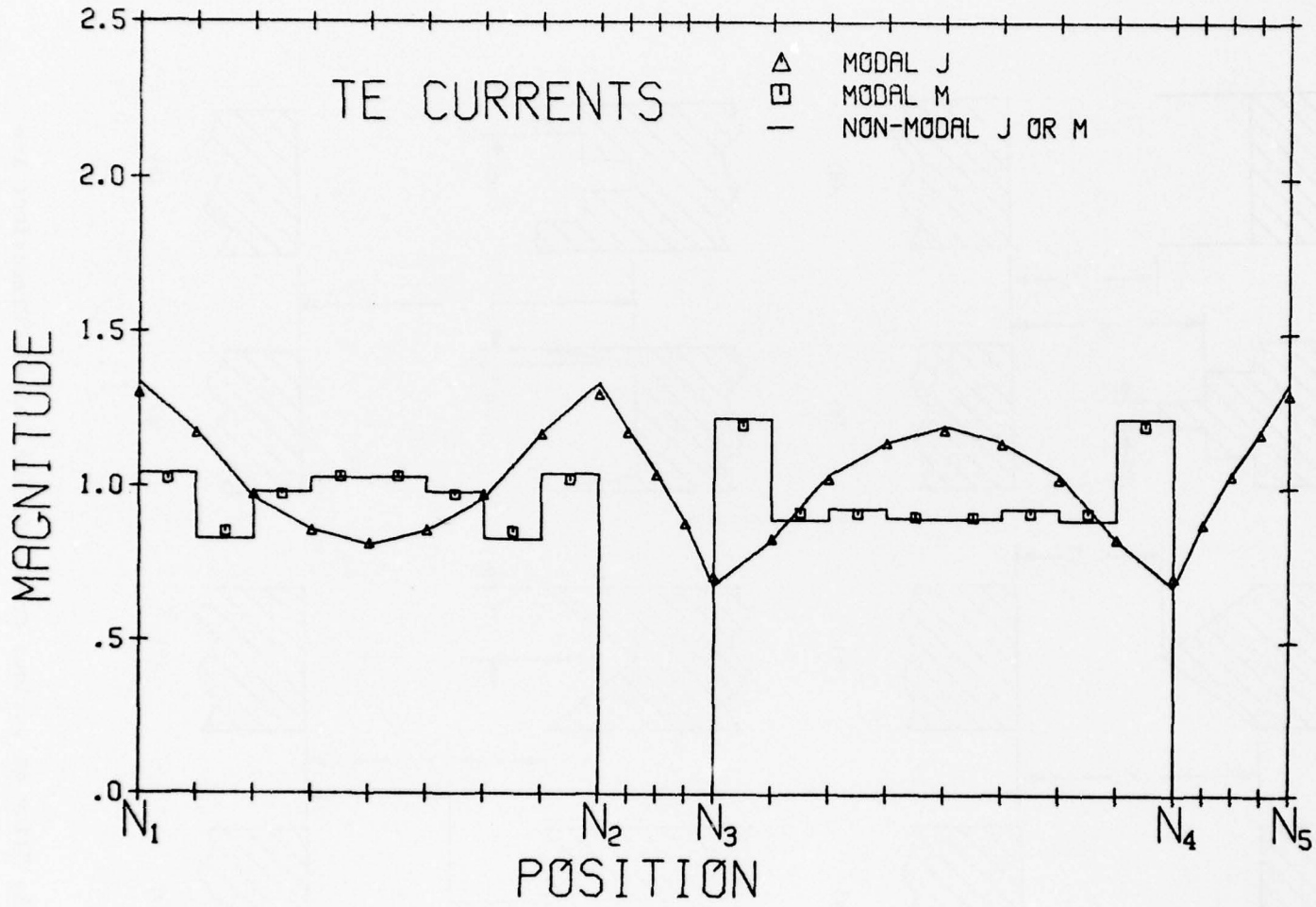

Fig. 17. TE Plane wave incident at $\phi^i = 0^o$ on rectangular slit, $w = .8\lambda_o$, $d = .2\lambda_o$, $\varepsilon_b = \varepsilon_o$, $\Delta P = 0.20\%$, $J = \eta_o J^b$.

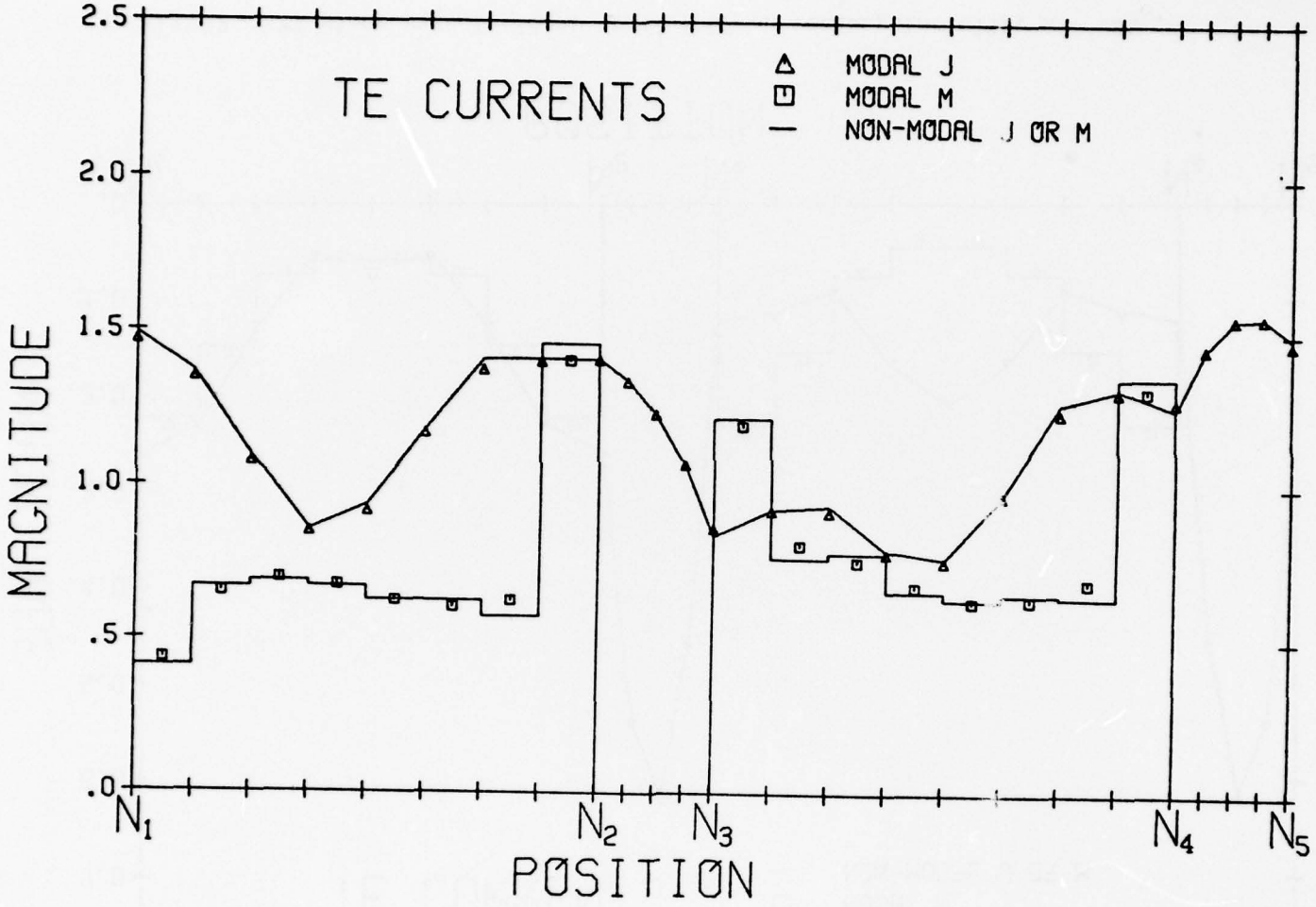

Fig. 18. TE Plane wave incident at $\phi^i = 45^o$ on rectangular slit, $w = .8\lambda_o$, $d = .2\lambda_o$, $\varepsilon_b = \varepsilon_o$, $\Delta P = 0.01\%$, $J = \eta_o J^b$.

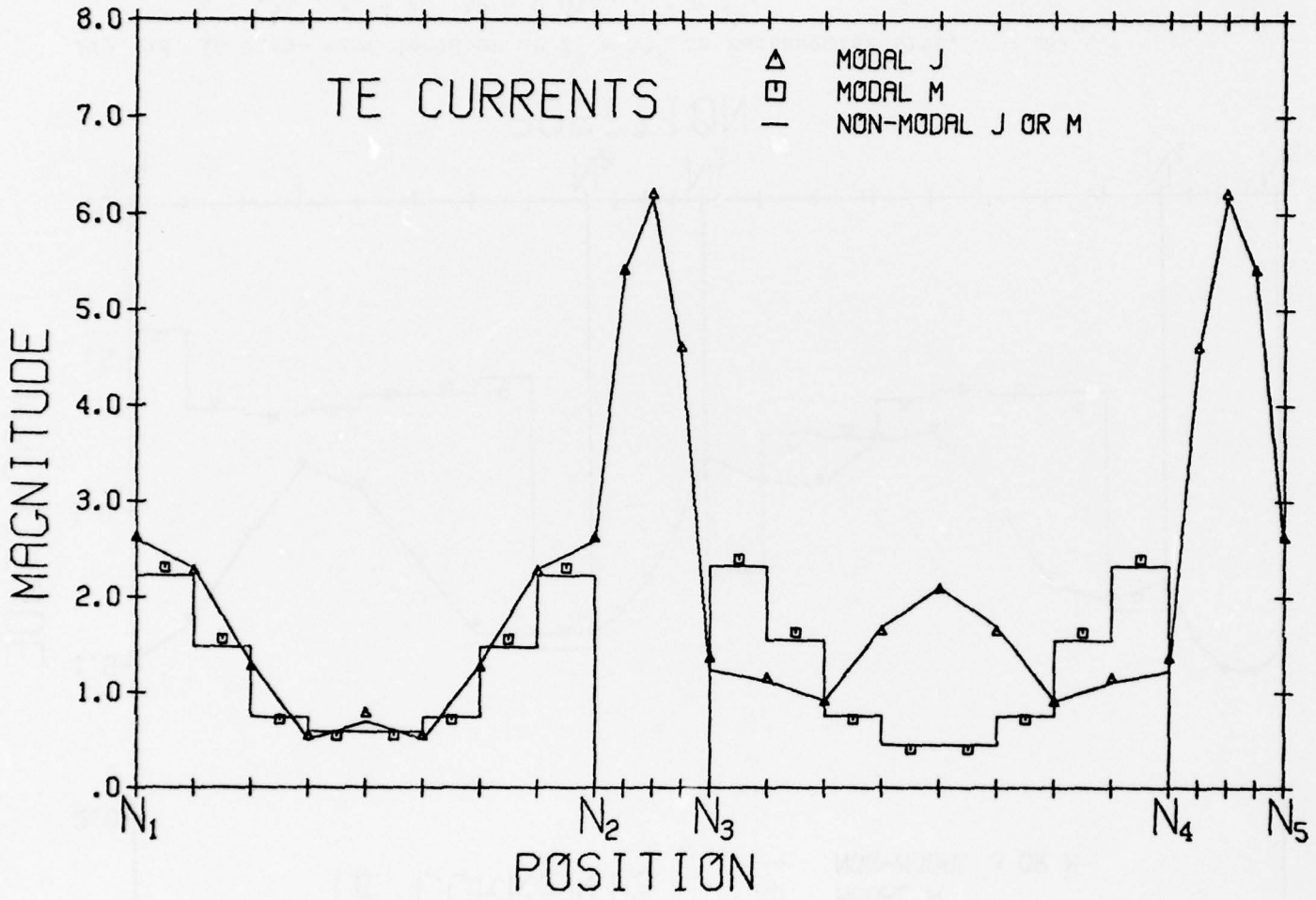

Fig. 19 . TE plane wave incident at $\phi^i = 0°$ on rectangular slit, $w = .8\lambda_o$, $d = .2\lambda_o$, $\varepsilon_b = 5\varepsilon_o$, $\Delta P = 0.50\%$, $J = \eta_o J^b$.

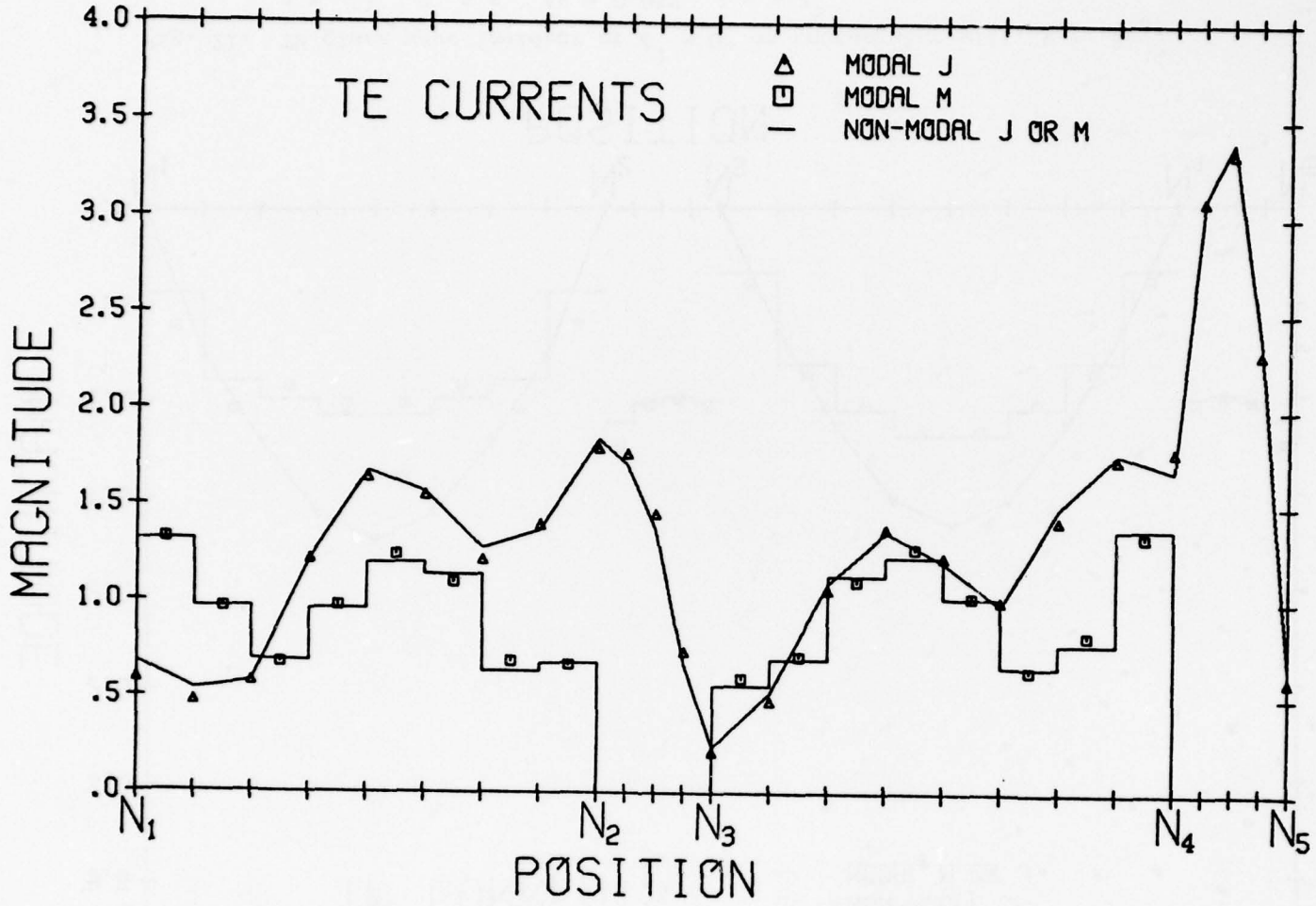

Fig. 20. TE plane wave incident at $\phi^i = 45°$ on rectangular slit, $w = .8\lambda_o$, $d = .2\lambda_o$, $\varepsilon_b = 5\varepsilon_o$, $\Delta P = 0.33\%$, $J = \eta_o J^b$.

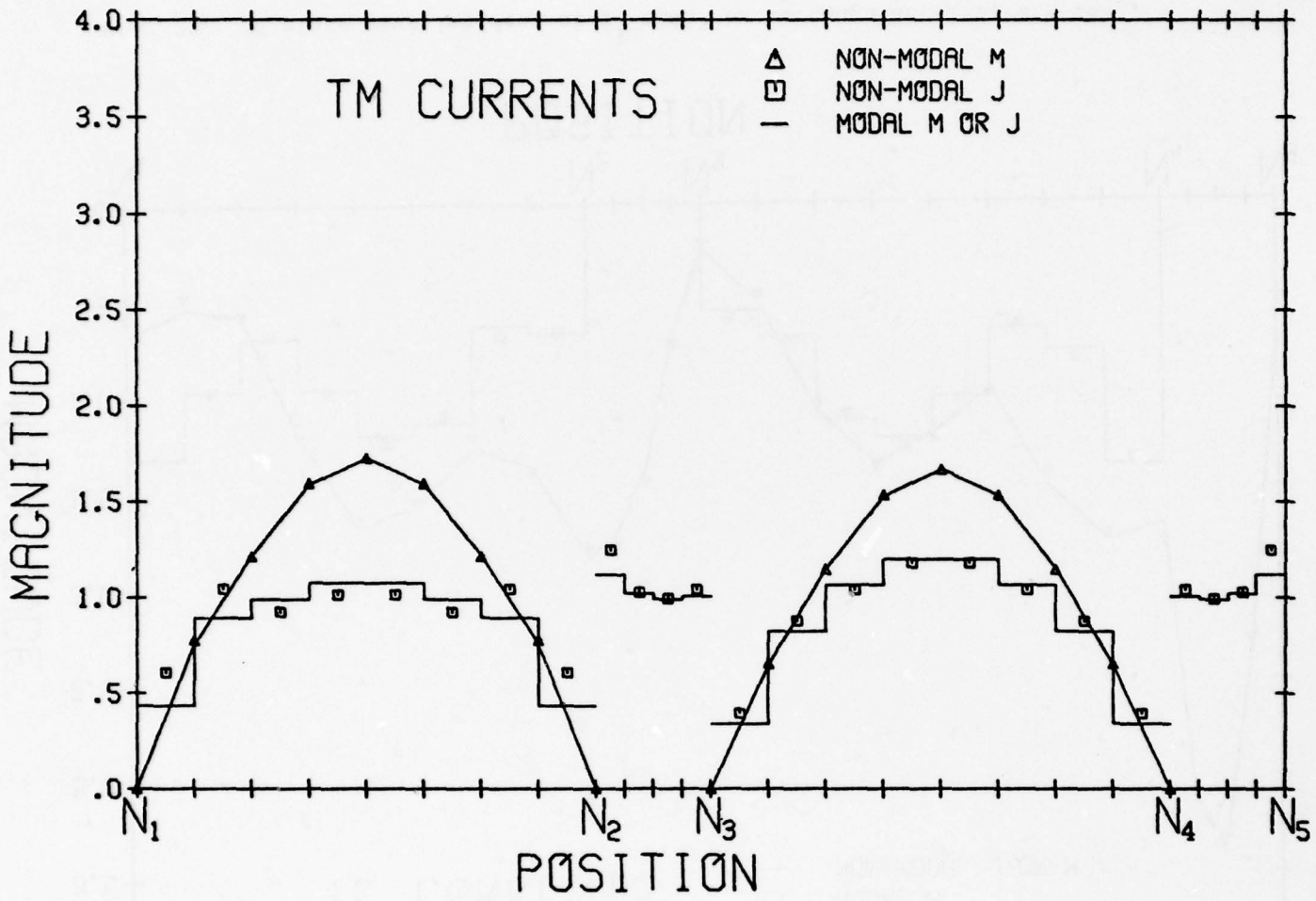

Fig. 21. TM plane wave incident at $\phi^i = 0°$ on rectangular slit, $w = .8\lambda_o$, $d = .2\lambda_o$, $\varepsilon_b = \varepsilon_o$, $\Delta P = 0.05\%$, $J = \eta_o J^b$.

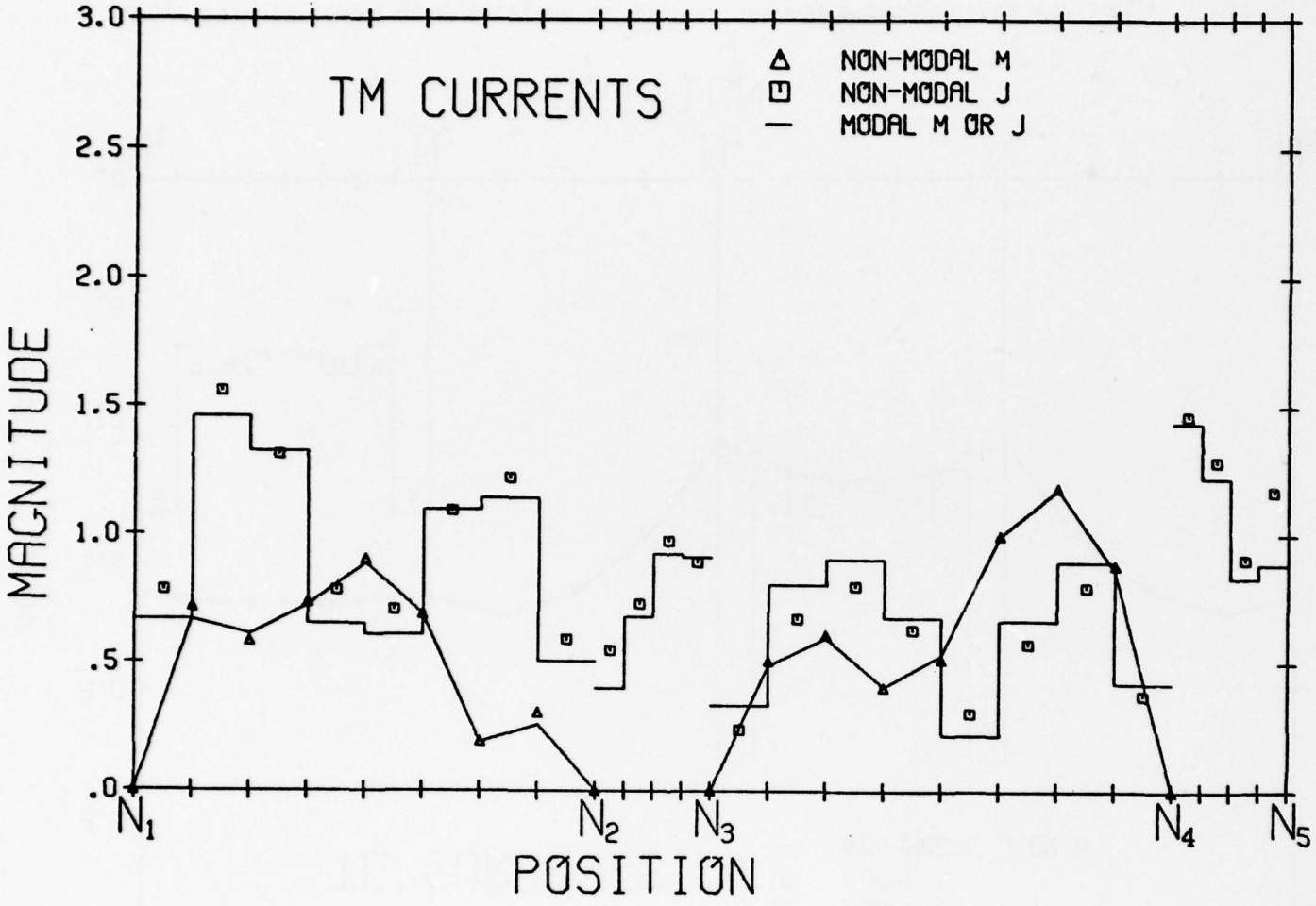

Fig. 22. TM plane wave incident at $\phi^i = 45°$ on rectangular slit, $w = .8\lambda_o$, $d = .2\lambda_o$, $\varepsilon_b = 5\varepsilon_o$, $\Delta P = 0.02\%$, $J = \eta_o J^b$.

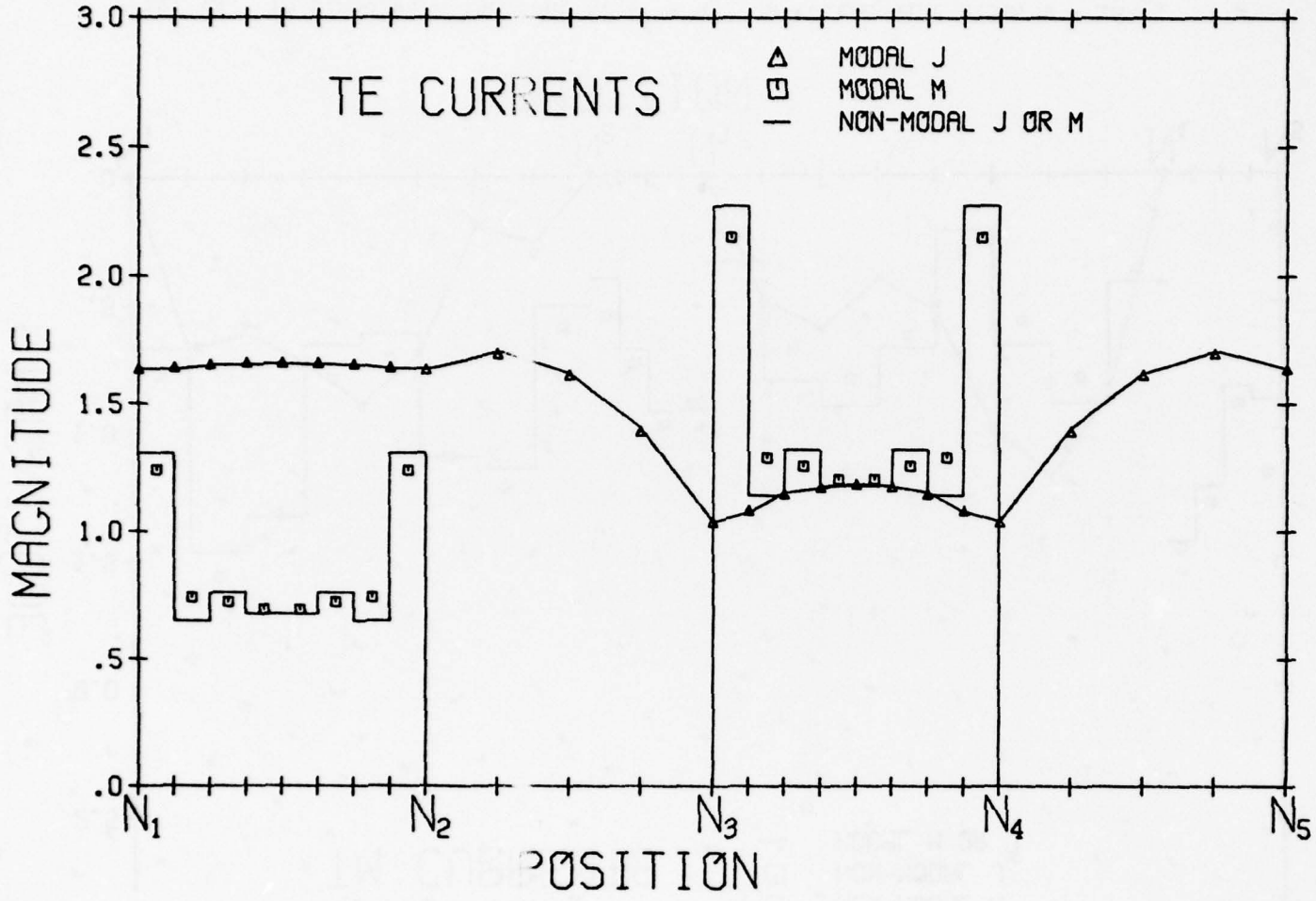

Fig. 23. TE plane wave incident at $\phi^i = 0°$ on rectangular slit, $w = .2\lambda_o$, $d = .2\lambda_o$, $\varepsilon_b = \varepsilon_o$, $\Delta P = 0.41\%$, $J = \eta_o J^b$.

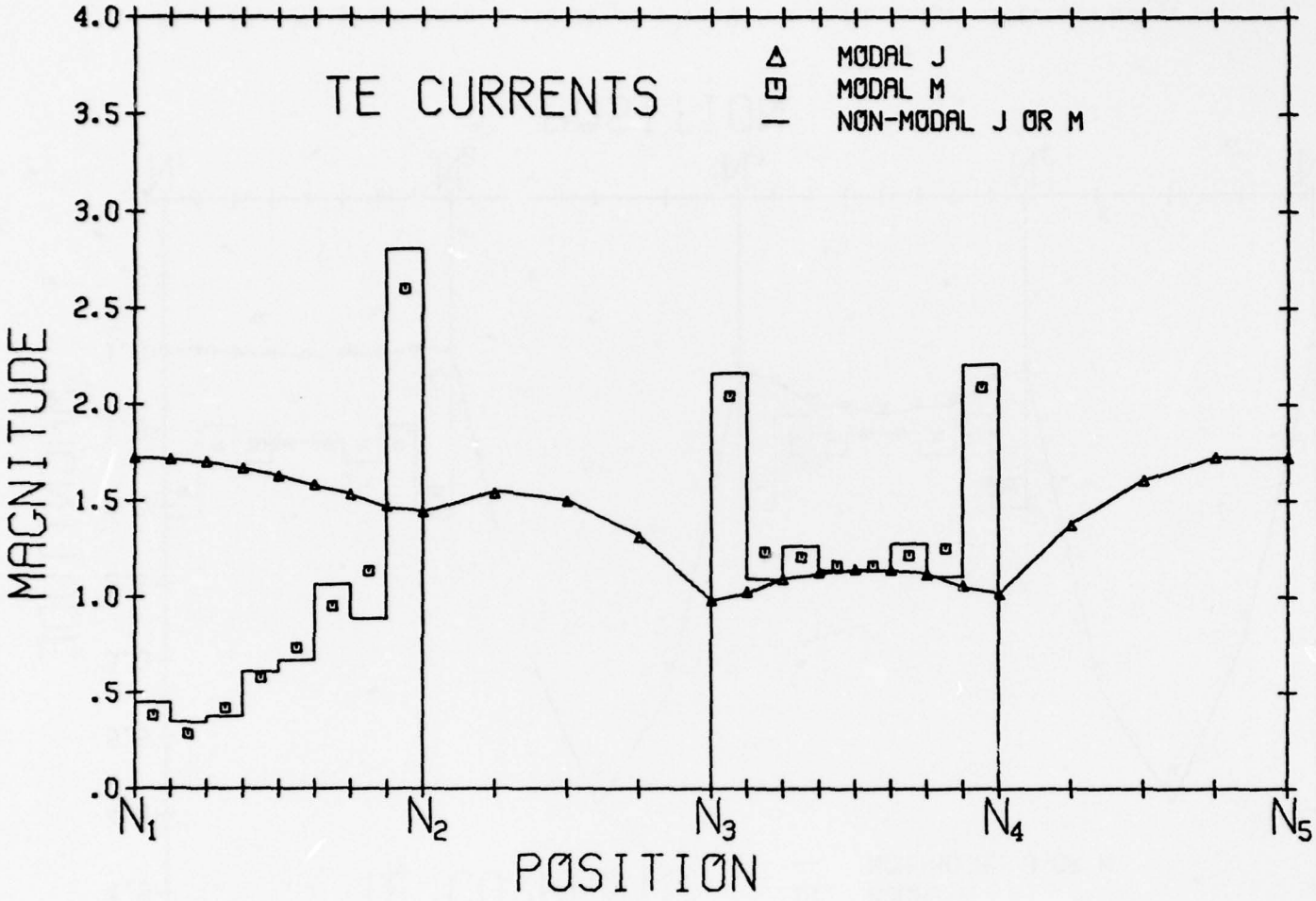

Fig. 24. TE plane wave incident at $\phi^i = 45°$ on rectangular slit, $w = .2\lambda_o$, $d = .2\lambda_o$, $\varepsilon_b = \varepsilon_o$, $\Delta P = 0.35\%$, $J = \eta_o J^b$.

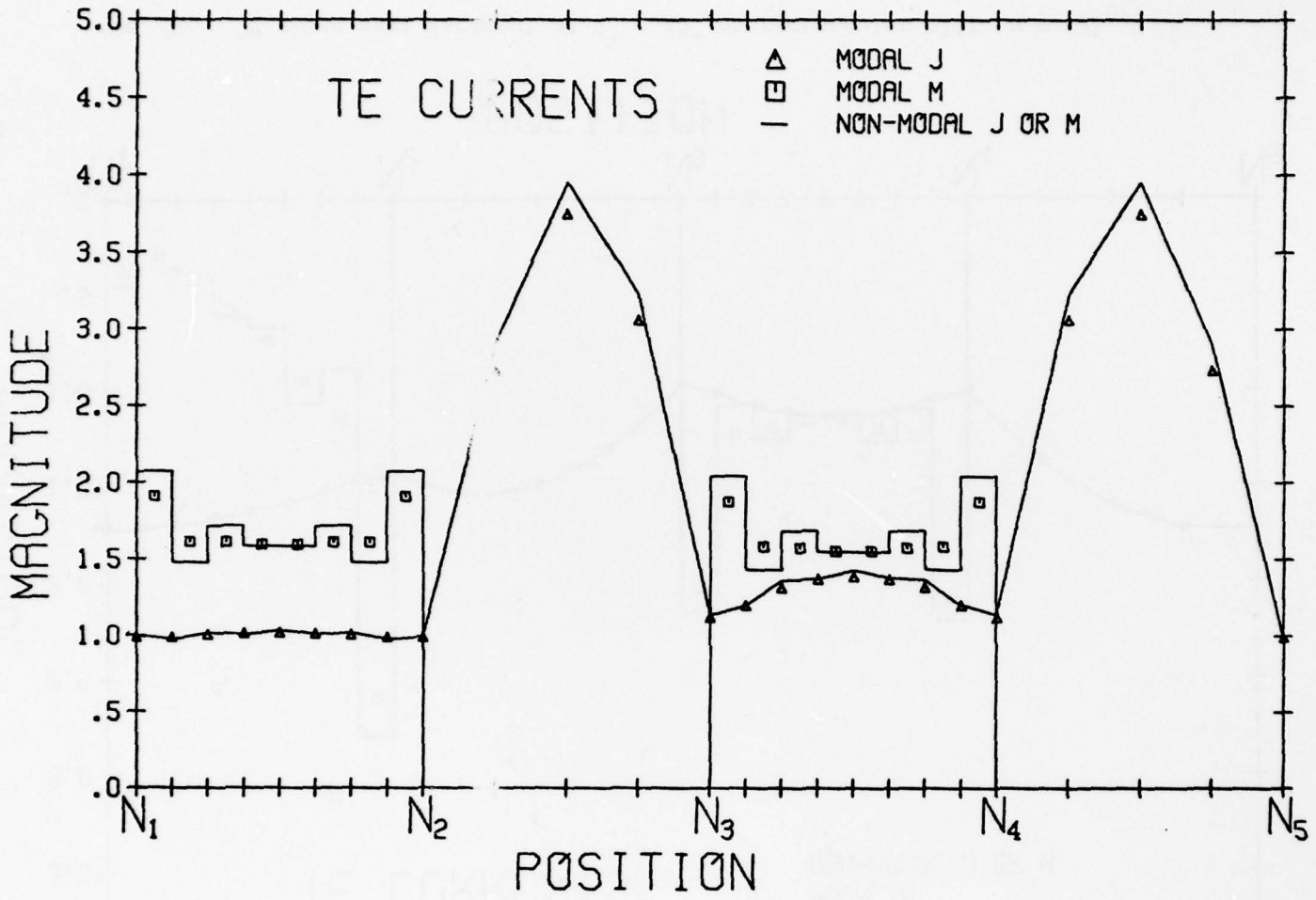

Fig. 25. TE plane wave i ident at $\phi^i = 0°$ on rectangular slit, $w = .2\lambda_o$, $d = .2\lambda_o$, $\varepsilon_b =$ $_o$, $\Delta P = 3.10\%$, $J = \eta_o J^b$.

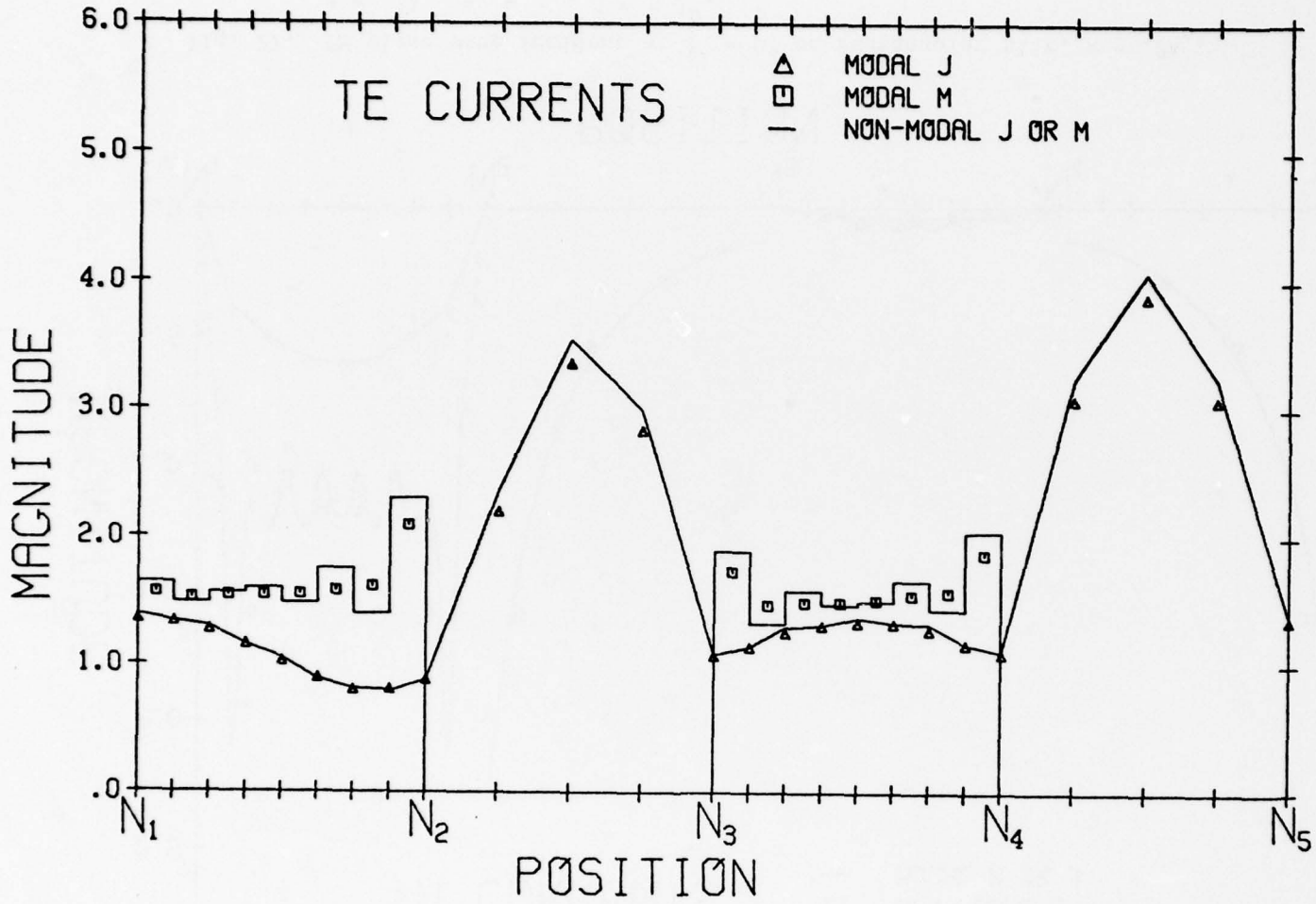

Fig. 26. TE plane wave incident at $\phi^i = 45°$ on rectangular slit, $w = .2\lambda_o$, $d = .2\lambda_o$, $\varepsilon_b = 5\varepsilon_o$, $\Delta P = 2.94\%$, $J = \eta_o J^b$.

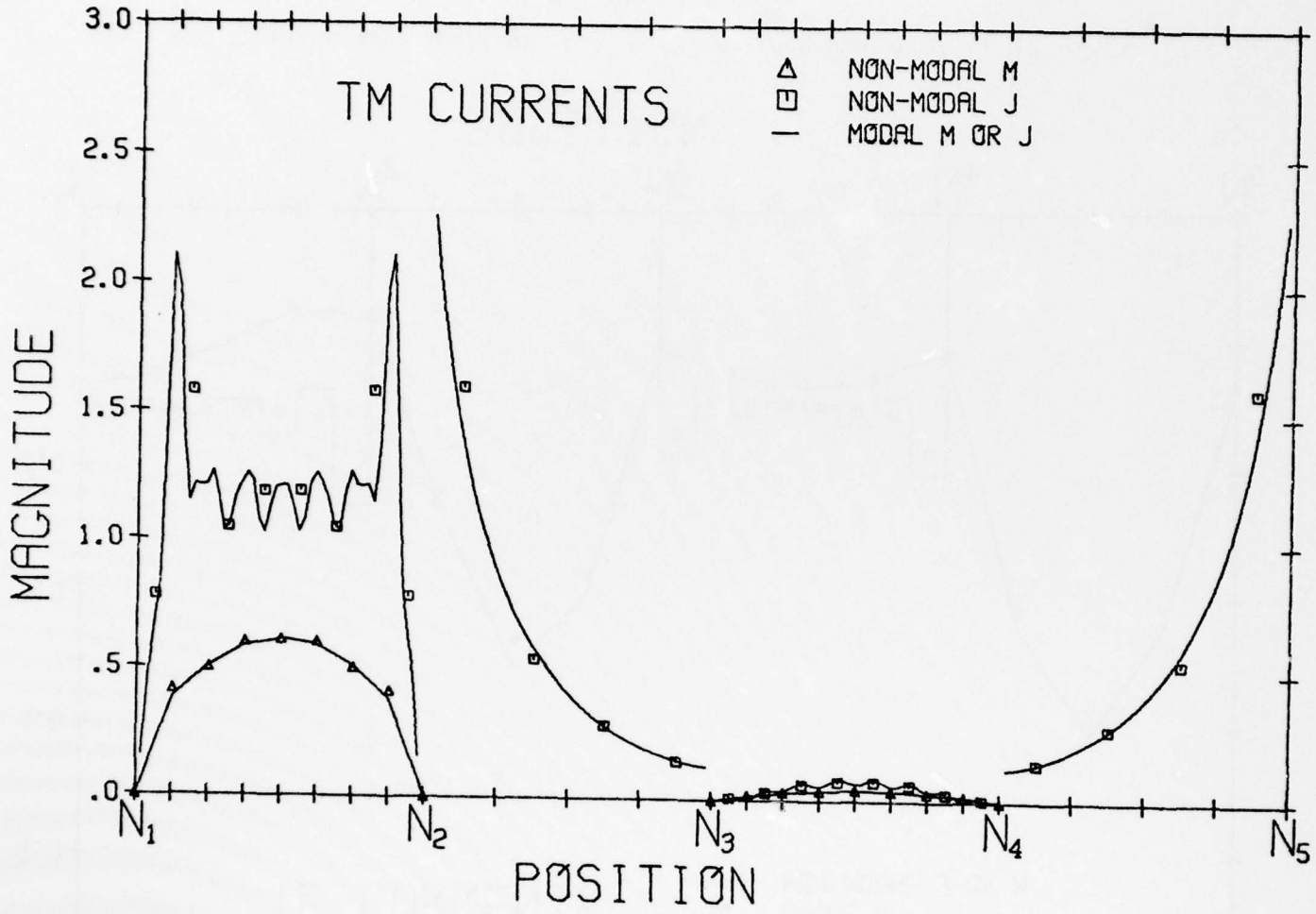

Fig. 27. TM plane wave incident at $\phi^i = 0°$ on rectangular slit, $w = .2\lambda_o$, $d = .2\lambda_o$, $\varepsilon_b = \varepsilon_o$, $J = \eta_o J^b$.

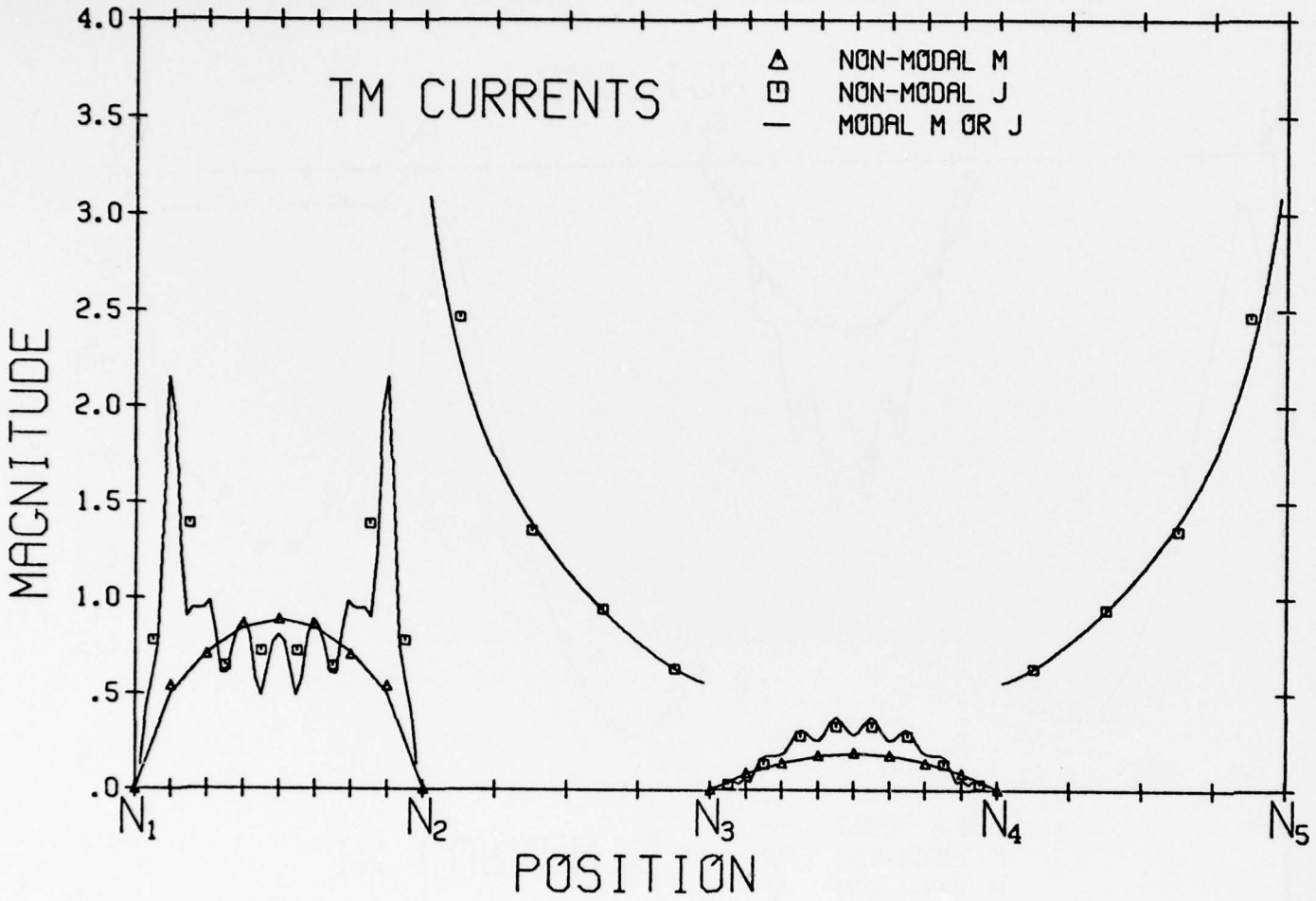

Fig. 28. TM plane wave incident at $\phi^i = 0°$ on rectangular slit, $w = .2\lambda_o$, $d = .2\lambda_o$, $\varepsilon_b = 5\varepsilon_o$, $J = \eta_o J^b$.

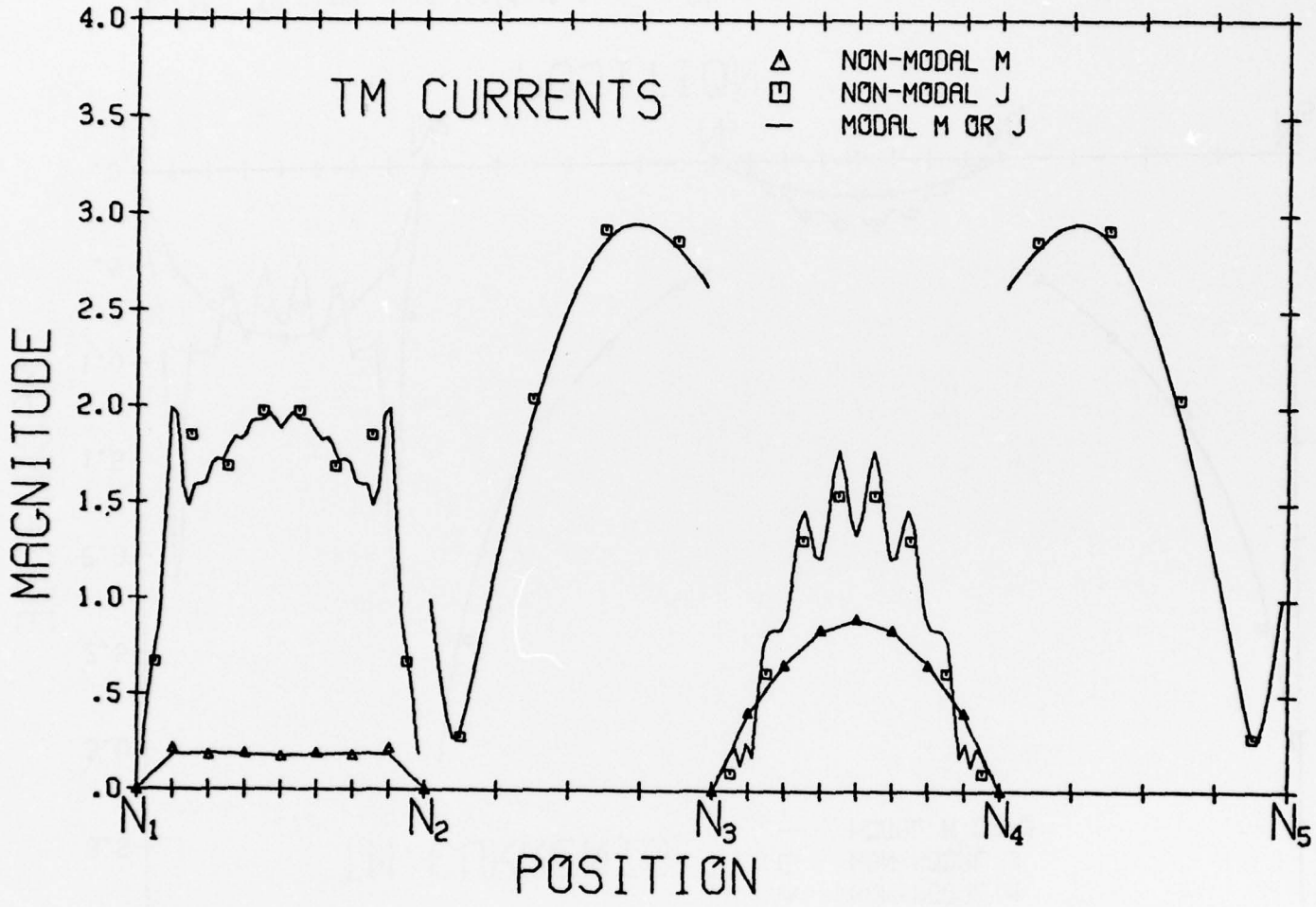

Fig. 29. TM plane wave incident at $\phi^i = 0°$ on rectangular slit, $w = .2\lambda_o$, $d = .2\lambda_o$, $\varepsilon_b = 10\varepsilon_o$, $J = \eta_o J^b$.

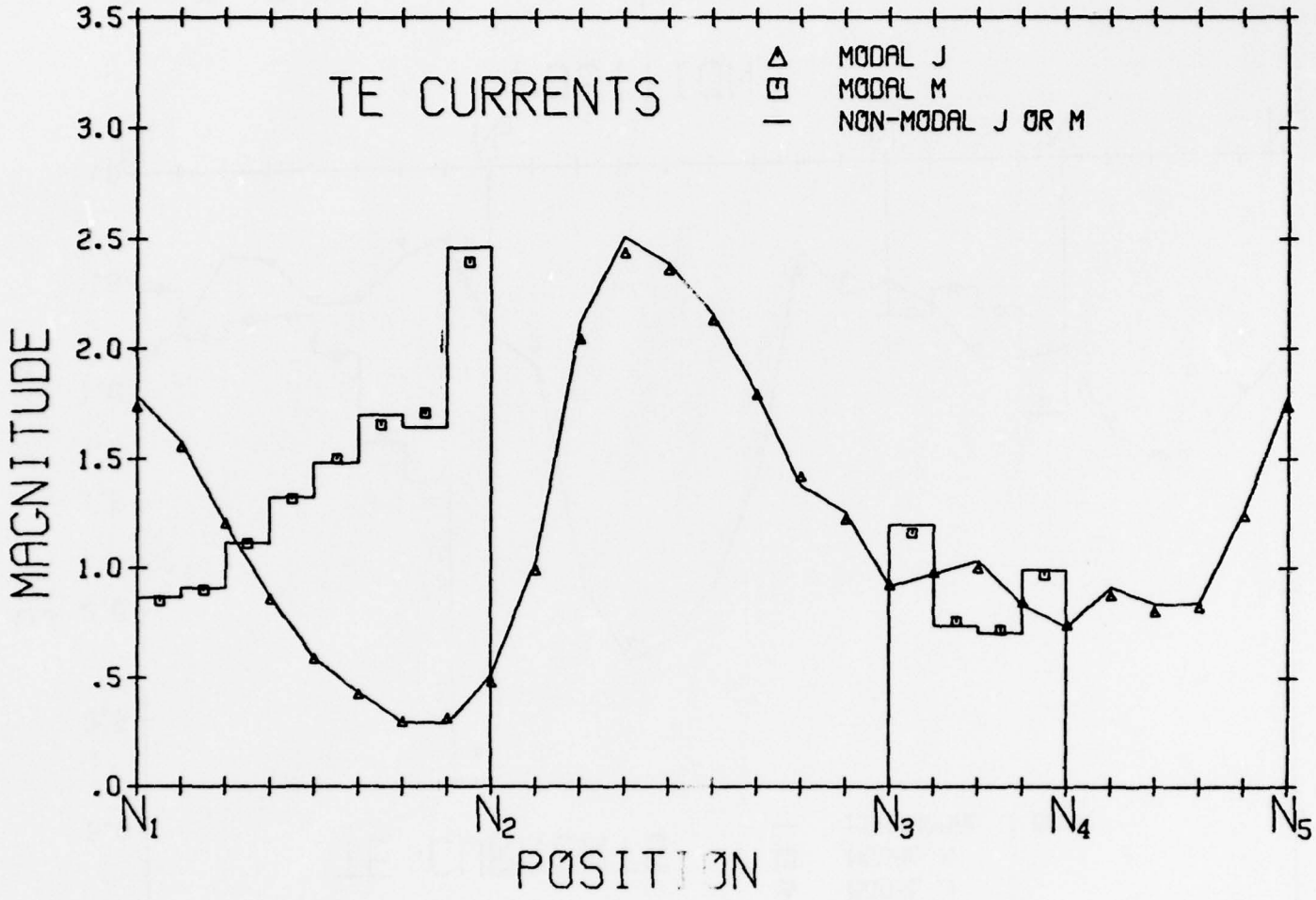

Fig. 30. TE plane wave incident at ϕ^i = 0° on slit of Fig. 15, $\varepsilon_b = \varepsilon_o$, ΔP = 1.49%, $J = \eta_o J^b$.

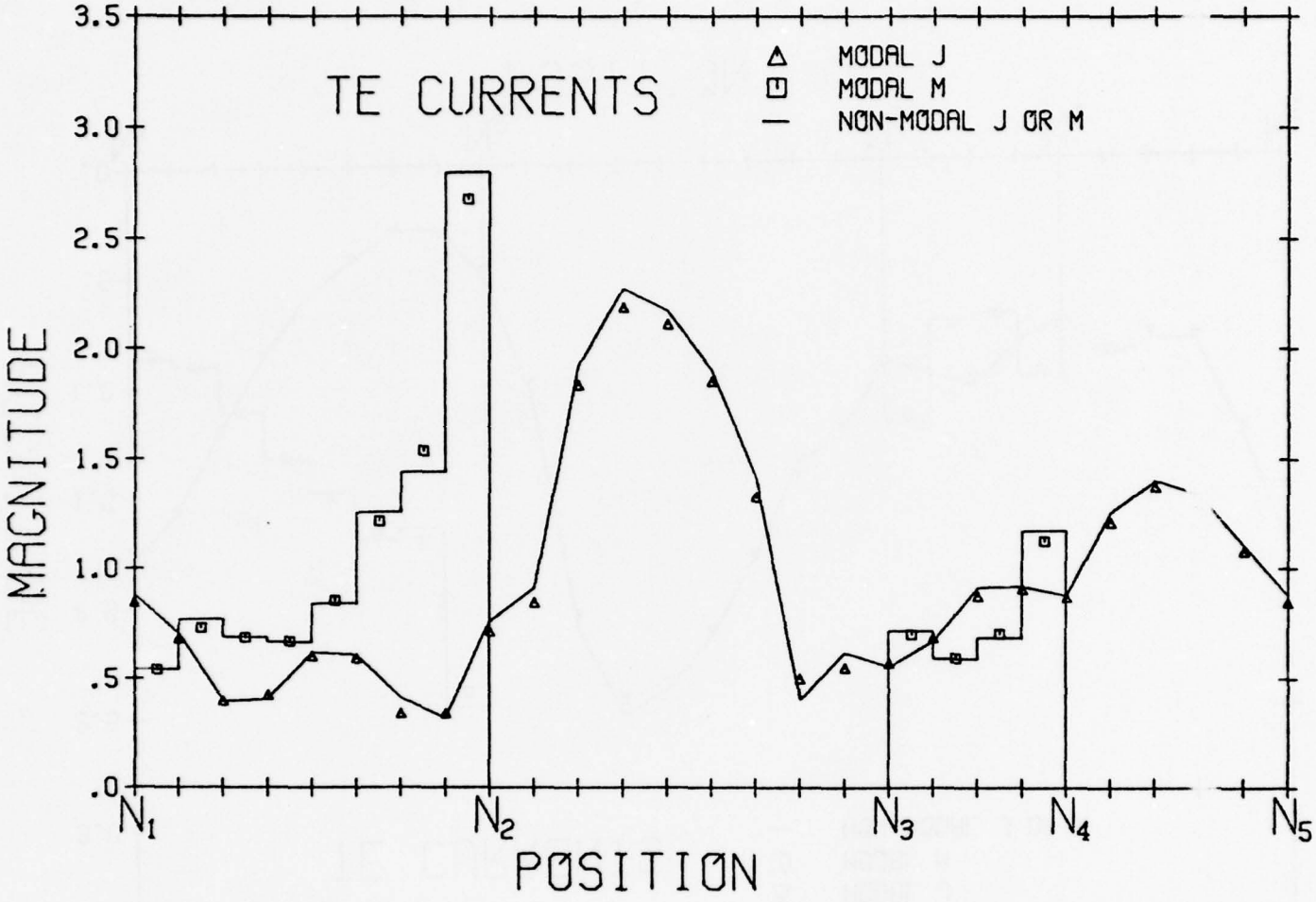

Fig. 31. TE plane wave incident at $\phi^i = 60°$ on slit of Fig. 15, $\varepsilon_b = \varepsilon_o$, $\Delta P = 0.57\%$, $J = \eta_o J^b$.

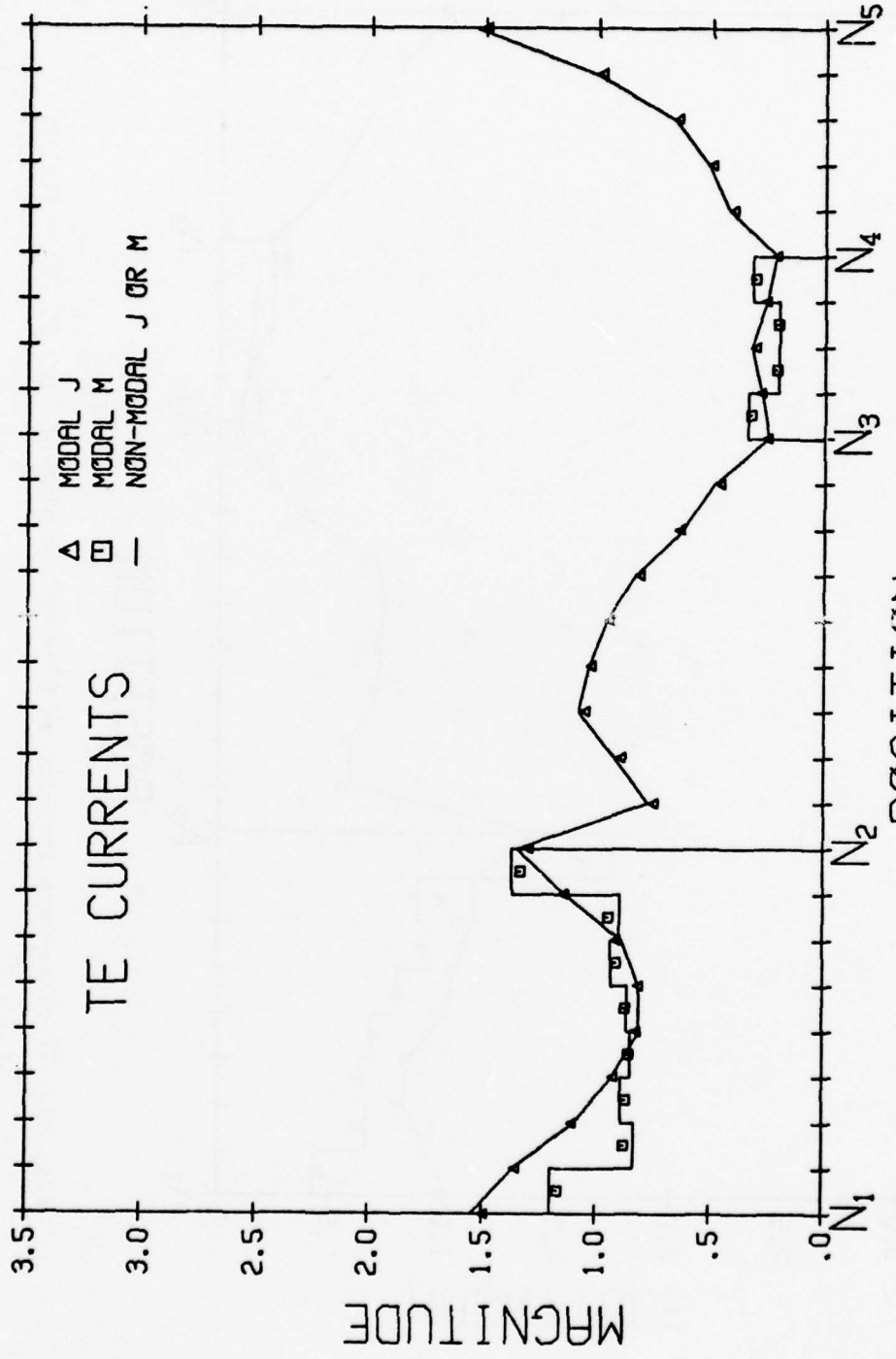

Fig. 32. TE plane wave incident at $\phi^i = 0°$ on slit of Fig. 15, $\epsilon_b = (1-j)\epsilon_o$, $J = \eta_o J^b$.

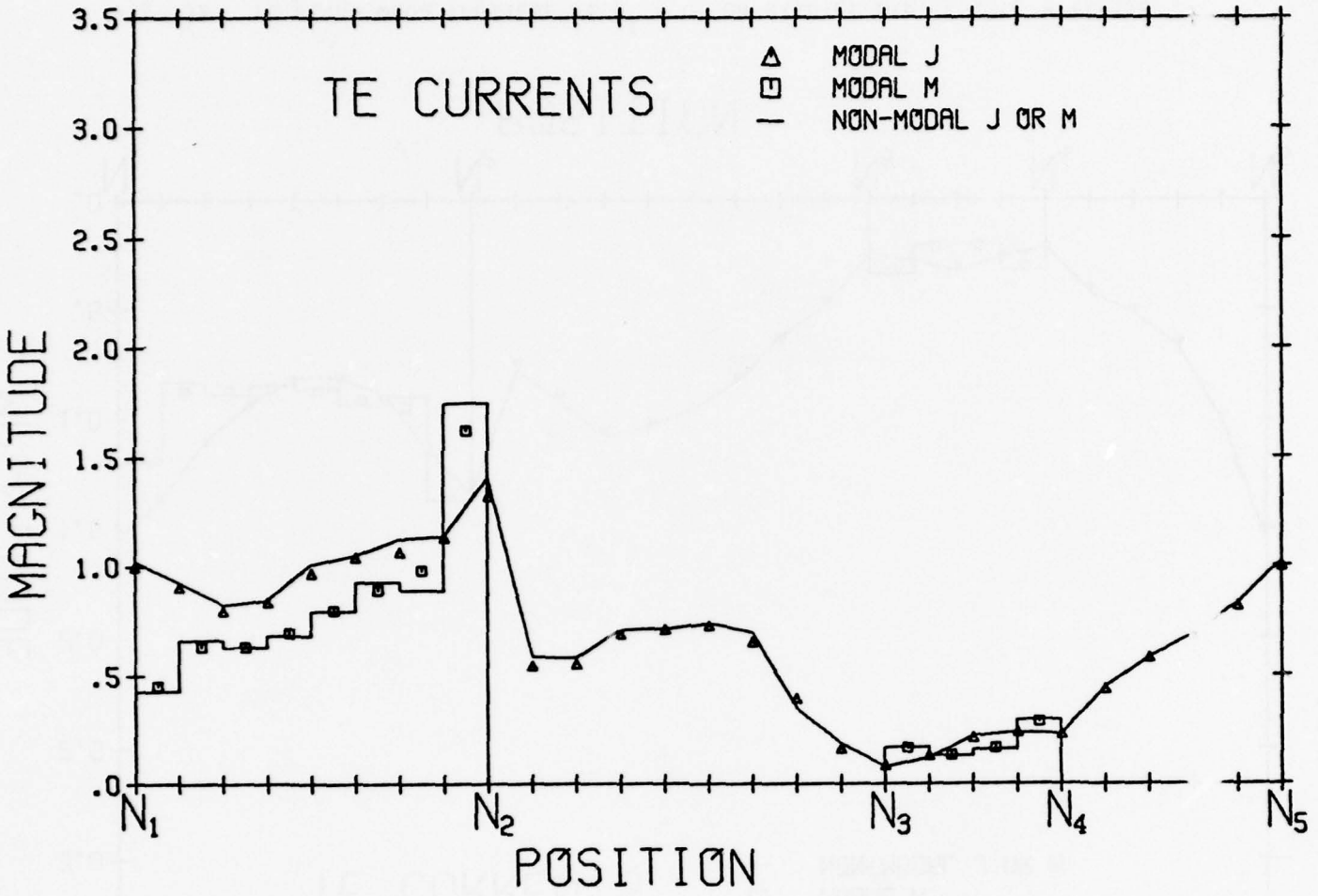

Fig. 33. TE plane wave incident at $\phi^i = 60°$ on slit of Fig. 15, $\varepsilon_b = (1-j)\varepsilon_o$ $J = \eta_o J^b$.

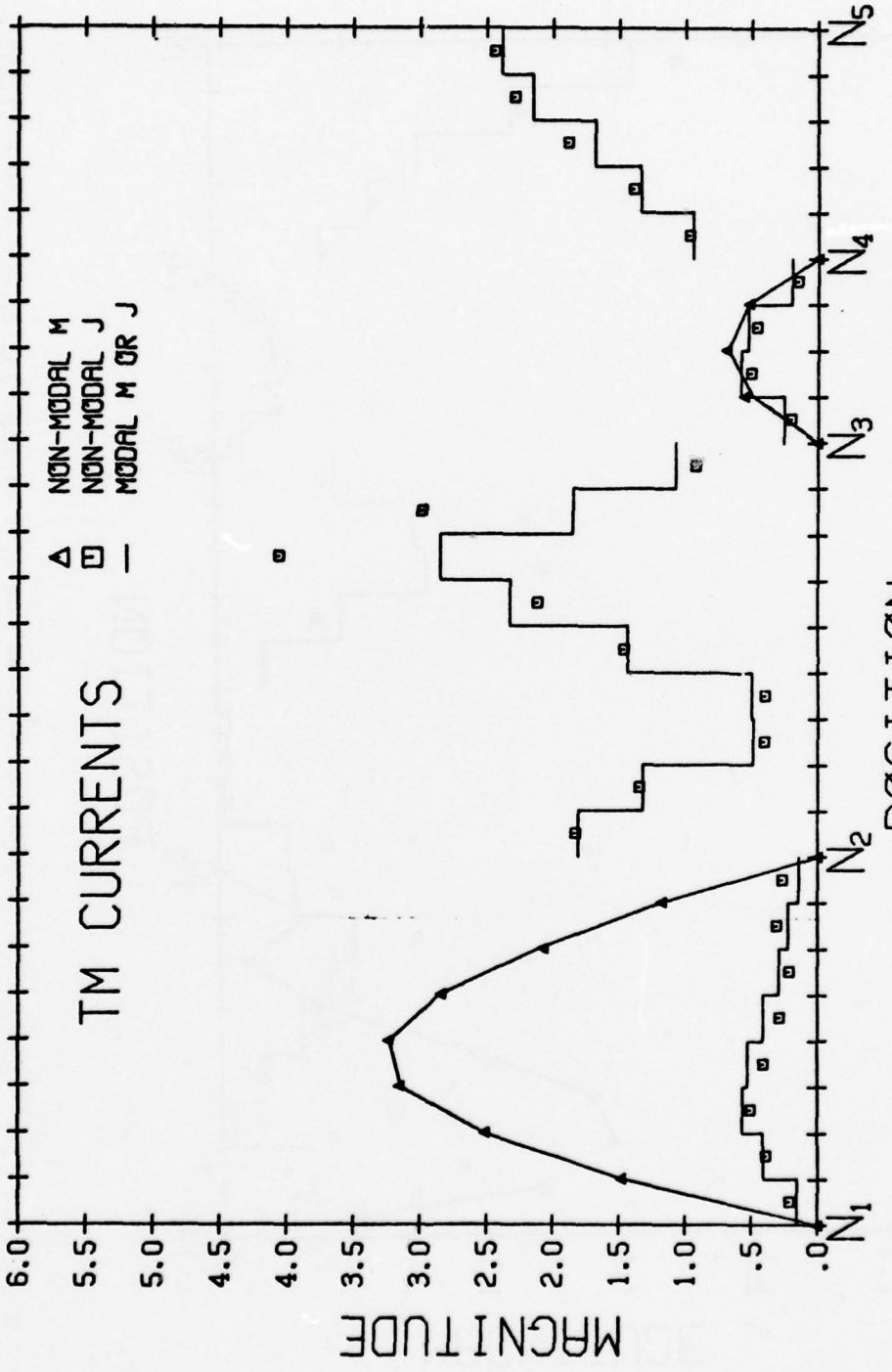

Fig. 34. TM plane wave incident at $\phi^i = 0°$ on slit of Fig. 15, $\varepsilon_b = \varepsilon_o$, $\Delta P = 2.88\%$, $J = \eta_o J^b$.

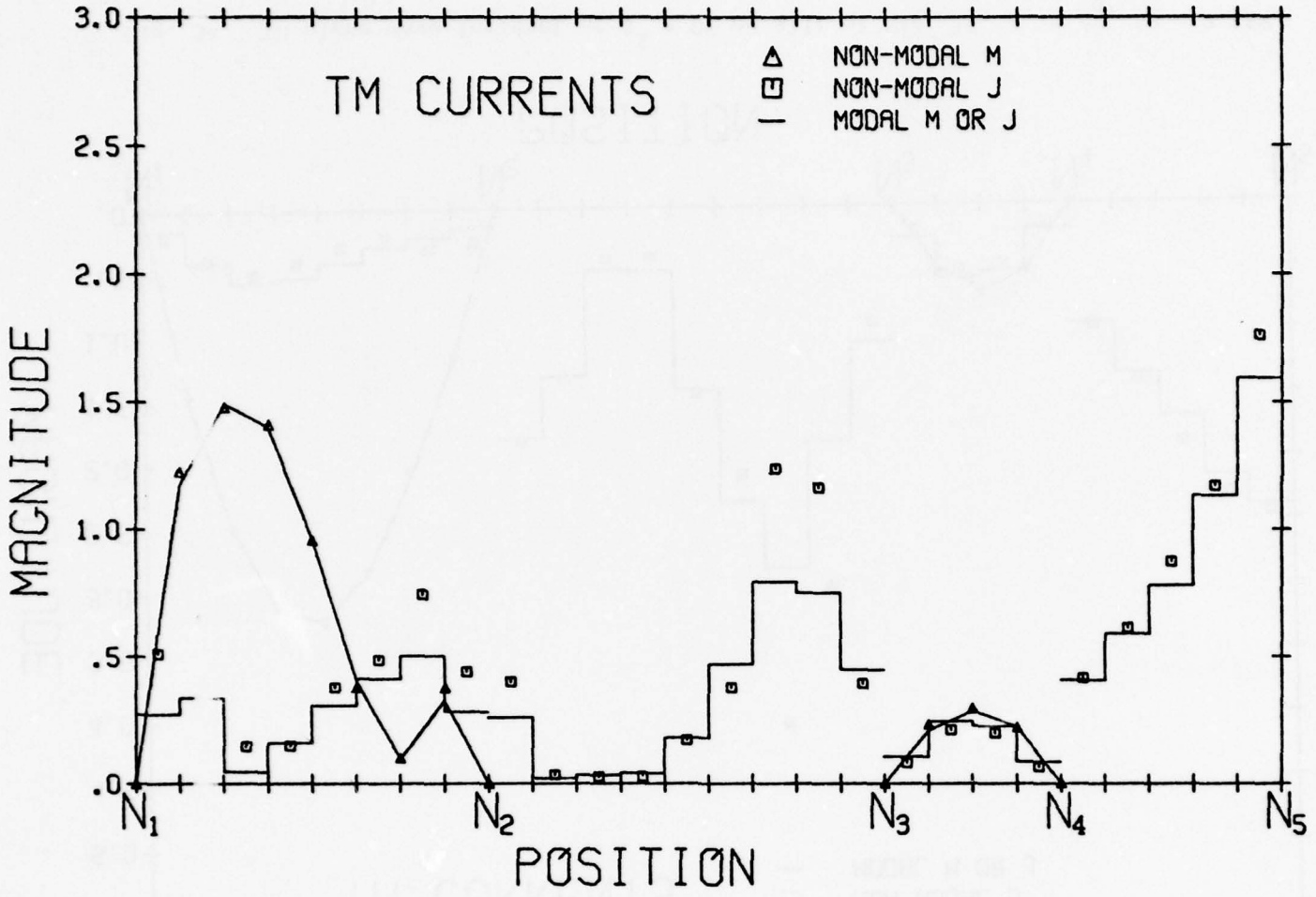

Fig. 3[illegible]. TM plane wave incident at $\phi^i = 60°$ on slit of Fig. 15, $\varepsilon_b = \varepsilon_o$, $\Delta P = 17.25\%$, $J = \eta_o J^b$.

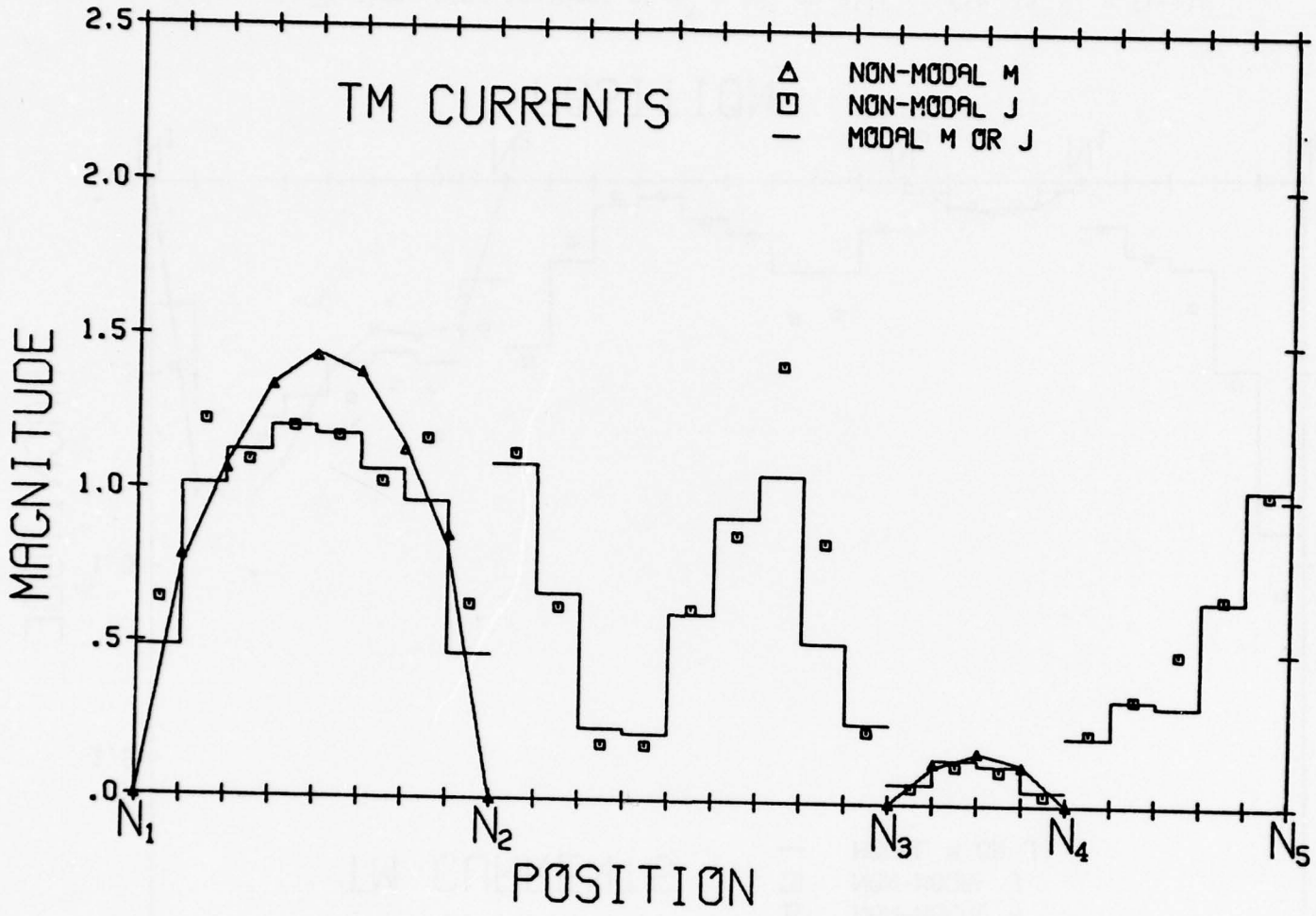

Fig. 36. TM plane wave incident at $\phi^i = 0°$ on slit of Fig. 15, $\varepsilon_b = (1-j)\varepsilon_o$, $J = \eta_o J^b$.

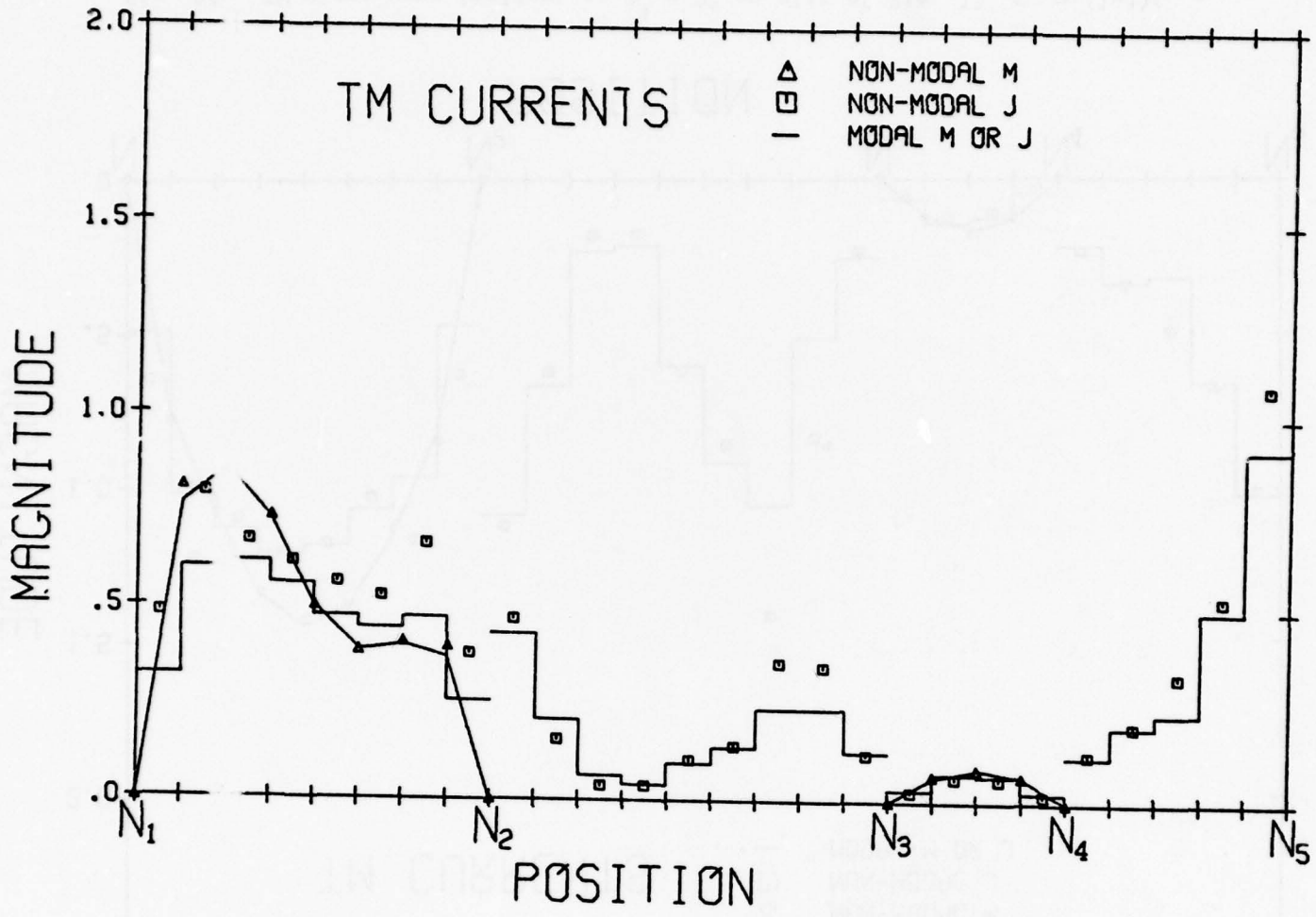

Fig. . TM plane wave incident at $\phi^i = 60°$ on slit of Fig. 15, $\varepsilon_b = (1-j)\varepsilon_o$, $J = \eta_o J^b$.

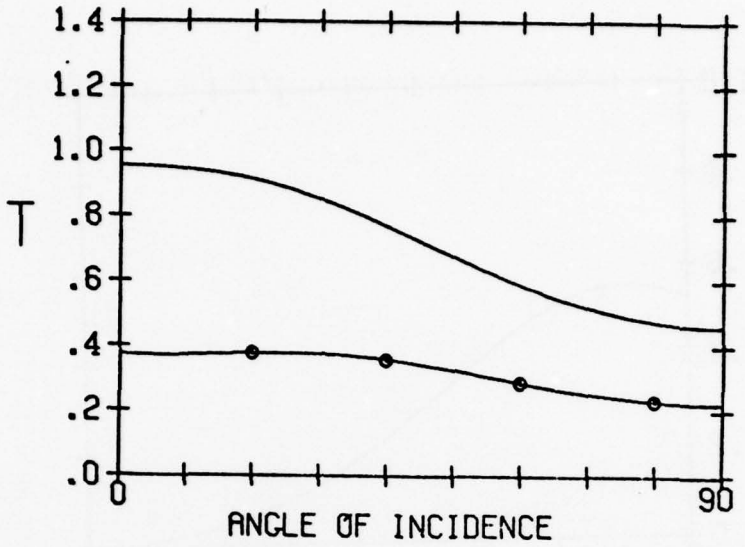

Fig. 38. TE Transmission coefficients vs. ϕ^i for slit of Fig. 15 (circles) and rectangular slit $w = .8\lambda_o$, $d = .5\lambda_o$, $\varepsilon_b = \varepsilon_o$.

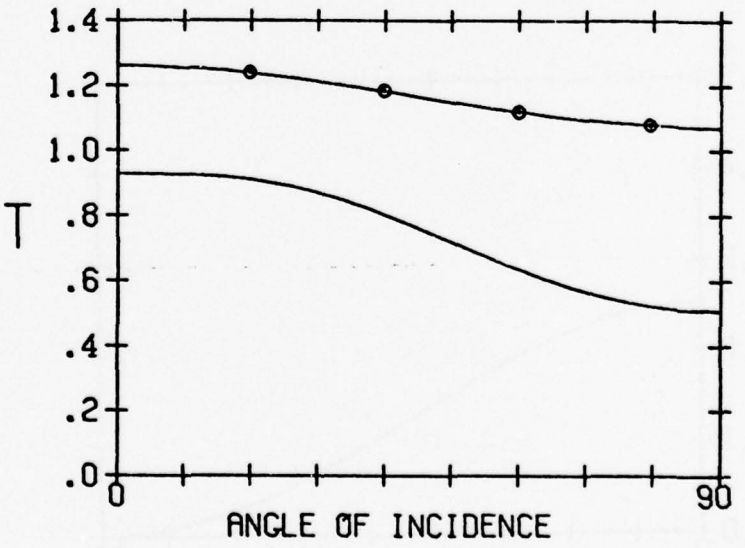

Fig. 39. TE transmission coefficients vs. ϕ^i for rectangular slit $w = .2\lambda_o$, $d = .2\lambda_o$ (circles) and rectangular slit $w = .8\lambda_o$, $d = .2\lambda_o$, $\varepsilon_b = \varepsilon_o$.

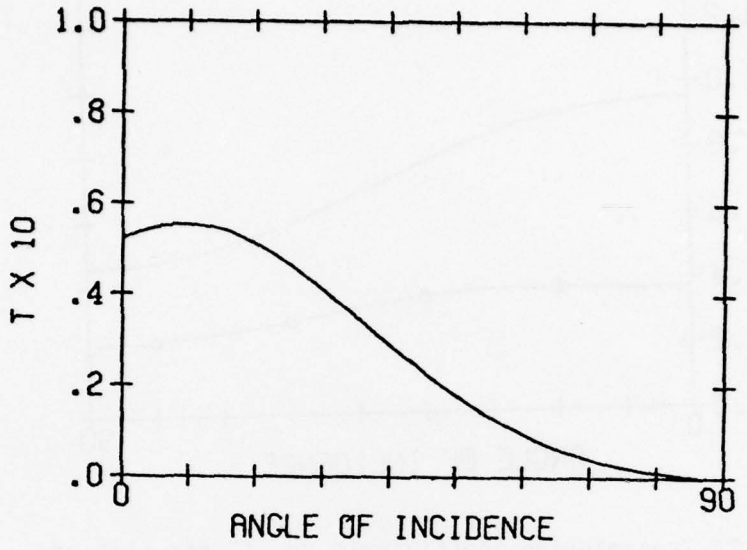

Fig. 40. TM transmission coefficient vs. ϕ^i for slit of Fig. 15, $\varepsilon_b = \varepsilon_o$.

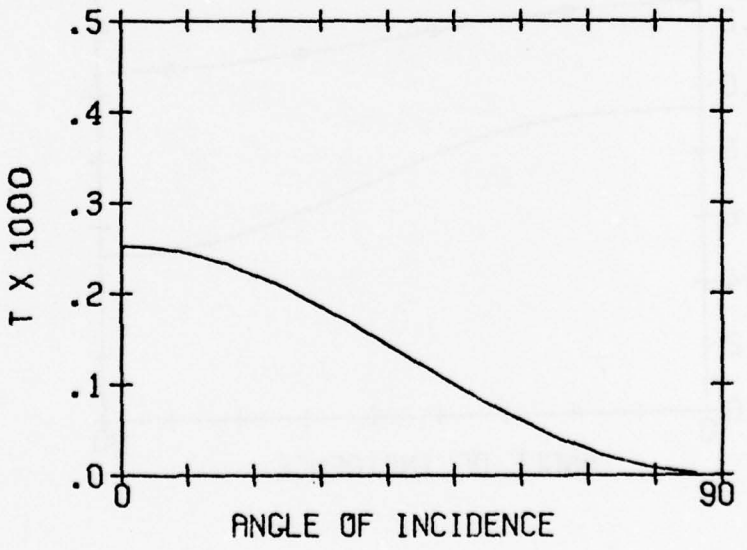

Fig. 41. TM transmission coefficient vs. ϕ^i for rectangular slit $w = .2\lambda_o$, $d = .2\lambda_o$, $\varepsilon_b = \varepsilon_o$.

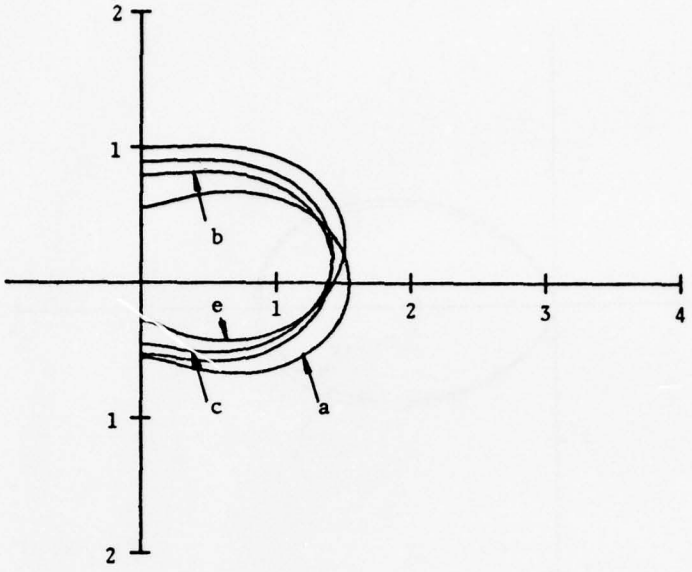

GAIN PATTERN

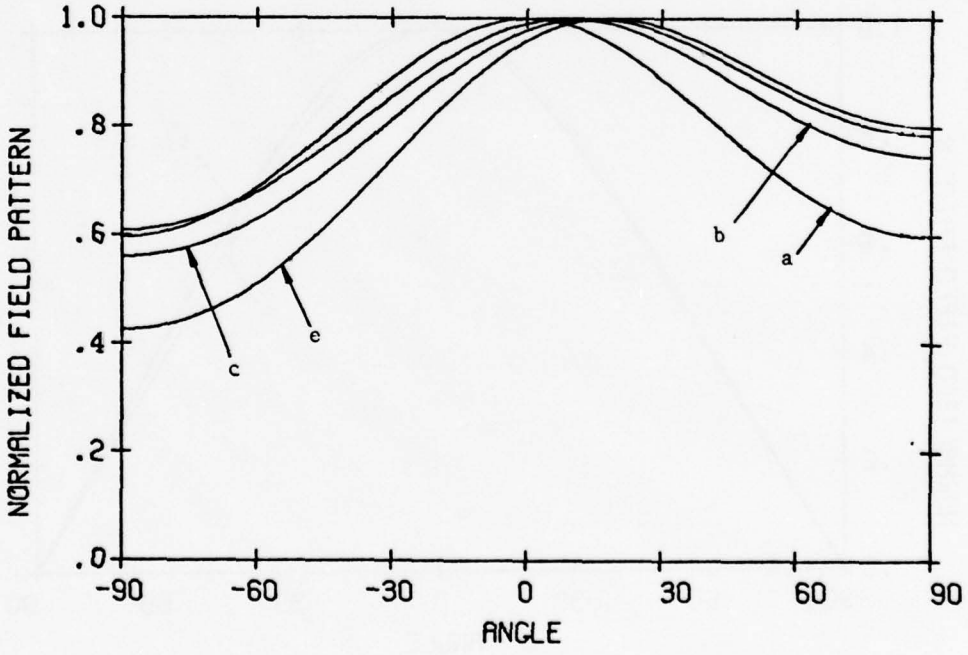

Fig. 42. TE gain and normalized field patterns for slits of Figs. 16a, b, c, and e for $\phi^i = 0°$.

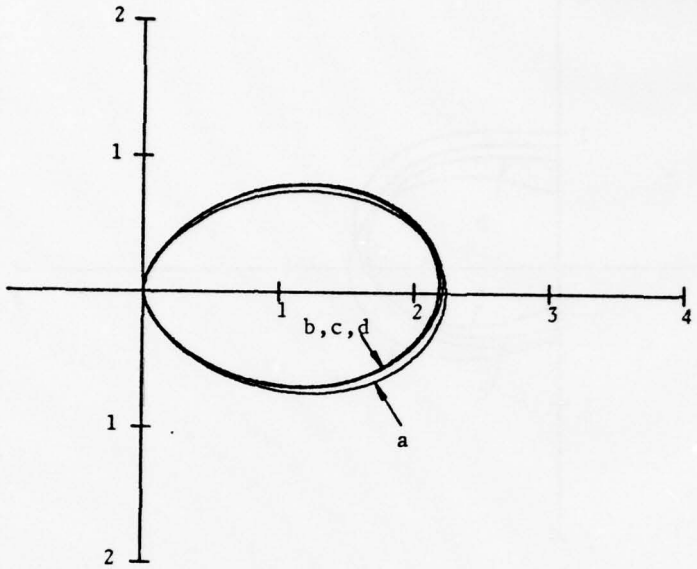

GAIN PATTERN

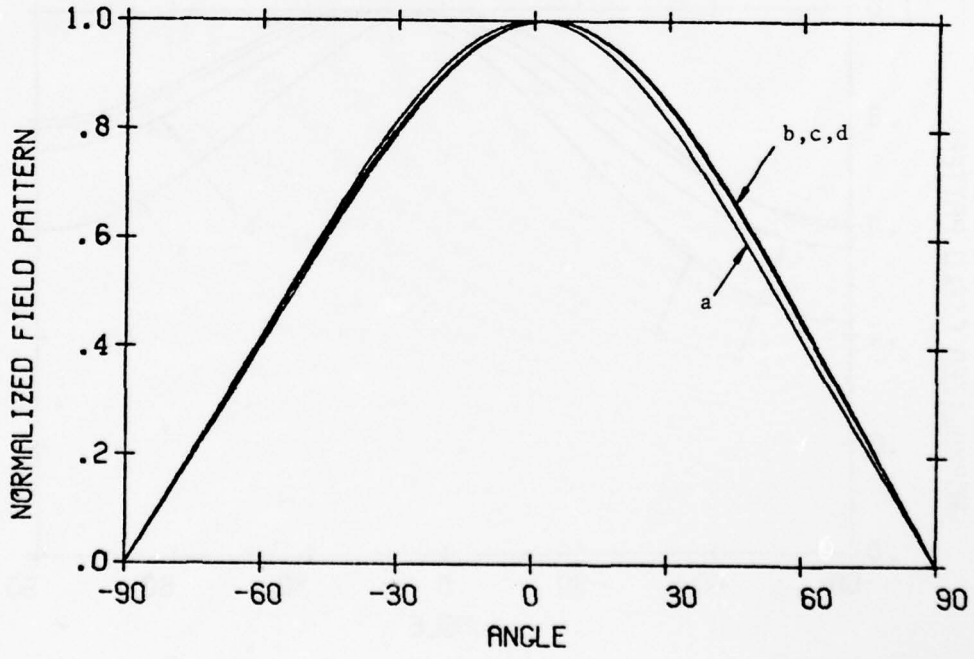

Fig. 43. TM gain and normalized field patterns for slits of Figs. 16a, b, c, and d for $\phi^i = 0°$.

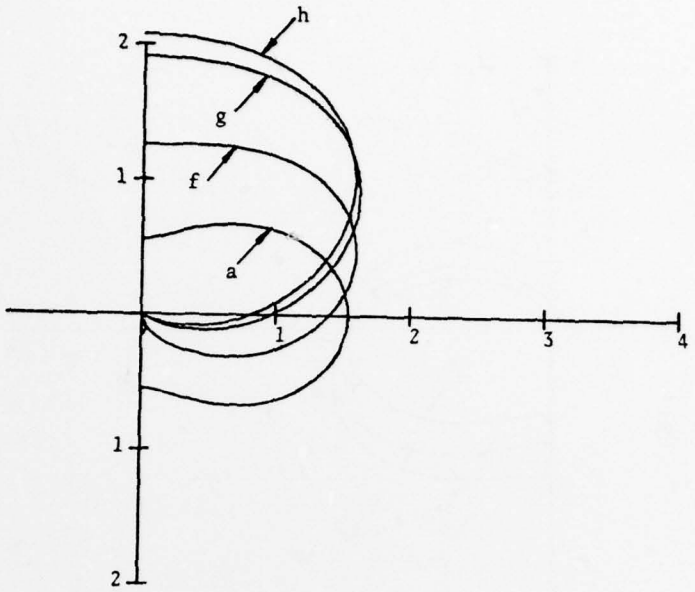

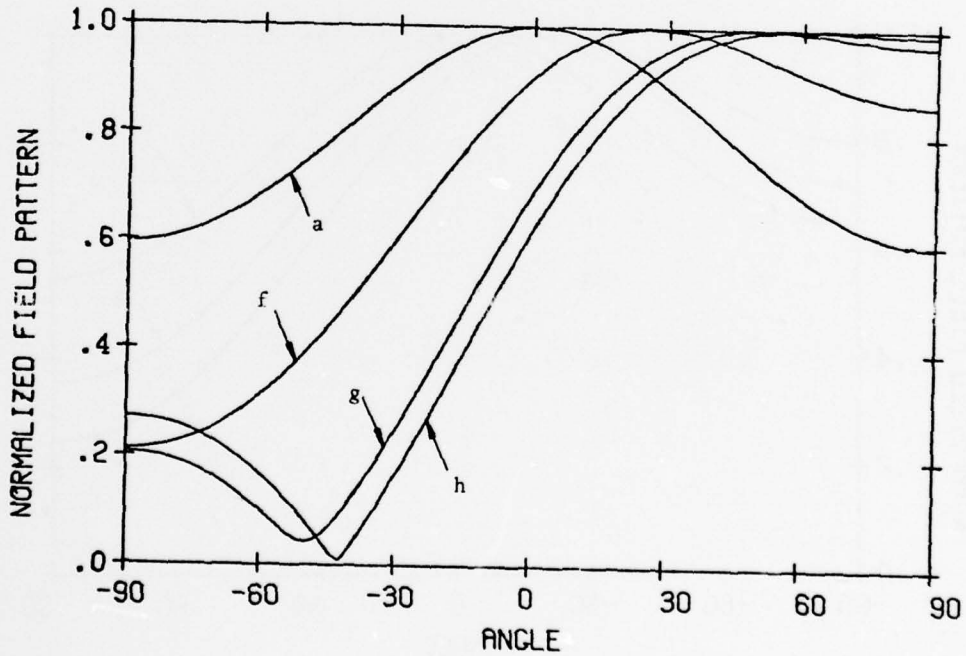

Fig. 44. TE gain and normalized field patterns for slits of Figs. 16a, f, g, and h for $\phi^i = 0°$.

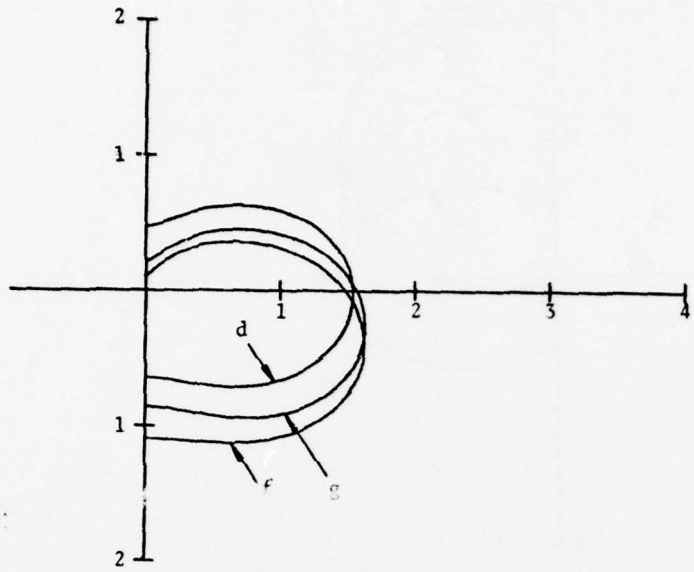

GAIN PATTERN

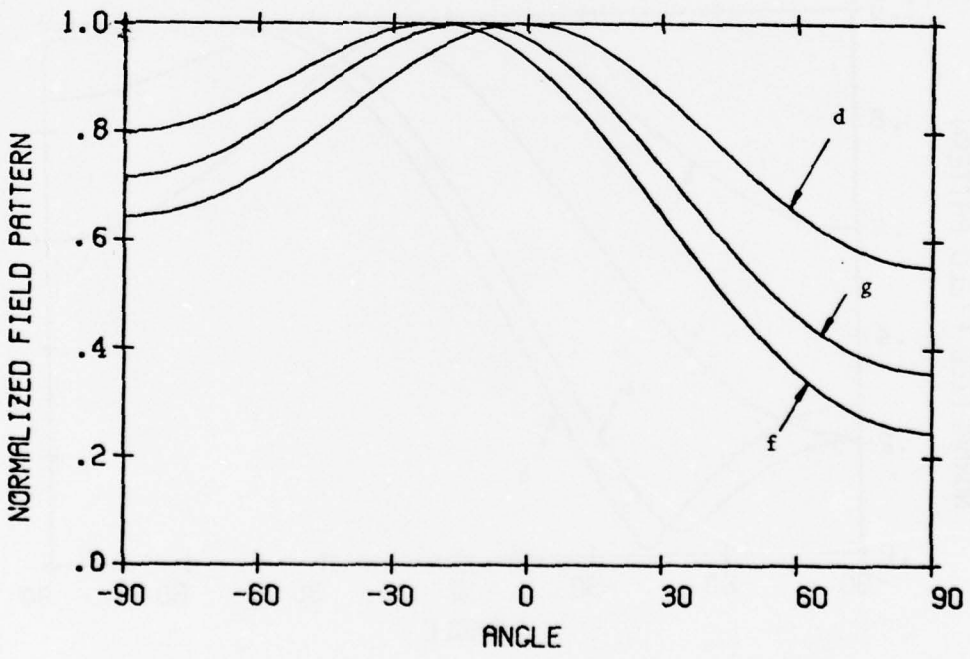

Fig. 45. TE gain and normalized field patterns for slits of Figs. 16 d, f, and g for $\phi^i = 45°$.

8.2. Slit Impedance and Equivalent Circuit for TE Case

When the slit cross section is rectangular, several approximate solutions for the transmission characteristics are readily available after making suitable assumptions. The first cases considered are when regions a, b, and c are filled with free space and the slit width w is such that $k_o w << 1$. As discussed in Chapter 5, the transmission characteristics may then be determined from a slit impedance for the TE case, and a slit polarizability for the TM case. The TE case is very important in electromagnetic shielding problems since there is always a propagating mode in the waveguide region b. If the condition $k_o w << 1$ is satisfied and $d > w$ then the two assumptions are made:

1) Each half space may be represented by a lumped impedance.

2) Region b behaves like a uniform transmission line.

This suggests the equivalent circuit shown in Fig. 46. Regions a and c

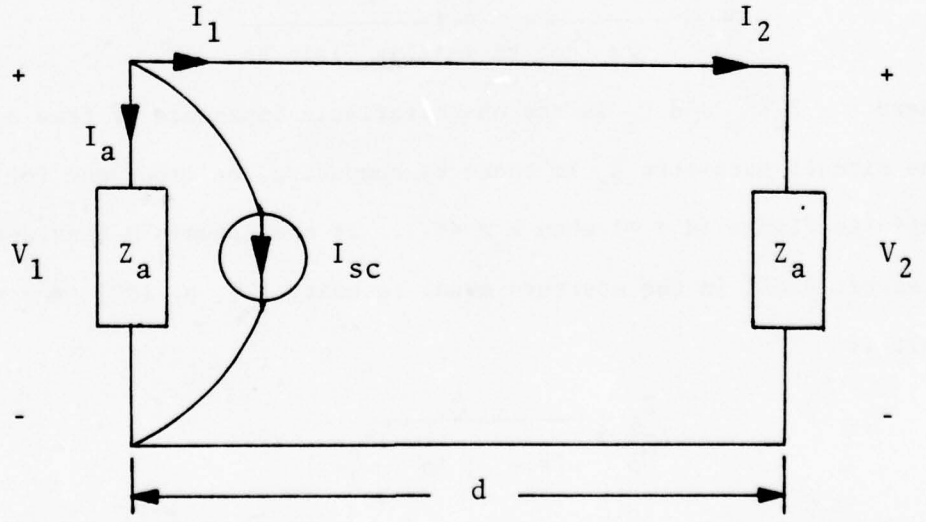

Fig. 46. Equivalent circuit model for rectangular slit when $k_o w << 1$.

are identical and are represented by the lumped impedance Z_a which is defined by

$$Z_a = \frac{V_1}{I_a} = \frac{V_2}{I_2} \tag{8-2}$$

The excitation, I_{sc}, is equal to the negative of the electric current which would exist at Γ_1 if Γ_1 were completed by a perfect electric conductor. This is a form of the equivalence principle used by Collin [30]. The voltages V_1 and V_2 are obtained by integrating the electric field (magnetic currents) across the aperture faces Γ_1 and Γ_3 respectively. It is desired to find the slit impedance defined by Eq. (5-28) which may be rewritten in terms of the equivalent circuit parameters as

$$Z = \frac{V_2}{I_{sc}} \tag{8-3}$$

From transmission line theory, one may easily obtain

$$\frac{Z}{\eta_o} = -\frac{1}{2z^{-1}\cos kd + j(1+z^{-2})\sin kd} \tag{8-4}$$

where $z = Z_a/\eta_o$ and η_o is the characteristic impedance of free space. The circuit parameter Z_a is found by computing the impedance for an infinite flange ($d \to \infty$) when $k_o w << 1$. If one assumes a constant electric field in the aperture equal to unity [24, p. 180], the result is

$$\frac{Z_a}{\eta_o} = \frac{\lambda_o}{w[\pi - 2j \ln (\frac{\gamma k_o w}{2e^2})]} \tag{8-5}$$

where $\gamma = 1.781$ and $e = 2.71828...$ Another formula, based on a static

solution of the flange problem, is given by [31]

$$\frac{Z_a}{\eta_o} = \frac{\lambda_o}{w[\pi - 2j \ln (\frac{\gamma k_o w}{e\pi})]} \tag{8-6}$$

For comparison purposes, one last formula is obtained which uses the assumption that the electric field in the aperture is that obtained for a slit in a zero thickness conducting plane [32] and is given by

$$\frac{Z_a}{\eta_o} = \frac{\lambda_o}{w[\pi - 2j \ln (\frac{\gamma k_o w}{8})]} \tag{8-7}$$

For $k_o w$ small enough, there is little difference between these formulas.

The transmission coefficient may also be obtained from the equivalent circuit by determining the power delivered to the load Z_a at the distance d and dividing by the power delivered to the circuit by I_{sc} when $Z_a = \eta_o$. Thus one may obtain

$$T = \frac{4}{\eta_o} |Z|^2 \, \mathrm{Re}\{1/Z_a\} \tag{8-8}$$

Some plots of Z/η_o and T versus d/λ_o are shown in Figs. 47-49 for rectangular slits of various widths. The solid curves represent computations from the equivalent circuit in Fig. 46 where Z_a is determined from Eq. (8-7). Circles and triangles are used to mark results obtained from the modal solution of the rectangular slit computed for each value of w and d. Agreement is excellent for slits whose widths are even as large as $0.2\lambda_o$. For wider slits, the slit impedance Z loses its usefulness since it can no longer accurately

determine the transmitted fields.

It is interesting to note that, as w becomes smaller, the transmission coefficient tends to a peak value when d is close to a multiple of $\lambda_o/2$. These peaks approach a value of $1/w\pi$ for small w which can be shown from the equivalent circuit. This behavior is predictable in that a resonance condition is achieved when the reactance of Z_a, at the distance d, cancels that of Z_a at the source I_{sc}. Thus, even though very little incident energy impinges upon the slit for small w, the transmission coefficient may be quite large for some thickness d when compared to the d = 0 case.

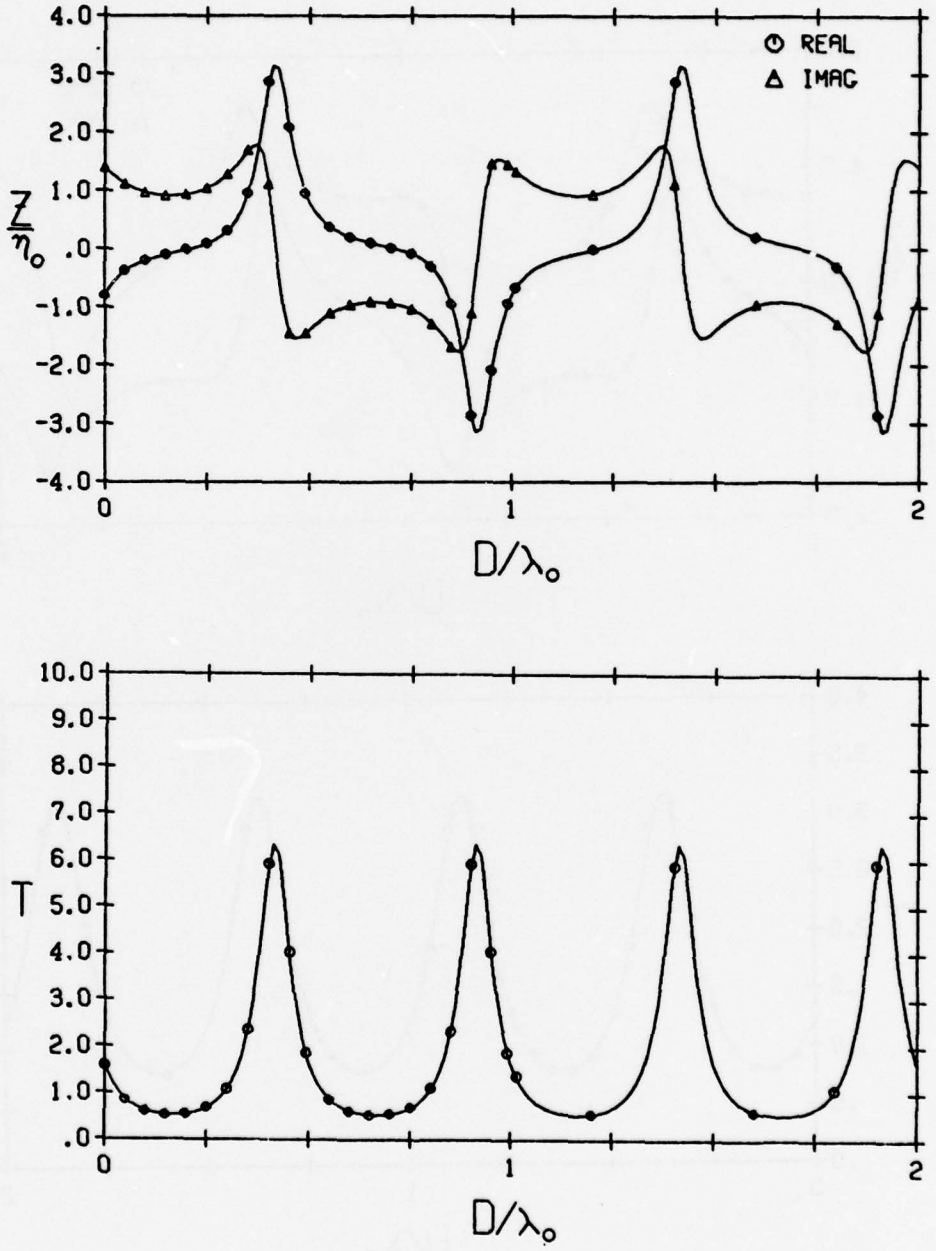

Fig. 47. Slit impedance and transmission coefficient vs. d/λ_o for $w = .05\lambda_o$. Circles and triangles denote modal results, solid lines denote equivalent circuit model.

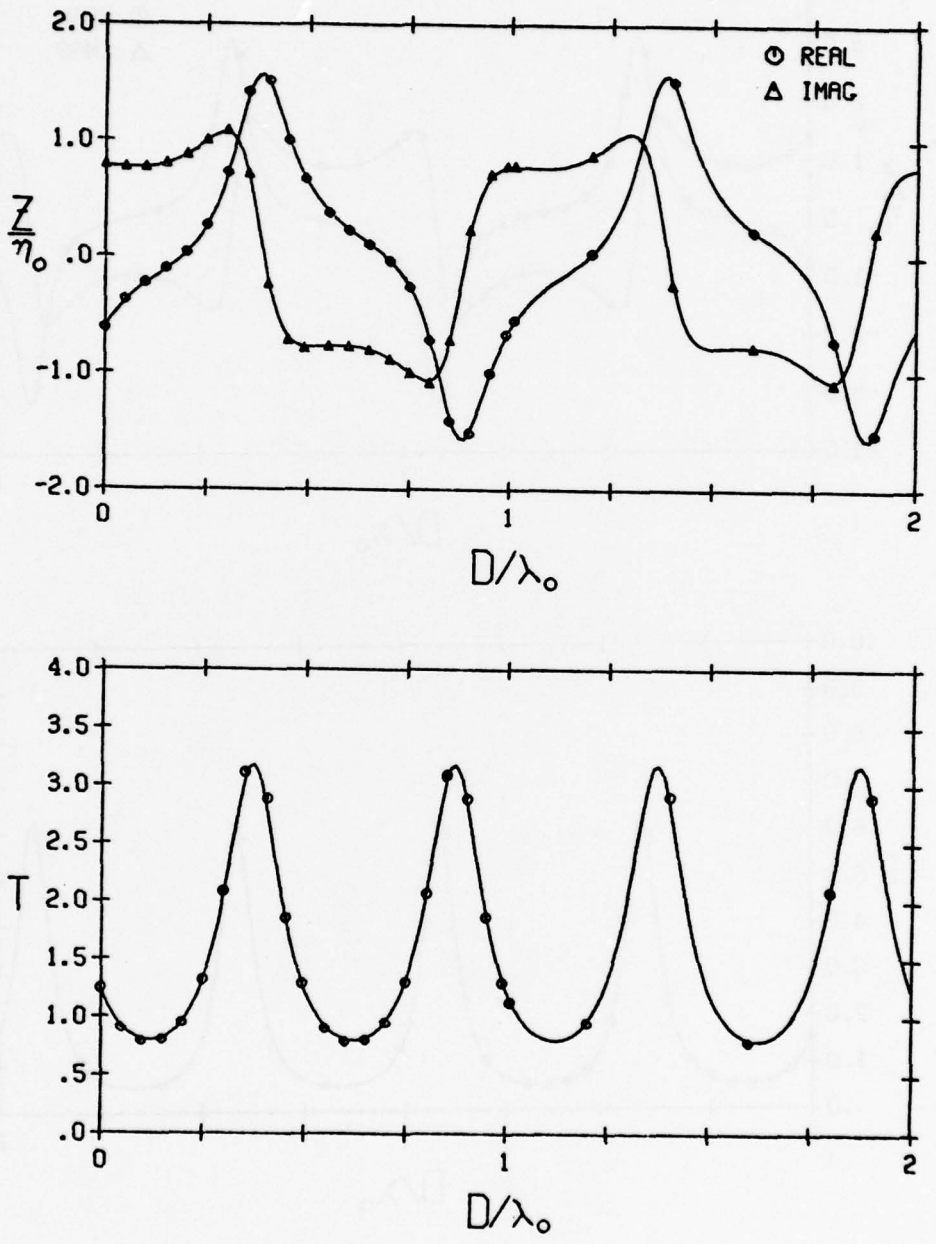

Fig. 48. Slit impedance and transmission coefficient vs. d/λ_o for $w = 0.1\lambda_o$. Circles and triangles denote modal results, solid lines denote equivalent circuit model.

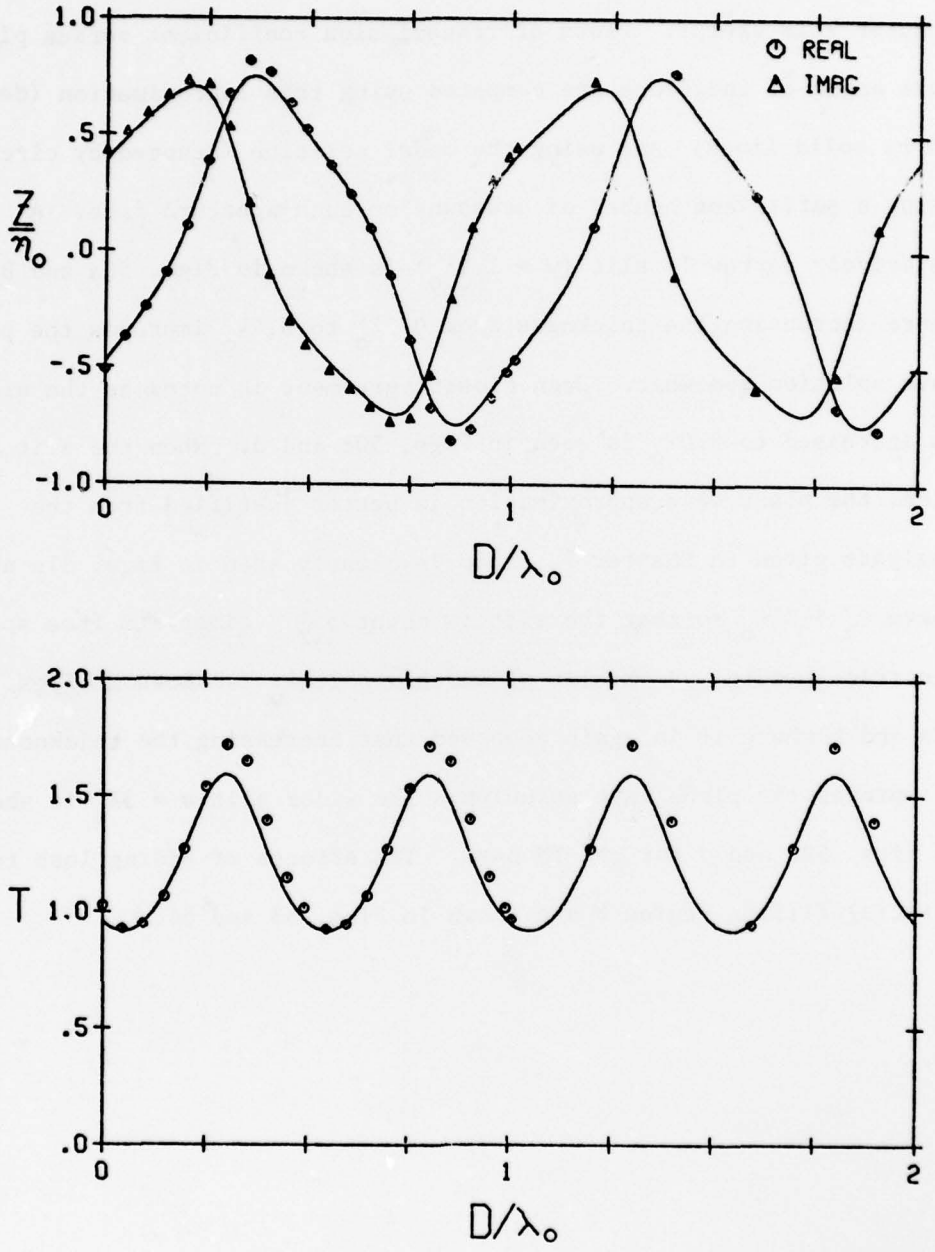

Fig. 49. Slit impedance and transmission coefficient vs. d/λ_o for $w = 0.2\lambda_o$. Circles and triangles denote modal results, solid lines denote equivalent circuit model.

8.3. Plane Wave Approximate Solution

For wider rectangular slits, the plane wave approximation of Chapter 7 is useful. Plots of transmission coefficient versus plane wave angle of incidence are computed using this approximation (denoted by solid lines) and using the modal solution (denoted by circles) using a sufficient number of unknowns on each aperture face. A relatively narrow TE slit ($w = 1.4\lambda_o$) is shown in Figs. 50a and b where increasing the thickness from $0.2\lambda_o$ to $0.4\lambda_o$ improves the plane wave solution somewhat. Even closer agreement is noted as the width is increased to $3.0\lambda_o$ as seen in Figs. 50c and d. When the slit is wide, the plane wave approximation is better justified from the analysis given in Chapter 7. This is clearly seen in Figs. 51a and b where $\varepsilon_b = 30\varepsilon_o$ so that the slit is about $5\frac{1}{2}$ times its free space electrical width. A TM slit of width $w = 1.4\lambda_o$ is shown in Figs. 52a and b where it is again observed that increasing the thickness d improves the plane wave solution. The wider slit $w = 3\lambda_o$ is shown in Figs. 52c and d for the TM case. The effects of adding loss to the material filling region b are shown in Figs. 53 and 54.

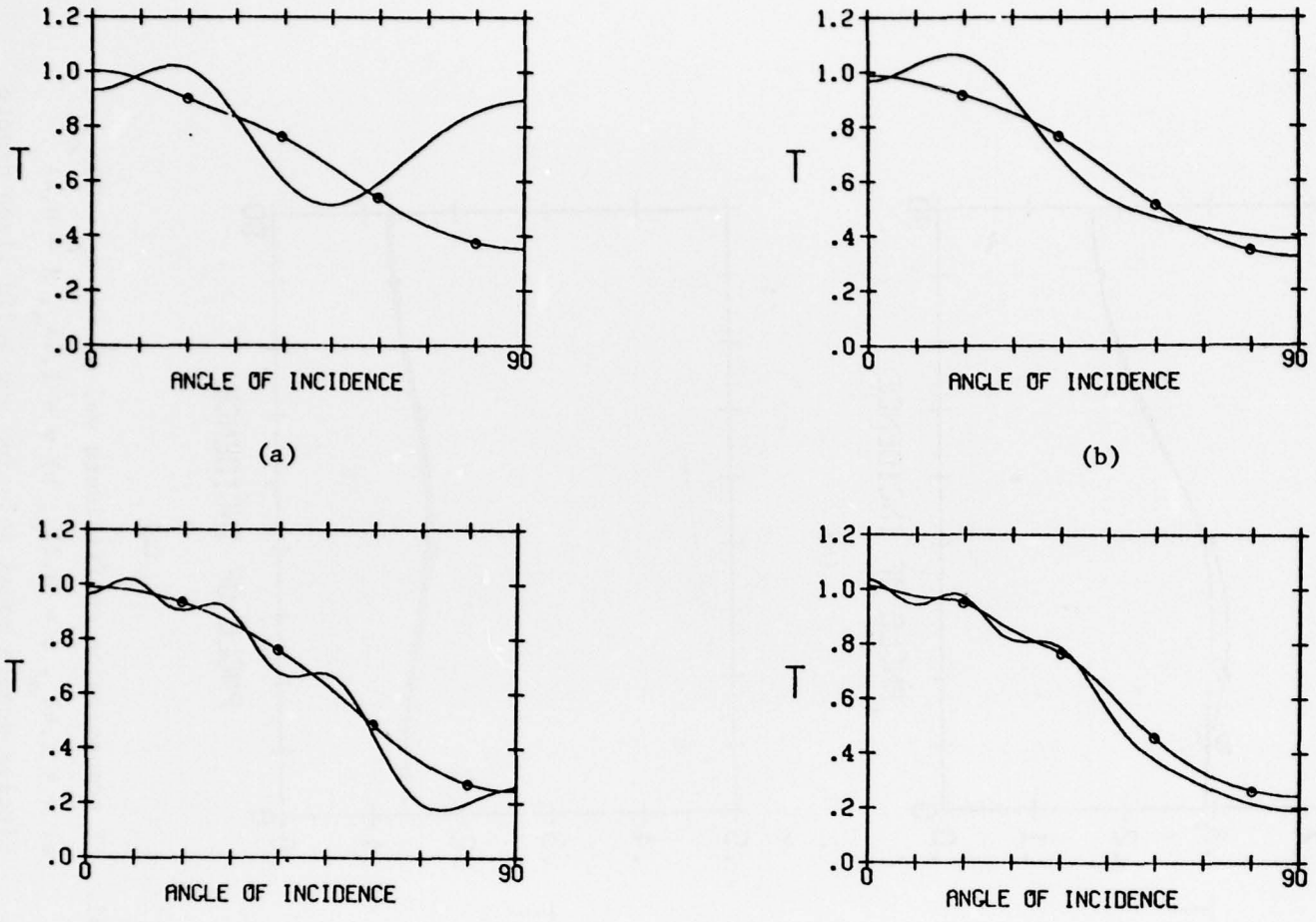

Fig. 50. TE transmission coefficients vs. ϕ^i for $\varepsilon_b = \varepsilon_o$, a) $w = 1.4\lambda_o$, $d = 0.2\lambda_o$; b) $w = 1.4\lambda_o$, $d = 0.4\lambda_o$; c) $w = 3\lambda_o$, $d = 0.2\lambda_o$; d) $w = 3\lambda_o$, $d = 0.4\lambda_o$. Circles denote modal solution and solid lines denote plane wave approximation.

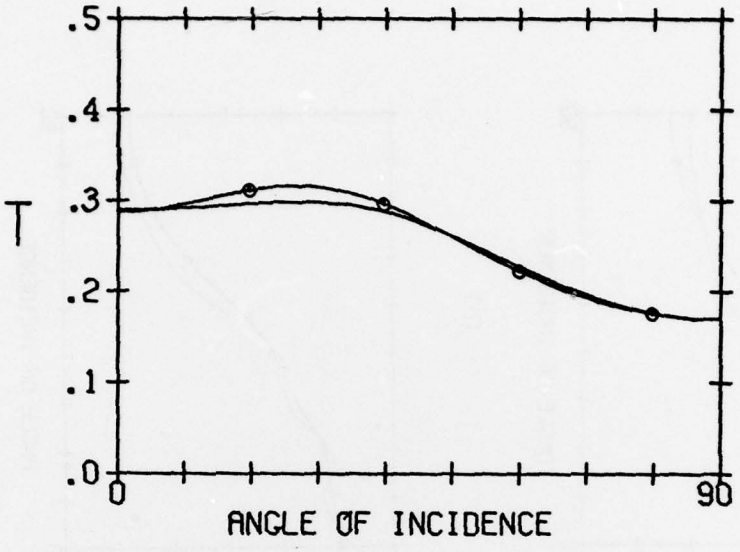

(a)

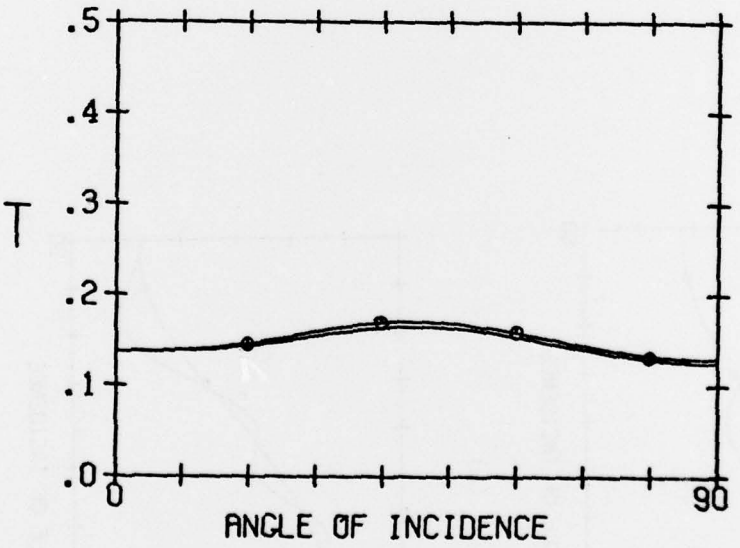

(b)

Fig. 51. TE transmission coefficients vs. ϕ^i for $\varepsilon_b = 30\varepsilon_o$, a) $w = 1.4\lambda_o$, $d = 0.2\lambda_o$; b) $w = 1.4\lambda_o$, $d = 0.4\lambda_o$. Circles denote modal solution and solid lines denote plane wave approximation.

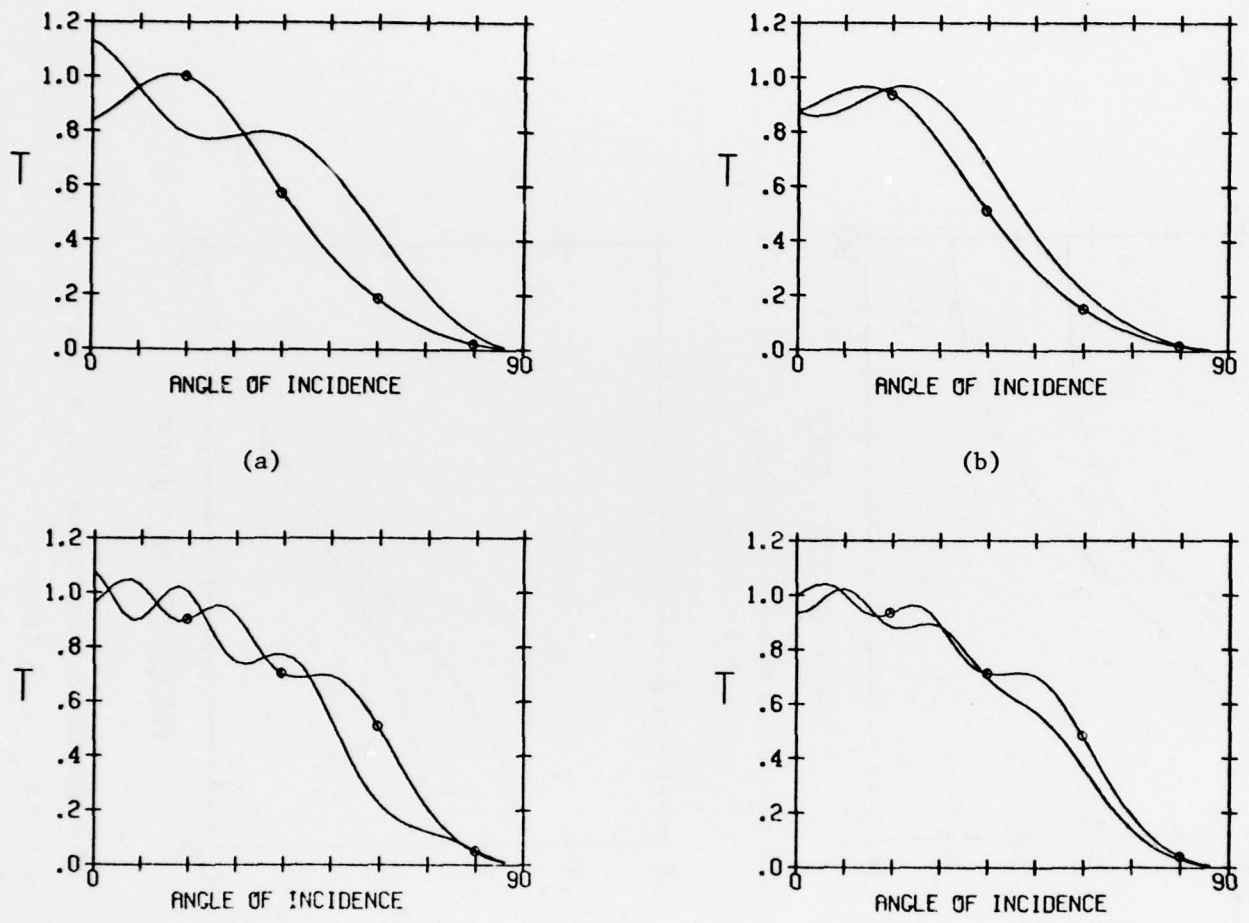

Fig. 52. TM transmission coefficients vs. ϕ^i for $\varepsilon_b = \varepsilon_o$, a) $w = 1.4\lambda_o$, $d = 0.2\lambda_o$; b) $w = 1.4\lambda_o$, $d = 0.4\lambda_o$; c) $w = 3\lambda_o$, $d = 0.2\lambda_o$; d) $w = 3\lambda_o$, $d = 0.4\lambda_o$. Circles denote modal solution and solid lines denote plane wave approximation.

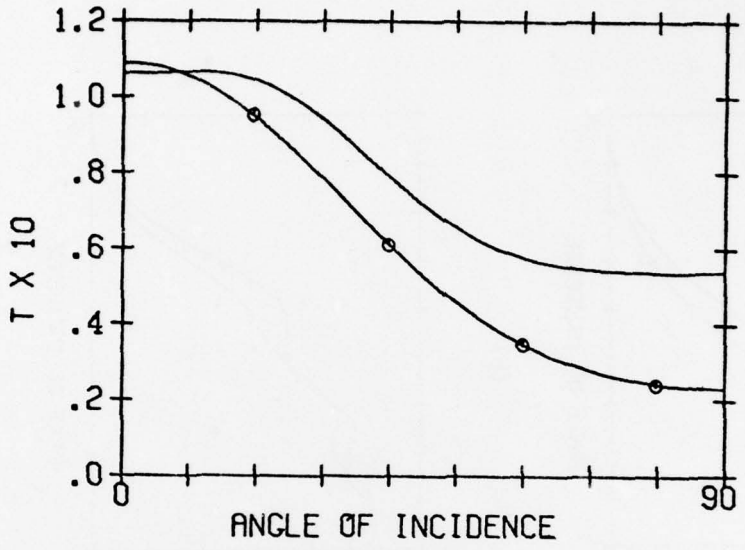

Fig. 53. TE transmission coefficient vs. ϕ^i for $w = 1.4\lambda_o$, $d = 0.4\lambda_o$, $\varepsilon_b = (1-j)\varepsilon_o$.

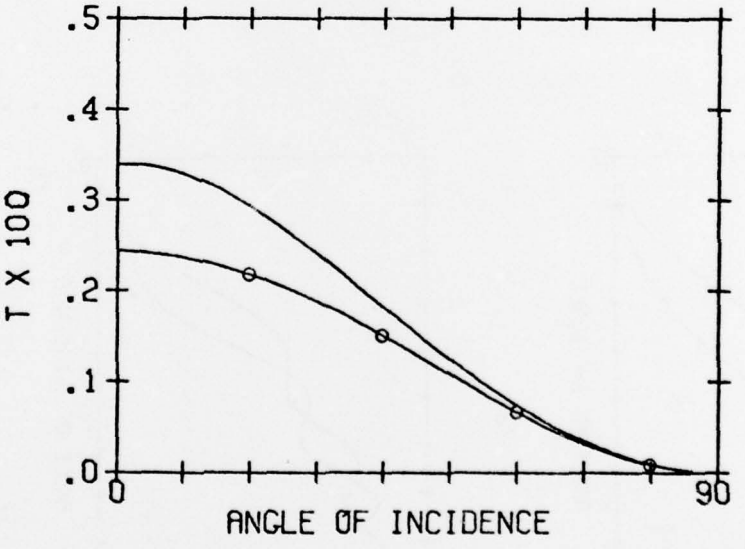

Fig. 54. TE transmission coefficient vs. ϕ^i for $w = 0.7\lambda_o$, $d = 0.4\lambda_o$, $\varepsilon_b = (1-j)\varepsilon_o$.

Chapter 9

CONCLUSIONS AND RECOMMENDATIONS

A non-modal formulation has been developed for studying electromagnetic transmission through a slit of arbitrary cross section cut in a perfectly conducting ground plane of finite thickness. The term "arbitrary cross section" means that the two slit faces, represented by lines Γ_1 and Γ_3, are coincident with the planes $x = 0$ and $x = d$, respectively, and that the rest of the cross section, lines Γ_2 and Γ_4, may be specified in an arbitrary manner. After some modification, which is not undertaken in this report, the formulation can also be applied to cases where the material filling the slit, and hence lines Γ_1 and Γ_3, may protrude out into the half space regions a and c.

A modal solution is presented to treat slits with a cross section which may be represented by a chain of two-dimensional rectangular cavities which are coupled to each other by an aperture. This chain coupling approach yields a block tri-diagonal matrix which allows special computational considerations. In dealing with a cross section composed of more than one rectangular sub-region, the same number of parallel plate guide modes is taken in each sub-region to compute the fields. This number is more or less arbitrarily picked while checking to see that the real power flow across each aperture face is essentially the same.

The above two formulations, which are also applicable when the material filling the slit is lossy, are compared to one another in

various examples. The advantage of the non-modal solution lies in the arbitrary nature of the specification of the slit cross section whereas the modal solution may be used when the material filling the slit has certain types of inhomogeneities. The computational effort is usually greater in the non-modal solution, especially as the slit cross secton becomes larger. The convergence of the numerical solutions is only investigated in the sense that the mean difference between the two solutions is observed to decrease as the number of unknowns is increased.

A brief exposition of some approximate solutions has also been presented. It is well known that a small hole in a conducting plane may be represented in terms of an electric and magnetic dipole moment. For the two-dimensional slit, the TE case is of more importance than the TM case, because there is then always a propagating mode in the parallel plate cross section no matter how small the width. Here, a slit impedance is defined from which one may compute the transmission characteristics of the slit. Next, an equivalent circuit is postulated, based on a transmission line model, in terms of the aperture impedance of an infinite flange. It is found that this equivalent circuit accurately models the slit for widths as large as 0.2 wavelengths. As the slit width becomes very small, the transmission coefficient becomes very large for conducting planes whose thickness corresponds to the distances at which the equivalent circuit resonates. This circuit model, obtained for slits of a rectangular cross section, could be extended to more complicated cross sections

by using results from waveguide junction theory.

For slits whose cross section is again rectangular but whose widths are large with respect to the wavelength in the material filler, a so-called plane wave approximation can be used. This greatly simplifies the block tri-diagonal matrix which arises in the modal solution and allows very rapid computation. It is found that this approximation yields accurate results when $k_b w \gg 1$ and is slightly better in the TE case. This approximate solution could also be applied to slits which are filled with layers of dense material.

Three computer programs have been written which implement the non-modal, modal, and approximate solutions discussed in this report. They are listed and documented in [34].

Appendix

NUMERICAL APPROXIMATION OF INTEGRALS

In Chapters 3 and 4, several integrals appear which must be computed numerically. These integrals are defined on straight line segments in the x-y plane. The Hankel functions $H_0^{(2)}$ and $H_1^{(2)}$ are encountered in the integrands and, since they are computed using polynomial approximations [29], it is natural to choose a quadrature formula which gives the highest degree of precision for integrating polynomials. Thus the well known Gaussian quadrature formulae [33] are used. With reference to Fig. 5, consider the integral

$$I_n = \int_{t_n}^{t_{n+1}} F(|\underline{r} - \underline{r}'|)dt' \qquad \text{(A-1)}$$

where $\underline{r}$ is a field point not on ΔC_n, $\underline{r}'$ is a source point on ΔC_n, and F is a well defined function on ΔC_n. Rewriting $\underline{r}'$ as

$$\underline{r}' = \underline{R}_n + t'\hat{\underline{t}}_n$$

where $\underline{R}_n$ is a vector from the origin to the midpoint of ΔC_n one may rewrite (A-1) as

$$I_n = \frac{\Delta C_n}{2} \int_{-1}^{1} F(|\underline{r} - \frac{\Delta C_n}{2} u'\hat{\underline{t}}_n - \underline{R}_n|)du' \qquad \text{(A-2)}$$

where $t' = \frac{\Delta C_n}{2} u'$. This is now in the form to approximate by

$$I_n \approx \frac{\Delta C_n}{2} \sum_{j=1}^{Q} A_j^{(Q)} F(|\underline{r} - \frac{\Delta C_n}{2} u_j^{(Q)}\hat{\underline{t}}_n - \underline{R}_n|) \qquad \text{(A-3)}$$

where $u_j^{(Q)}$ are the roots of the Legendre polynomial of degree Q

$$P_Q(u_j^{(Q)}) = 0$$

and $A_j^{(Q)}$ are the weighting coefficients determined by

$$A_j^{(Q)} = \frac{2}{[1 - (u_j^{(Q)})^2][P'_Q(u_j^{(Q)})]^2}$$

Tables of $u_j^{(Q)}$ and $A_j^{(Q)}$ for various values of Q are readily available [33, p. 337]. The foregoing rule can be applied in succession to multiple integrals. For example, if I_n is well defined on ΔC_m, then we have the formula

$$\int_{t_m}^{t_{m+1}} I_n dt \approx \frac{\Delta C_m \Delta C_n}{4} \sum_{i=1}^{Q} \sum_{j=1}^{Q} A_i^{(Q)} A_j^{(Q)} F(\left|\frac{\Delta C_m}{2} u_i^{(Q)} \underline{t}_m - \frac{\Delta C_n}{2} u_j^{(Q)} \hat{\underline{t}}_n + \underline{R}_{mn}\right|) \qquad \text{(A-4)}$$

REFERENCES

[1] A. N. Akhiezer, "On the Inclusion of the Effect of the Thickness of the Screen in Certain Diffraction Problems," Sov. Phys.-Tech. Phys., vol. 2 (6), 1957, pp. 1190-1196.

[2] K.H.L. Garb, et al., "Effect of Wall Thickness in Slot Problems of Electrodynamics," Radio Engineering and Electronic Physics, vol. 13, No. 12, 1968, pp. 1888-1896.

[3] N. A. McDonald, "Electric and Magnetic Coupling through Small Apertures in Shield Walls of Any Thickness," IEEE Trans. on Microwave Theory and Techniques, vol. MTT-20, No. 10, Oct. 1972, pp. 689-695.

[4] A. A. Oliner, "The Impedance Properties of Narrow Radiating Slots in the Broad Face of Rectangular Waveguide, Part I - Theory," IRE Trans. on Antennas and Propagation, vol. AP-5, January 1957, pp. 4-11.

[5] A. A. Oliner, "The Impedance Properties of Narrow Radiating Slots in the Broad Face of Rectangular Waveguide, Part II - Comparison with Measurement," IRE Trans. on Antennas and Propagation, vol. AP-5, January 1957, pp. 12-20.

[6] M.A.K. Hamid, "Diffraction by a Slit in a Thick Conducting Screen," Journal of Applied Physics, vol. 40, 1969, pp. 3882-3883.

[7] L. Deryck, "Diffraction d'une onde sphérique par une fente dans un écran conducteur épais," Fisica Della Radiazion, Fondazione" Giorgio Ronchi," Florence, Italy, vol. 28, No. 4, July-August 1973, pp. 523-544.

[8] S. C. Kashyap, et al., "Diffraction Pattern of a Slit in a Thick Conducting Screen," Journal of Applied Physics, vol. 42, No. 2, February 1971, pp. 894-895.

[9] K. Hongo, "Diffraction of Electromagnetic Plane Waves by Infinite Slit Perforated in a Conducting Screen with Finite Thickness," Electronics and Communications in Japan, vol. 54-B, No. 8, 1971, pp. 90-96.

[10] K. Hongo and G. Ishii, "Diffraction of an Electromagnetic Plane Wave by a Thick Slit," IEEE Trans. on Antennas and Propagation, vol. AP-26, No. 3, May 1978, pp. 494-499.

[11] S. C. Kashyap and M.A.K. Hamid, "Diffraction Characteristics of a Slit in a Thick Conducting Screen," IEEE Trans. on Antennas and Propagation, vol. AP-19, No. 4, July 1971, pp. 499-507.

[12] L. N. Litvenenko, et al., "Diffraction of a Planar, H-Polarized Electromagnetic Wave on a Slit in a Metallic Shield of Finite Thickness," Radio Engineering and Electronic Physics, vol. 22, March 1977, pp. 35-43.

[13] J. L. Roumiguieres, et al., "Etude de la Diffraction par une Fente Pratiquee dans un Ecran Infiniment Conducteur d' Epaisseur Quelconque," Optics Communications, vol. 9, No. 4, December 1973, pp. 368-372.

[14] A. Wirgin, "Influence de l'Épaisseur de l'Écran sur la Diffraction par une Fente," C.R. Acad. Sc. Paris, t. 270, Série, B., June 1970, pp. 1457-1460.

[15] F. L. Neerhoff and G. Mur, "Diffraction of a Plane Electromagnetic Wave by a Slit in a Thick Screen Placed Between Two Different Media," Appl. Sci. Res., vol. 28, July 1973, pp. 73-88.

[16] D. T. Auckland and R. F. Harrington, "Electromagnetic Transmission Through a Filled Slit in a Conducting Plane of Finite Thickness, TE Case," IEEE Trans. on Microwave Theory and Techniques, vol. MTT-26, No. 7, July 1978, pp. 499-505.

[17] H. Henke, et al., "Irradiation in a Slotted Half Space and Diffraction by a Slit in a Thick Screen," Nachrichtentech. Z., vol. 29, 1976, pp. 401-405.

[18] H. Henke, et al., "Diffraction by a Flanged Parallel-Plate Waveguide and a Slit in a Thick Screen," Radio Science, vol. 14, No. 1, January-February 1979, pp. 11-18.

[19] G. W. Lehman, "Diffraction of Electromagnetic Waves by Planar Dielectric Structures - I, Transverse Electric Excitation," Journal of Mathematical Physics, vol. 11, No. 5, May 1970, pp. 1522-1535.

[20] N. Morita, "Diffraction of Electromagnetic Waves by a Two-Dimensional Aperture with Arbitrary Cross-Sectional Shape," Electronics and Communications in Japan, vol. 54-B, No. 5, 1971, pp. 58-61.

[21] P.L.E. Uslenghi, "A Simple Model for Electromagnetic Field Penetration Through Gaskets and Seams," Alta Frequenza, vol. 45, No. 10, October 1976, pp. 616-620.

[22] J. R. Mautz and R. F. Harrington, Boundary Formulations for Aperture Coupling Problems, Technical Report TR-79-1, January 1979, Syracuse University, Syracuse, New York, 13210.

[23] S. A. Schelkunoff, "On Diffraction and Radiation of Electromagnetic Waves," Phys. Rev., vol. 56, August 15, 1939, pp. 308-316.

[24] R. F. Harrington, Time-Harmonic Electromagnetic Fields, McGraw-Hill Book Company, New York, 1961.

[25] R. F. Harrington, Field Computation by Moment Methods, The Macmillan Co., New York, 1968.

[26] K. Rektorys, Variational Methods in Mathematics, Science, and Engineering, D. Reidel Publishing Co., Dordrecht, Holland, 1977, Chapter 14.

[27] D. S. Jones, The Theory of Electromagnetism, Pergamon Press, New York, 1964, pp. 565-569.

[28] J. Meixner, "The Behavior of Electromagnetic Fields at Edges," IEEE Trans. on Antennas and Propagation, vol. AP-20, No. 4, July 1972, pp. 442-446.

[29] M. Abramowitz and I. Stegun, Handbook of Mathematical Functions, Dover Publications Inc., New York, 1965.

[30] R. E. Collin, Field Theory of Guided Waves, McGraw-Hill Book Co., New York, 1969, p. 286.

[31] N. Marcuvitz, Waveguide Handbook, Radiation Laboratory Series, McGraw-Hill Book Co., New York, 1951, p. 184.

[32] C. M. Butler and D. R. Wilton, "General Analysis of Narrow Strips and Slots," submitted for publication, April 1979.

[33] V. I. Krylov, Approximate Calculation of Integrals, translated by A. H. Stroud, The Macmillan Co., New York, 1962, pp. 107-122.

[34] D. T. Auckland and R. F. Harrington, Computer Programs for Electromagnetic Transmission through a Filled Slit of Arbitrary Cross Section in a Conducting Plane of Finite Thickness, Technical Report TR-79-8, July 1979, Syracuse University, Syracuse, New York.

MISSION
of
Rome Air Development Center

RADC plans and executes research, development, test and selected acquisition programs in support of Command, Control Communications and Intelligence (C^3I) activities. Technical and engineering support within areas of technical competence is provided to ESD Program Offices (POs) and other ESD elements. The principal technical mission areas are communications, electromagnetic guidance and control, surveillance of ground and aerospace objects, intelligence data collection and handling, information system technology, ionospheric propagation, solid state sciences, microwave physics and electronic reliability, maintainability and compatibility.